REPORT NO. DOT-TSC-OST-73-29, X

CONCEPT FOR A SATELLITE-BASED ADVANCED AIR TRAFFIC MANAGEMENT SYSTEM

Volume X. Subsystem Performance Requirements

J. B. King
C. I. Chen
R. P. Utsumi

FEBRUARY 1974
FINAL REPORT

DOCUMENT IS AVAILABLE TO THE PUBLIC THROUGH THE NATIONAL TECHNICAL INFORMATION SERVICE, SPRINGFIELD, VIRGINIA 22151.

Prepared for

DEPARTMENT OF TRANSPORTATION
OFFICE OF THE SECRETARY
Office of Systems Engineering
Washington DC 20590

NOTICE

The contents of this report reflect the views of Rockwell International/Autonetics Division. The contents do not necessarily reflect the official views or policy of the Department of Transportation. This report does not constitute a standard, specification, or regulation.

NOTICE

This document is distributed under the sponsorship of the Department of Transportation in the interest of information exchange. The United States Government assumes no responsibility for contents or use, thereof.

Technical Report Documentation Page

1. Report No.	2. Government Accession No.	3. Recipient's Catalog No.
DOT-TSC-OST-73-29, X		

4. Title and Subtitle	5. Report Date
CONCEPT FOR A SATELLITE-BASED ADVANCED AIR TRAFFIC MANAGEMENT SYSTEM Volume X. Subsystem Performance Requirements	February 1974
	6. Performing Organization Code
7. Author(s) *J. B. King, C. I. Chen, R. P. Utsumi	8. Performing Organization Report No. DOT-TSC-OST-73-29, X
9. Performing Organization Name and Address Autonetics 3370 Miralome Avenue Anaheim CA 92803	10. Work Unit No. (TRAIS) OS404/R-4509
	11. Contract or Grant No. DOT-TSC-508
12. Sponsoring Agency Name and Address Department of Transportation Office of the Secretary Office of Systems Engineering Washington DC 20590	13. Type of Report and Period Covered Final Report October 1972 to November 1973
	14. Sponsoring Agency Code

15. Supplementary Notes

*Under contract to: Department of Transportation, Transportation Systems Center, Kendall Square, Cambridge, MA 02142

16. Abstract

This volume presents the results of the subsystem performance requirements study for an Advanced Air Traffic Management System (AATMS). The study determined surveillance and navigation subsystem requirements for terminal and enroute area operations. It also established the approach guidance requirements for VOR, Category I, and Category II landing conditions. Subsystem requirements were based on a specified system operating point, namely, a peak busy hour runway capacity of over 100 operations/hour, protection against blunder accelerations of 22 ft/sec^2 or less, and an IFR separation standard of 1.5 nmi without considering the effects of wake turbulence. The study assumed that requirements for surveillance and navigation position accuracy should be identical to provide a fail-operational system. The enroute surveillance and navigation subsystem requirements were based on the same safety level as used in the terminal area (i.e., protection against blunders of less than 22 ft/sec^2) and on specified separation distances of 5, 7, and 10 nmi. The results of the VVOR suitability analysis indicated that approach guidance requirements for VOR landing conditions were approximately the same as those for terminal area operations. A discussion of the methodology used in the study and a description of the models and simulations utilized to establish the subsystem performance requirements is also presented.

17. Key Words	18. Distribution Statement
Subsystem requirements, approach guidance, terminal area operations, enroute area operations, VVOR, surveillance, and navigation.	DOCUMENT IS AVAILABLE TO THE PUBLIC THROUGH THE NATIONAL TECHNICAL INFORMATION SERVICE, SPRINGFIELD, VIRGINIA 22151.

19. Security Classif. (of this report)	20. Security Classif. (of this page)	21. No. of Pages	22. Price
UNCLASSIFIED	UNCLASSIFIED	96	

Form DOT F 1700.7 (8-72)

* U. S. GOVERNMENT PRINTING OFFICE : 1973 725-504/328

CONTENTS

ILLUSTRATIONS

ILLUSTRATIONS (continued)

TABLES

GLOSSARY

AATMS	Advanced Air Traffic Management System
ACC	Airport Control Center
ADF	Automatic Direction Finder
ADIZ	Air Defense Identification Zone
AGL	Above Ground Level
AMF	Analog Matched Filter
AOPA	Aircraft Owners and Pilots Association
ARINC	Aeronautical Radio, Inc.
ARTCC	Air Route Traffic Control Center
ARTS	Automated Radar Terminal System
ATC	Air Traffic Control
ATCAC	Air Traffic Control Advisory Committee
ATCRBS	Air Traffic Control Radar Beacon System
ATCS	Air Traffic Control System
ATM	Air Traffic Management
CA	California
CARD	Civil Aviation Research and Development
CAS	Collision Avoidance System
CCC	Continental Control Center
CNI	Communication Navigation Identification
CNMAC	Critical Near Midair Collisions
COMM	Communications
CONUS	Continental United States
CP	Central Processor
CST	Central Standard Time
CW	Continuous Wave

GLOSSARY (continued)

DABS	Discrete Address Beacon System
DOD	Department of Defense
DOT	Department of Transportation
DME	Distance Measuring Equipment
DNSDP	Defense Navigation Satellite Development Program
DNSS	Defense Navigation Satellite System
ERP	Effective Radiated Power
ESRO	European Satellite Reserach Organization
EST	Eastern Standard Time
ETA	Estimated Time of Arrival
FAA	Federal Aviation Administration
F&E	Facilities and Equipment
FL	Florida
FM	Frequency Modulation
FSS	Flight Service Station
GA	General Aviation
GAATMS	Ground-Based Advanced Air Traffic Management System
GDOP	Geometric Dilution of Precision
GFE	Government Furnished Equipment
IAC	Instantaneous Airborne Count
ICAO	International Civil Aviation Organization
ID	Identification
IFR	Instrument Flight Rules
ILS	Instrument Landing System
IMC	Instrument Meteorological Conditions

GLOSSARY (continued)

I/O	Input/Output
IOP	Input Output Processor
IPC	Intermittent Positive Control
IPS	Instructions Per Second
IR	Infrared
JFK	Kennedy International Airport
LA	Los Angeles
LAT	Latitude
LAX	Los Angeles International Airport
LORAN	Long Range Navigation
LOS	Line-of-sight
LRR	Long Range Radar
MIPS	Million Instructions Per Second
MLS	Microwave Landing System
MODEM	Modulator-Demodulator
MSL	Mean Sea Level
MTBF	Mean Time Between Failures
NAFEC	National Aviation Facilities Experimental Center
NAD	North American Datum
NAS	National Airspace System
NASA	National Aeronautics and Space Administration
NAV	Navigation
NDB	Non-Directional Radio Beacon
NEF	Noise Exposure Factor
NFCC	National Flow Control Center

GLOSSARY (continued)

NMAC	Near Midair Collisions
NOTAM	Notice to Airmen
NOZ	Normal Operating Zone
NWS	National Weather Service
O&M	Operations and Maintenance
PCA	Positively Controlled Airspace
PIREPS	Pilot Reports
PN	Pseudo-Noise
PPM	Pulse Position Modulation
PWI	Pilot Warning Indicator
RAM	Random Access Memory
RCAG	Remote Control Air-to-Ground Facility (Present System)
RCAGT	Remote Communication Air-Ground Terminal
RCC	Regional Control Center
R&D	Research and Development
RDT&E	Research, Development, Test, and Evaluation
RF	Radio Frequency
RNAV	Area Navigation
ROM	Read-Only Memory
SAATMS	Satellite-Based Advanced Air Traffic Management Syste
SAMUS	State Space Analysis of Multisensor System
SID	Standard Instrument Departure
S/N	Signal-to-Noise
SNC	Surveillance, Navigation, Communication
STAR	Standard Arrival Routes
STC	Satellite Tracking Center
STOL	Short Takeoff and Landing

GLOSSARY (continued)

TACAN	Tactical Air Navigation
T&E	Test and Evaluation
TCA	Terminal Controlled Airspace
TOA	Time of Arrival
TRACAB	Terminal Radar Approach/Tower Cab
TRACON	Terminal Radar Approach Control
TRSA	Terminal Radar Service Areas
TRW	Thompson Ramo Wooldridge
TSC	Transportation Systems Center
TX	Texas
VFR	Visual Flight Rules
VHF	Very High Frequency
VMC	Visual Meteorological Conditions
VOR	Very High Frequency Omni-Directional Range
VORTAC	Very High Frequency Omni-Range TACAN
VVOR	Virtual VOR
2D	Two Dimensional
3D	Three Dimensional
4D	Four Dimensional

1. INTRODUCTION AND SUMMARY

1.1 Introduction

The objectives of the Subsystem Performance Requirements Study were to establish the performance requirements of the surveillance and navigation subsystems of a generic Advanced Air Traffic Management System (AATMS) for enroute and terminal area operations and to assess the suitability of Virtual VHF Omni-Range (VVOR) and Satellite Navigation techniques for approach guidance. This volume presents the results of that study.

Section 2 of this volume presents a discussion of the general methodology used to determine the subsystem requirements. The approach involved the use of digital models and simulations representing the operation of an AATMS in terminal and enroute areas. These models relate the system performance measures of capacity, safety, and delay to the position and velocity accuracies of the surveillance and navigation subsystem along with the rate at which surveillance and navigation data must be received to meet the desired system performance levels. This section presents a brief description of the models and simulations (a more detailed description is presented in Volumes V and IX of this report) and a general description of the procedures used to derive the subsystem performance requirements.

Section 3 of this volume presents the detailed procedure used to establish the subsystem requirements for enroute and terminal area operations. It presents the basic assumptions used in the derivation of the requirements, the ranges of system and subsystem parameters investigated, and the rationale for the specification of the system performance levels. The system performance levels used as a basis for the subsystem requirements study are as follows:

(1) The capacity of a single runway during peak busy hour must be at least 100 operations per hour.

(2) The average delay for all operations must be less than 8 min.

(3) The safety level must be at least that afforded by the present system.

The subsystem performance requirements are presented as sets of parameter values that will satisfy the system performance specification.

The subsystem parameters for which requirements are defined include the following:

(1) Surveillance position accuracy, σ_s

(2) Navigation position accuracy, σ_n

(3) Surveillance velocity accuracy, $\sigma_{\dot{s}}$

(4) Navigation velocity accuracy, $\sigma_{\dot{n}}$

(5) Surveillance update interval, τ_s

(6) Navigation update interval, τ_n

This section also presents a discussion of the influence of these parameters on the communication subsystem and data processing requirements. It will discuss the impact of the selection of specific surveillance and navigation requirements on system cost.

Section 4 presents the investigation into the suitability of VVOR and satellite navigation techniques for approach guidance. It describes the VVOR concept and the models used to establish the runway delivery window as a function of visibility and the aircraft control limits on velocity, turn rate, and rate of change of turn rate. This section also describes the methodology used to establish the position-keeping accuracy required to intersect the delivery window for visibility conditions representing VOR, Category I, and Category II operations. This section presents the accuracy of the surveillance or navigation systems required to achieve the position keeping accuracy necessary to achieve entry into the runway delivery window.

1.2 Summary

The Subsystem Performance Requirements Study was conducted to establish the requirements for an Advanced Air Traffic Management System capable of satisfying the demand for services postulated for the 1995 and post-1995 time frame. During the Satellite-Based Advanced Air Traffic Management System (SAATMS) performance evaluation, the demand and capacity of the airports in the Los Angeles region were compared. To meet the post-1995 peak busy hour demand, either the number of runways in the area or the capacity of the existing runways must be increased. A runway capacity in excess of 100 operations per hour could satisfy the IFR traffic demand. To achieve this capacity, the IFR separation standard is required to be at most 1.5 nmi. While the analysis that lead to this 1.5 nmi requirement was not concerned with the means for achieving this separation standard, the first nine volumes of this report describe a system that will allow safe operation with this reduced separation. These two values of capacity and separation standard were specified as the desired system operating point, along with the specification that safety be maintained at its present level. The present safety level corresponds to protecting individual aircraft against blunder accelerations of 22 ft/sec^2, assuming that a constant commanded return acceleratio of 16 ft/sec^2 is employed by the system. It was further stipulated that 99.87 percent of all aircraft experiencing a blunder acceleration of 22 ft/sec^2 would come no closer than 300 ft of an adjacent aircraft. Using these specifications and selected representative mixes of aircraft that comprise the traffic demand, an analysis was made to determine the resultant peak busy hour delays. The average aircarrier delays under these conditions ranged from 2.5 to 3.5 min, while the general aviation aircraft could experience maximum average delays from 5 to 8 min.

The subsystem performance requirements were then established for the specified level of system performance, using the computer models and simulations developed during the SAATMS system performance evaluation. The requirements for both terminal area and enroute area operations were determined. The basic assumption used in the study was that the surveillance position accuracy and navigation position accuracy must be approximately the same value to achieve a fail-operational system. Then, in the event that either of the subsystems failed, data from the remaining subsystem could be utilized to maintain acceptable system performance. The assumption of a highly automated system also requires a high degree of reliability to achieve the desired performance.

The results of the study are presented graphically in the text of the report, since the development of the requirements involves a multi-dimensional analysis. The relationship between the specified separation standard and the subsystem parameters is

$$Q_s^* \text{ (1.5 nmi)} = Q_s \left(A_B, A_R, \sigma_s, \sigma_s^{\bullet}, \tau_s, \sigma_n, \sigma_n^{\bullet}, \tau_n, \tau_D, K_s\right)$$

where

A_B = Specified blunder acceleration for which protection is provided (22 ft/sec^2)

A_R = Assumed return acceleration commanded (16 ft/sec^2)

σ_s = Surveillance position accuracy

$\sigma_s^{\bullet}$ = Surveillance velocity accuracy

τ_s = Surveillance update interval

σ_n = Navigation position accuracy

$\sigma_n^{\bullet}$ = Navigation velocity accuracy

τ_n = Navigation update interval

τ_D = System delay time

K_s = 3σ, a specified number related to the percentage of aircraft for which protection is provided

The subsystem performance requirements are not equally dependent upon all of the preceding parameters. Hence, the values of certain of these parameters were assumed and were fixed throughout the study. These fixed parameters were as follows:

System delay time, $\tau_D = 4$ sec

Navigation velocity accuracy, $\sigma_{\dot{n}} = 10$ ft/sec

Navigation update interval $\tau_n = 5$ sec

Sensitivity data showing the relationships between the subsystem performance requirements and those parameters considered as fixed are presented in Section 3 of this report.

The results of the requirements analysis indicate that the terminal area subsystem performance requirements are

(1) Surveillance and navigation position standard deviation from 300 to 500 ft

(2) Surveillance velocity standard deviation from 10 to 35 ft/sec (including wind uncertainties)

(3) Surveillance update interval from 4 to 7 sec

A more detailed determination of terminal area requirements is not possible without additional information, such as cost. With cost information, a minimum cost system can be defined, and tradeoff comparisons of subsystem mechanizations can be developed to establish a more detailed set of subsystem performance requirements.

Requirements were also established for enroute area operations. In enroute areas, capacity and delay are not important performance criteria. Safety and separation standard specifications were used as the basis for developing subsystem requirements. The safety level specified was identical to that selected for terminal area operations; the separation standards considered were separations of 5, 7, and 10 nmi. For the assumption of identical surveillance and navigation position accuracies, the results indicated that requirements in enroute areas can be relaxed considerably from those required in terminal areas. The enroute area requirements are

(1) Surveillance and navigation position standard deviations of 2200 ft for 5 nmi separations, 3300 ft for 7 nmi separations, and 4900 ft for 10 nmi separations

(2) Surveillance update intervals from 6 to 8 sec

(3) Surveillance and navigation velocity standard deviations from 10 to 50 ft/sec

(4) Navigation update interval of 5 sec

Two additional cases were considered for enroute area operations. The first case assumed that the navigation position accuracy was fixed as σ_n = 1000 ft and the surveillance position accuracy requirements were then established (all other parameters were fixed as previously stated). The second case considered a fixed surveillance position accuracy of σ_s = 1000 ft and established the requirements on the navigation position accuracy. The results for the first case show that the one sigma (1-σ) surveillance position accuracy requirement for a 5 nmi separation is 3000 ft; for a 7 nmi separation the requirement is 4700 ft; and for a 10 nmi separation the requirement is 7350 ft. For the second case (σ_s = 1000 ft), the 1-σ navigation position accuracy requirements are 3400 ft for 5 nmi separations, 5200 ft for 7 nmi separations, and 7900 ft for 10 nmi separations. The study results show that the position accuracy requirements vary almost linearly with separation standards and are very insensitive to other subsystem parameters.

The suitability of VVOR and satellite navigation techniques for approach guidance were also investigated. Navigation position accuracy and navigation update interval requirements were established for approach guidance under three landing conditions, i.e., VOR, Category I, and Category II. Visibility ranges for these three conditions are 6000 ft, 2600 ft, and 1200 ft, respectively. A further criterion used was that 99.74 percent of all aircraft would be able to safely approach and land on the runway without being required to make a second approach. This corresponds to a wave-off of 26 aircraft out of 10,000 aircraft approaches.

The basic procedure involved establishing the size and shape of the delivery window (or aircraft control limit window) through which the aircraft must pass to land. The window is a function of visibility range, aircraft velocity, and aircraft control characteristics such as maximum turn rates and turn rate change. This window was then considered as a boundary of a joint position-keeping probability density function, whose volume within the window is 0.9974. The two functions involved are the vertical position-keeping error standard deviation, σ_z, and the cross-track or horizontal position-keeping error standard deviation, σ_y. Once the integration of the joint probability density function is complete, the required values for σ_z and σ_y are established as a function of the ratio of σ_z/σ_y. The ratio σ_z/σ_y that can be obtained is dependent on mechanization and, hence, was treated parametrically in the study.

A computer simulation of an aircraft control and position-keeping process was used to determine the navigation position accuracy and update interval required to maintain the desired position-keeping accuracy.

The results of the study indicated that for VOR conditions (6000 ft visibility) the requirements are essentially those established for terminal area operations. That is,

(1) Navigation position standard deviation of about 500 ft

(2) Navigation update interval of about 5 sec

(3) Navigation velocity standard deviation of about 10 ft/sec

These requirements assume a vertical position-keeping accuracy of approximately 50 ft ($\sigma_z/\sigma_y = 0.1$). The requirements for other landing conditions, such as Categories I and II, are more stringent and may require auxiliary landing aids such as ILS or MLS. Without a more detailed analysis of these cases, the capability of the VVOR concept cannot be determined. Any navigation technique, whether satellite navigation or VVOR, capable of satisfying the terminal area requirements should be suitable for approach guidance under present day VOR landing conditions.

The SAATMS VVOR concept, which uses ground processed surveillance data to provide the user's navigation data, appears to have the capability to provide the required navigation position accuracy and update interval for VOR landing conditions.

A summary of the terminal and enroute surveillance and navigation requirements is shown in Table 1-1. The VVOR requirements are shown in Table 1-2.

Table 1-1. Summary of Surveillance and Navigation Requirements

	Surveillance Accuracy (ft)	Surveillance Update Rate (sec)	Velocity Accuracy (ft/sec)*	Navigation Accuracy (ft)	Navigation Update Rate (sec)
Terminal Area	300 to 500	4 to 7	10 to 35	300 to 500	4 to 7
Enroute Area					
5 nmi Separation	2200	6 to 8	10 to 50	2200	6 to 8
7 nmi Separation	3300	6 to 8	10 to 50	3300	6 to 8
10 nmi Separation	4900	6 to 8	10 to 50	4900	6 to 8

Table 1-2. Summary of VVOR Subsystem Requirements

	Velocity Accuracy (Ft/Sec)*	Navigation Accuracy (Ft)	Navigation Update Rate (Sec)
VVOR Approaches	10	≃500	5
Category I Approaches	10	≃200	5
Category II Approaches	10	≃ 20	5

*Both Navigation and Surveillance

2. METHODOLOGY

During the concept definition study for a Satellite-Based Advanced Air Traffic Management System (SAATMS), analytical models and computer simulations were developed to analyze the relationships among the variables affecting air traffic control system operations, to identify those variables which most significantly impact the performance of the system, and to evaluate the performance of the SAATM system. A more detailed description of these models is presented in Volume IX of this report.

The evaluation of SAATMS performance was concerned with three specific system performance measures: safety, delay, and capacity. Safety is defined in terms of the blunder acceleration protection afforded an individual aircraft. Individual aircraft delay is a measure of the difference between the actual time it takes to travel a given distance due to the presence of other aircraft and the time it would take in the absence of other aircraft. The capacity of an air traffic element, such as an airport or a single runway, is defined in two ways. Saturation capacity is the absolute maximum number of aircraft the element can service or handle with an unspecified limit to the average delay imposed on the aircraft. Capacity efficiency is the number of aircraft the element can service with a specified average delay or with a specified delay distribution.

The dominant subsystem parameters which impact these system performance measures are the surveillance and navigation subsystem accuracies, the surveillance and navigation data update rates, and the system delay time. These parameters significantly impact system performance throughout a wide range of scenarios. The scenario constraints imposed on the system include factors, such as

(1) The demand level (aircraft per unit time), the mix of aircraft types comprising the demand, and the characteristics of each aircraft type

(2) The structure of the airspace (tubes, corridors, routes)

(3) Airport configurations

(4) The operational rules and procedures of the system.

The basic configuration of the system models developed during the SAATMS performance evaluation efforts is shown in Fig. 2-1.

The system models were used to establish the input-output relationships between subsystem parameters and system performance. The process is shown in Fig. 2-2.

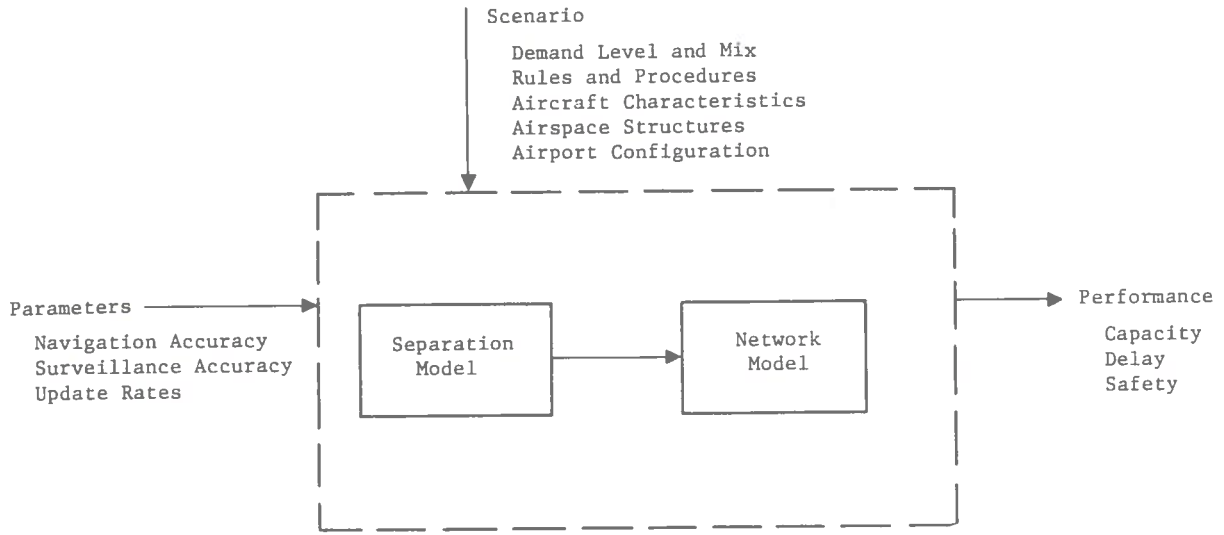

Fig. 2-1. Basic Model Configuration

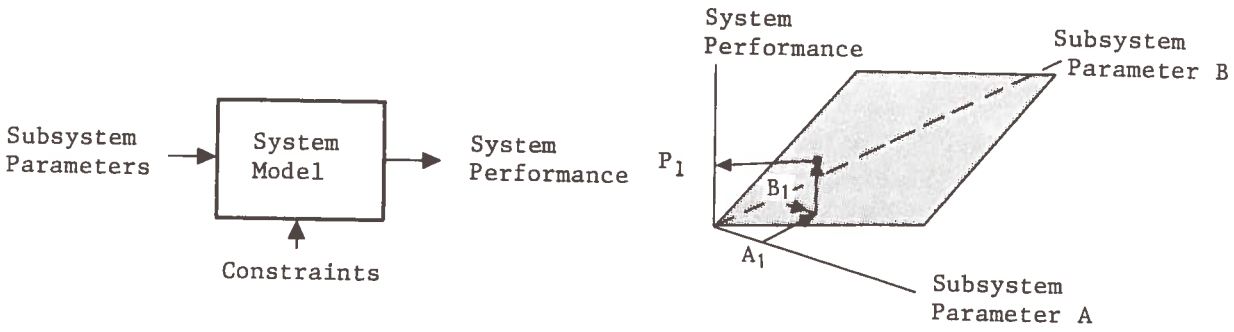

Fig. 2-2. Input-Output System Performance Relationships

The process of establishing the input-output relationships can also be considered as a mapping $f:x \rightarrow y$, where x is an element of the subsystem parameter space X, and y is an element of the system performance measure space Y.

To determine the subsystem performance requirements, the models can be used in a reverse manner. While a given combination of subsystem parameters yields a unique system performance value, a specific system performance value may be achieved by many different combinations of subsystem parameters. That is the inverse mapping function, $f^{-1}: y \rightarrow x$, is not unique. It is necessary to search through the subsystem parameter space in the region of practical value for all possible combinations of parameters that yield the specified performance.

Figure 2-3 illustrates the use of the system models to develop subsystem requirements.

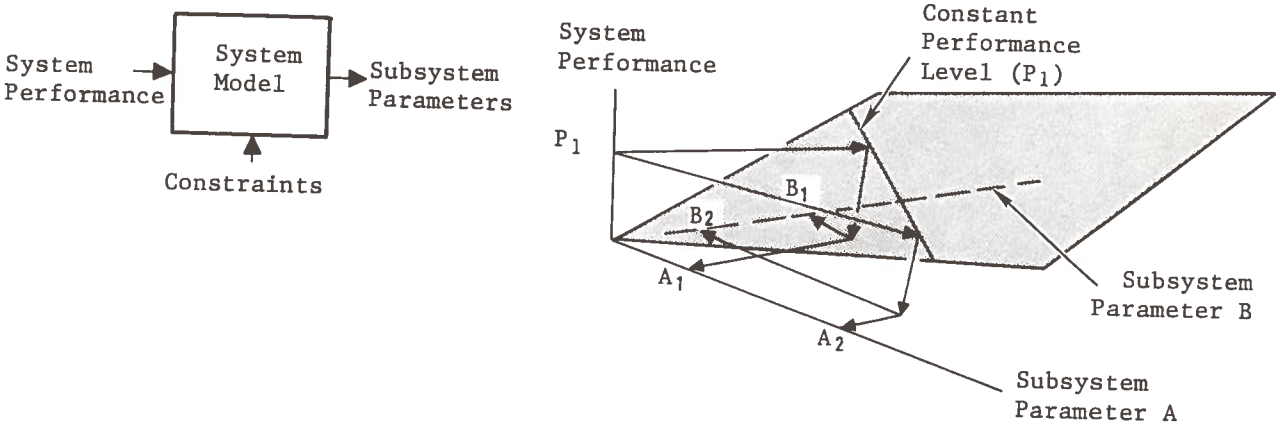

Fig. 2-3. Input-Output Subsystem Requirements Relationships

The figure illustrates that a number of values of subsystem parameters A and B (such as A_1, B_1 and A_2, B_2) will yield a specific system performance value, P_1. Since the set of subsystem parameters required to yield a specific performance level is not unique, additional measures or constraints, such as cost, must be introduced to order the subsystem parameter combinations so that a most preferable set of parameters can be identified. A more detailed discussion of the constraints introduced during the study is presented in Section 3.

The following sections present a brief description of the models and their utilization in the development of the subsystem performance requirements for an AATMS.

2.1 MODEL DESCRIPTION

Models based on analytical expressions and digital computer simulations are used to establish (1) the relations between subsystem parameters and system parameters and (2) the relations between system parameters and system performance measures. Simulation techniques are required due to the complexity of the system. The models can be divided into two basic portions. Separation standard models, which consider the more detailed aspects of an individual aircraft movement, provide the relationships between subsystem parameters and the separation standard. These models are applicable in both terminal and enroute areas. The other portion, the network model, is a simulation of movement of aircraft in a specific portion of the space with given airport configuration and airspace structures. The model yields the relations between subsystem parameters and the performance measures.

2.1.1 Separation Standard Models

Separation standard, Q_s, for the air traffic system is considered to be composed of several distances, as given by

$$Q_s = \frac{W_{NF}}{2} + W_{BF} + W_{BL} + \frac{W_{NL}}{2} + W_{T_{LF}} + W_M \qquad (1)$$

where

W_{NF} = Width of the Normal Operating Zone (NOZ) for the following aircraft

W_{NL} = Width of the NOZ for the leading aircraft

W_{BF} = Width of the Buffer Zone (BZ) for the following aircraft

W_{BL} = Width of the BZ for the leading aircraft

$W_{T_{LF}}$ = Wake turbulence danger distance (function of the leading and following aircraft)

W_M = Aircraft miss distance for both aircraft experiencing maximum protected blunder acceleration

These compositions are shown in Fig. 2-4. For the case where $W_{NF} = W_{NL} = W_N$ and $W_B = W_{BF} = W_{BL}$, Eq. (1) becomes

$$Q_s = W_N + W_B + W_{T_{LF}} + W_M \qquad (2)$$

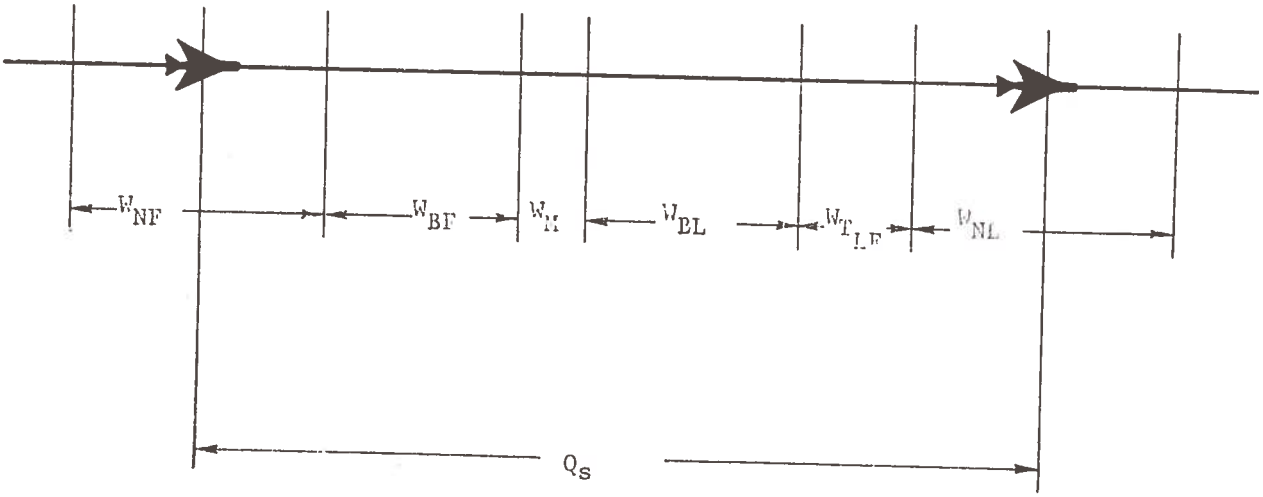

Fig. 2-4. Separation Standard Distances

The width of the Buffer Zone is obtained from the Buffer Zone model which is analytical in nature. The model establishes the values of the Buffer Zone which are needed to protect against specific levels of aircraft blunder accelerations. The blunder is measured in terms of aircraft acceleration, A_B, as it crosses the boundary of the NOZ. If the blundering aircraft cross the boundary of the NOZ immediately after the previous surveillance sample, it may travel beyond the NOZ for τ_S sec before it is detected, where τ_S is surveillance update interval. Because of system and pilot response delay, the correction acceleration cannot be applied until after another τ_D sec. In the model, return acceleration is assumed to be A_R. The maximum distance the blundering aircraft will travel beyond the NOZ can then be determined. The model also considers the uncertainty associated with surveillance position and velocity data and allows an additional zone to insure that the probability of not recognizing early enough that an aircraft has blundered across the normal operating zone threshold is limited to a certain value.

In line with the derivation in Volume V of this report, the width of Buffer Zone can be expressed as

$$W_B = \frac{A_B \tau^2}{2}\left(1 - \frac{A_B}{A_R}\right) - \frac{\dot{\sigma}_s^2}{2A_R} + K_S \left\{ \sigma_s^2 + \left[\tau\left(1 - \frac{A_B}{A_R}\right) - \frac{\hat{\dot{r}}_o}{A_R}\right]^2 \dot{\sigma}_s^2 + \frac{\dot{\sigma}_s^4}{2A_R^2} \right\}^{1/2} \qquad (3)$$

where

$\tau = \tau_S + \tau_D$

τ_S = Surveillance update interval

τ_D = System time delay

A_B = Amount of blunder acceleration the system will protect against

A_R = Return acceleration

σ_S = Standard deviation of position surveillance error

$\dot{\sigma}_S$ = Standard deviation of velocity surveillance error

K_S = A number related to probability of not recognizing in time that an aircraft has blundered across the NOZ threshold

$\hat{\dot{r}}_o$ = Measurement of aircraft velocity at time of crossing NOZ

For fixed values of A_B, A_R, τ, and K_S, the value of W_B increases as σ_S and $\dot{\sigma}_S$ increase. For very large values of σ_S, W_B is approximately linear in σ_S.

The width of the NOZ is obtained through simulation of the movement of an aircraft along its nominal path. The model is designated as the Track Model and is shown in Fig. 2-5.

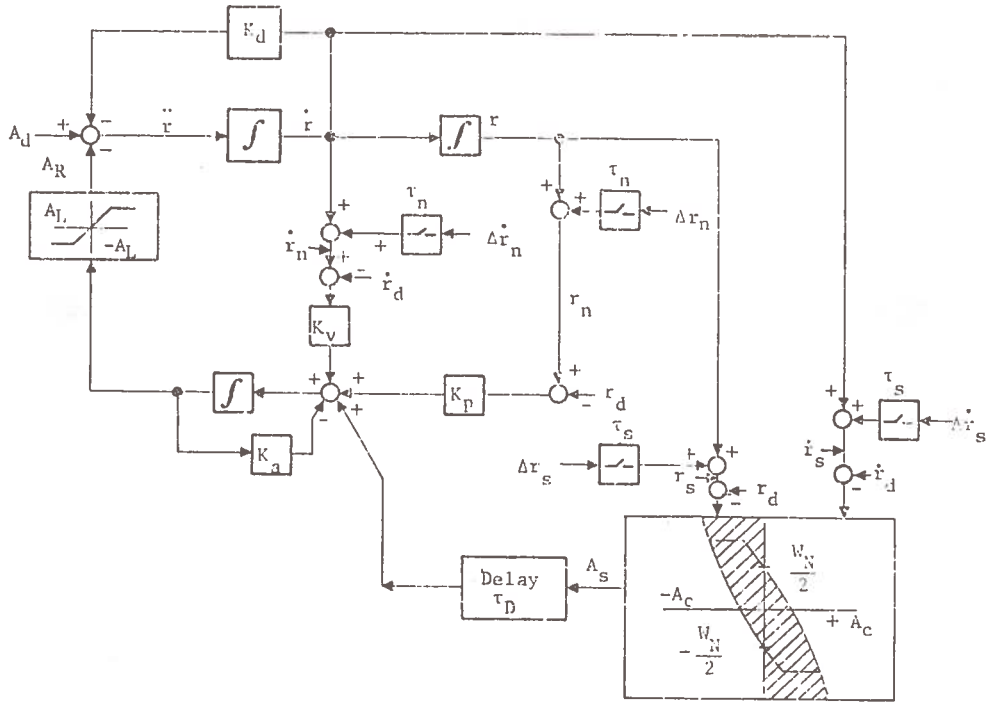

LEGEND:

A_d	Disturbance acceleration (includes blunder acceleration)
r, $\dot{r}$, $\ddot{r}$	Actual aircraft position, velocity, acceleration
r_d, $\dot{r}_d$	Desired aircraft position, velocity
$\Delta\dot{r}_n$, Δr_n	Navigation velocity and position errors
$\Delta\dot{r}_s$, Δr_s	Surveillance velocity and position errors
τ_n, τ_s	Navigation, surveillance update interval
$\dot{r}_n$, r_n	Navigation velocity and position
$\dot{r}_s$, r_s	Surveillance velocity and position
K_a	Aircraft response parameter
K_v, K_p	Velocity and position control loop gains
K_d	Aerodynamic drag term
A_s	Commanded ATC corrective acceleration, $\pm A_c$ (0 if aircraft in shaded region)
W_N	Width of NOZ
A_L	Limit on commanded acceleration

Fig. 2-5. Diagram of Track Model

In this model, there are two basic feedback control loops to determine the corrective acceleration needed so that the aircraft will maintain its nominal flying profile. In the model, the navigation data are assumed to be the actual position and velocity corrupted by navigation noises and the surveillance data are the actual position and velocity corrupted by surveillance noises. In the navigation loop, the navigation position and velocity are used by the pilot to regulate the states of the aircraft. Independent of the navigation loop, surveillance data are used by the surveillance subsystem to determine whether the aircraft remains in its NOZ. If the surveillance data show that the aircraft is outside the NOZ, a corrective command is issued to the pilot. The surveillance subsystem checks the state of the aircraft every τ_s sec. With subsystem parameters specified, the width of W_N is the amount of space needed for an aircraft to operate so that the frequency of intervention will be at a certain level.

The width of missed distance, W_M, is assumed to be equal to 300 ft, which is larger than the largest physical dimension of an aircraft in use today. Wake turbulance danger distance, $W_{T_{LF}}$, is not included here in establishing subsystem requirements. Further discussion of this quantity and its impact is given in Section 3.

2.1.2 Network Model

The movement of aircraft in the terminal area is simulated in the network model. The model determines the capacity and delay of the air traffic system as functions of the separation standard.

It is known that in addition to the separation standard, aircraft mix and demand distributions also play important roles in determining capacity and delay. In this study, aircraft are placed into six different classes according to their velocities and performances. Table 2-1 shows basic characteristics of the six classes.

Aircraft mixes in 43 airports in the Los Angeles hub have been analyzed, and 13 of these have been selected as representative of aircraft mixes in the runways. They range from an all-aircarrier mix to an all-general-aviation mix. The proportional make-ups of these 13 mixes can be found in Volume V of this report. Several of the typical mixes are considered in this study for the selection of a proper operating point.

Studies show that unregulated demand of air traffic can be closely represented by Poisson distributions. For each mix, a random sequence of Poisson-distributed demand is generated. A network structure consisting of nodes and connecting branches is used to represent the air space structure and airport configuration. Fig. 2-6 shows an example of the network structure for a single runway. The node number, location, and type are the variables which define a network structure.

Table 2-1. Aircraft Classes by Speed

Aircraft		Speed (knots)		Runway Occupancy Times (sec)	
Class	Type	Final Approach	Landing	Landing for Exit Speed of 50 fps*	Takeoff
A	Single Engine, GA	75	60	14	21
B	Multi-Engine and Turbo Prop, GA	90	75	19	23
C	Jet, GA	105	90	23	32
D	Ultra Short-Haul, Aircarrier	135	120	21	30
E	Light Weight, Aircarrier	150	135	24	38
F	Heavy Weight, Aircarrier	165	150	26	45

*Landing times for exit speed of 20 fps are 23 and 28 for Classes A and B, respectively.

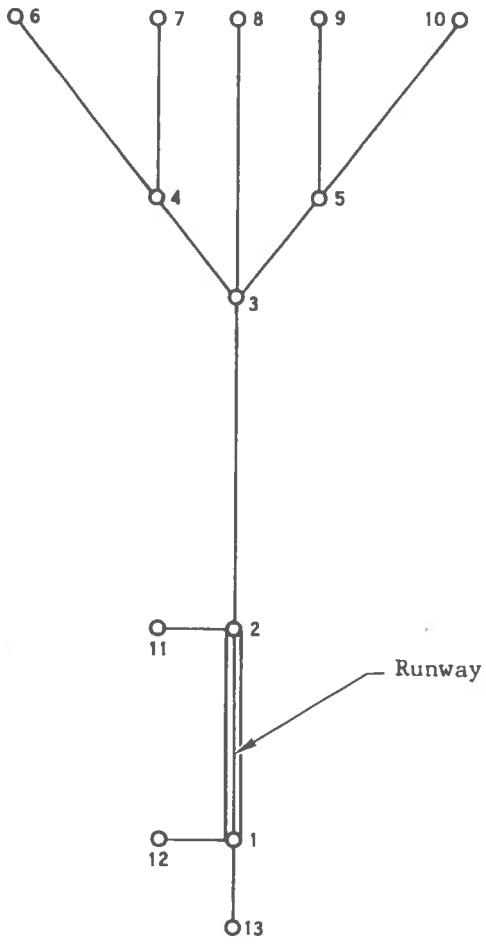

Fig. 2-6. Example of Network Structure for Single Runway

To reduce the computer time required for simulation of such a complex system, the network model is structured as an event-oriented simulation. Significant points of the airspace are considered as nodes and the basic event in the model occurs when an aircraft arrives at a new node. The simulation clock advances from one event to the next in a single step.

Aircraft move from node to node along the branches of the network. Only the time at which an aircraft passes a node will be used to describe states of the system. Detailed position and velocity of an aircraft will generally be available only at the nodes.

Inputs to the model consist of specification of the following:

Network: The x, y, z values of each node in the structure

Routes: The number and sequence of nodes in each route

Separation Standard: Minimum aircraft separation as a function of aircraft type and state

Demand: Aircraft types, arrival times, and velocity at each route node

Each aircraft constitutes an entity to the model. For each entity, the time and place (node) of the next event are recorded. The simulation clock advances from present time to the earliest time at which an event for any entity is to occur. The node where the event would take place is checked to see the last event that occurred there and to verify the availability of the node. If the node can accept the aircraft at its desired time, the event is then cleared and scheduled to take place. Otherwise, the event is delayed the necessary amount of time and a new schedule is given. The actual time of occurrence of the event is recorded and is also used to update the node occupation record. Statistics of delay are also generated as the simulation clock advances.

The following outputs are available from the model:

Capacity: Number of aircraft passing the specific nodes during the run

Delay: Average delay per aircraft, average delay per aircraft type, maximum delay, delay distribution

The model has been used for the simulation of IFR and VFR situations. In the IFR case, additional constraints concerning arrival-departure separation, departure-departure separation, and runway occupancy rules can also be properly introduced through selection of nodes and assignment of artificial velocities. Additional discussion of the model can be found in the model documentation report of the network model.

2.2 Methodology for Establishing Subsystem Performance Requirements

Using the separation standard models and the network model described in the previous section, it is possible to determine subsystem parameter requirements once the desired performance is specified. The outline of the procedure used for such calculation is given as follows.

The amount of the blunder acceleration to be protected against is first defined. With today's subsystem parameters, the relationships between separation standard, Q_S, and blunder acceleration, A_B, are determined and plotted as shown in Fig. 2-7. Since the separation standard of today's system is known, the amount of blunder acceleration protection provided by today's system can be determined.

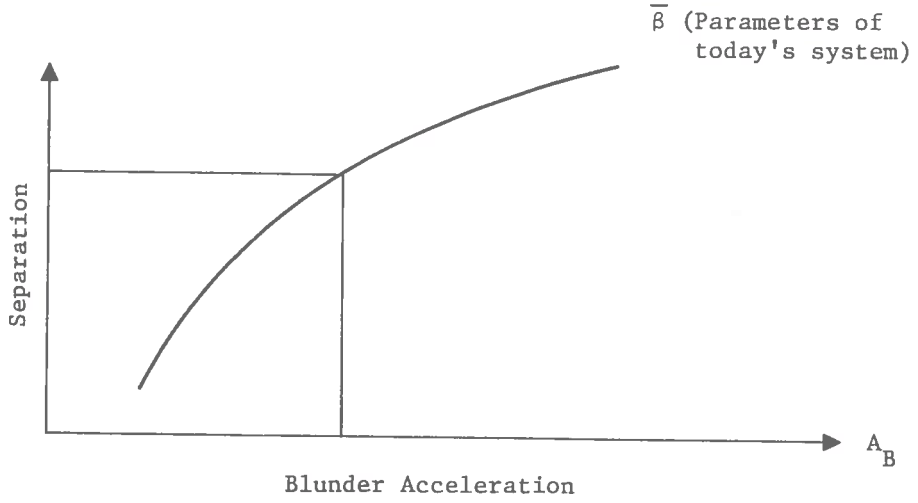

Fig. 2-7. Separation Standard vs Protected Blunder Acceleration for Today's System

The second step is to obtain the performance of an air traffic system for different separation standards. Figure 2-8 shows typical relationships among delay, capacity efficiency, and separation standard.

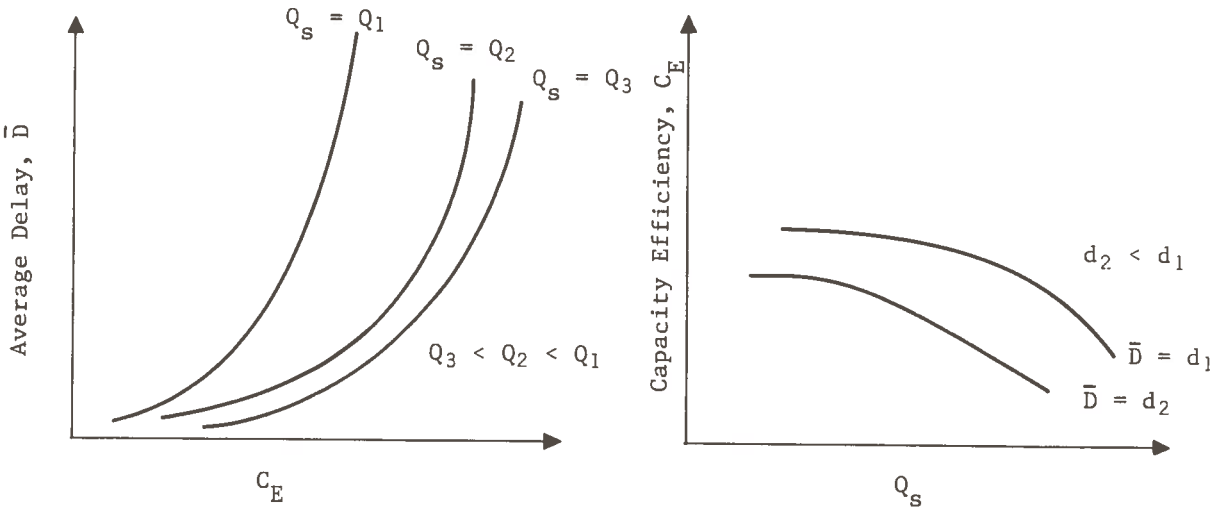

Fig. 2-8. Capacity and Delay vs Separation Standard, Q_s

The shapes of the curves indicate that reducing Q_s below a given value will not improve the capacity of the system effectively. Using the results of network simulation and considering the projected demand of the air traffic system, suitable capacity and delay requirements are established.

With capacity and delay specification given, it is then possible to determine the maximum separation which can meet performance specifications. Figure 2-9 shows the operating point for this case.

Once Q is determined, iteration procedures in the space of the subsystem parameters are performed to find the set of subsystem parameters which yield the desired separation Q. This procedure is shown in Fig. 2-10. Since the subsystem parameter space is of higher dimension, it is necessary to freeze certain parameters in this procedure so that the iteration can be carried out.

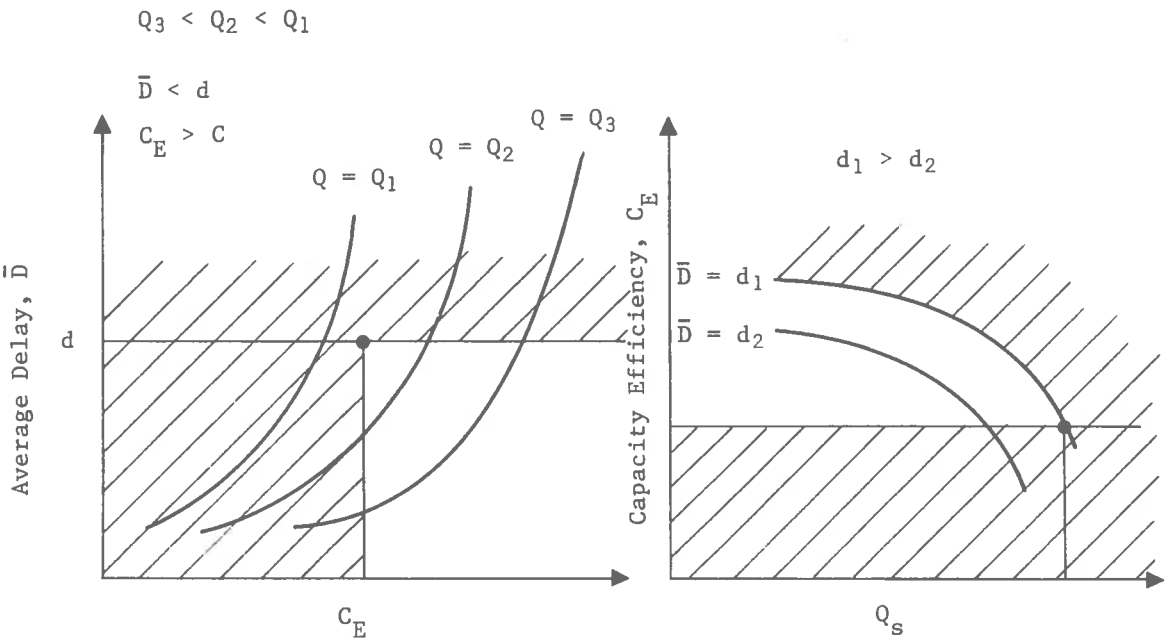

Fig. 2-9. Determination of Maximum Q_s Which Meets Performance Specification

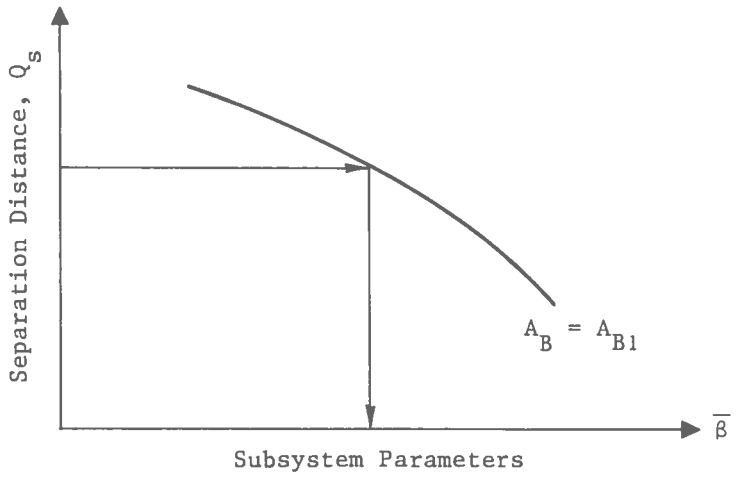

Fig. 2-10. Determination of Subsystem Parameter

3. SUBSYSTEM REQUIREMENTS

This section presents the results of the study to establish subsystem performance requirements for terminal and enroute area operations.

3.1 Terminal Area Requirements

To determine the subsystem requirements, a level of system performance must be specified. The combinations of subsystem parameters must be searched to find that most preferable set of parameters which will produce the desired performance. The parameters for which requirements have been established include the following:

(1) Standard deviation of surveillance position error, σ_s

(2) Standard deviation of surveillance velocity error, $\sigma_{\dot{s}}$

(3) Time interval between surveillance samples, τ_s

(4) Standard deviation of navigation position error, σ_n

(5) Standard deviation of navigation velocity error, $\sigma_{\dot{n}}$

(6) Time interval between navigation samples, τ_n

(7) Processing, decision, and communications delay, τ_D

(8) System time delay, τ ($\tau = \tau_s + \tau_D$)

The input-output relationships incorporated in the system models are limited in number; the number of variables or unknowns exceeds the number of known relationships. To establish the subsystem requirements and to reduce the search for suitable sets of subsystem parameters, additional constraints or assumptions must be introduced.

For terminal area operations, a failure of either the surveillance or navigation subsystems could result in a degradation in system performance. All three of the system performance measures, safety, capacity and delay, could be severely affected. To preclude such an occurrence, an advanced system must be designed to be fail-operational. That is, if either the surveillance or navigation subsystems should fail, the performance of the system will not be degraded. One method of insuring that the system is fail-operational is to use the surveillance and navigation data as backup for each other in the event that one subsystem fails. This requires that the surveillance and navigation data have the same quality. For the purposes of this study, the surveillance and navigation position accuracies are assumed to be the same. Additionally, the reliability of each subsystem must be high to achieve the degree of automation assumed for an advanced system.

The lower bound of position accuracy for the surveillance and navigation subsystems is taken to be 50 ft, system wide. While accuracies smaller than 50 ft can be achieved in a limited local area, an accuracy smaller than that value throughout the entire system would be difficult technologically and restrictive from the standpoint of cost.

The navigation velocity errors stem primarily from a lack of knowledge of wind velocities. The airspeed errors are generally small, but ground speed calculations are dependent on estimates of wind velocity. The accuracy of wind velocity estimates has not been investigated during this study. A nominal navigation velocity accuracy of 10 fps or 6 knots is assumed for this study and is considered to include errors caused by inaccurate wind velocity estimates. An investigation was performed to determine the sensitivity of the primary subsystem parameter values to navigation velocity errors. The results, shown in the following sections, show that the dependence of the requirements on navigation velocity errors is weak and that the assumption of 10 fps for navigation velocity accuracy is not constraining.

The surveillance velocity data can be obtained by using an aircraft's airspeed and estimating the wind velocity. In that case, the surveillance velocity accuracy is the same as the navigation velocity accuracy. Velocity data could also be obtained by filtering the surveillance position data. The surveillance velocity accuracy would be degraded under those conditions. It is also possible that the system could have more accurate wind information; more accurate wind data coupled with the aircraft's airspeed data could provide the surveillance subsystem a higher velocity accuracy then the navigation subsystem. The surveillance velocity accuracy is varied from 5 to 50 fps to encompass the potential schemes for obtaining velocity data. A limit of 5 fps or 3 knots was selected on the basis of technology and cost constraints.

The time interval between surveillance samples, τ_s, is varied from 2 to 12 sec. The lower bound was established from consideration of the data processing load and the attendant cost of processing data for the large demand postulated for the 1995 and post-1995 time frames. The upper bound is imposed from a consideration of the effects of aircraft maneuvers in a moderately dense airspace. Long update intervals could give rise to large inaccuracies in the estimation of aircraft position and velocity. This could result in a degradation of the safety level provided user aircraft. Surveillance position and velocity accuracies are highly sensitive to changes in the surveillance update interval. Long intervals require much higher surveillance position and velocity accuracies.

The navigation update interval is not as dominant a parameter as the surveillance update interval. Consideration of the fail-operational system requirement results in the assumption that the navigation update interval should be approximately the same as the surveillance update interval to maintain the same quality of data in the event of subsystem failure. The navigation update interval is varied from 5 to 10 sec in this study.

3.1.1 Selection of an AATMS Operating Point

The selection of the AATMS operating point is of prime importance in the development of the subsystem requirements. The operating point is defined in terms of the system performance measures and must be based on the overall system goals. The performance measures involved in the selection of the operating point are the capacity, safety, and delay. The operating point selected for use in the study is based on the desired performance at a single runway. The operating point defines the minimum peak busy hour capacity of the runway in operations per hour, the minimum safety afforded each individual aircraft during the approach to the runway, and the maximum allowable average delay for the aircraft using the runway.

3.1.1.1 Safety

The safety of each individual aircraft is expressed in terms of the magnitude of blunder acceleration for which protection is provided by the system. The specification of safety is that an advanced system must provide at lease the same safety level as provided by the present ATC system. The blunder protection provided by the present system is dependent upon its operating parameters. The data concerning the present system are not clearly established; many of the system parameters are range dependent, resulting in a non-uniform blunder protection. A reasonable estimate of these parameters is as follows:

(1) Surveillance position accuracy, σ_s = 1000 ft

(2) Surveillance velocity accuracy, $\sigma_s^{\bullet}$ = 10 fps

(3) Surveillance update interval, τ_s = 14 sec

(4) Navigation position accuracy, σ_n = 500 ft

(5) Navigation velocity accuracy, $\sigma_n^{\bullet}$ = 10 fps

(6) Navigation update interval, τ_n = 5 sec

(7) System time delay, τ_D = 4 sec

Assuming that today's system commands return accelerations of 16 ft/sec^2 and 32 ft/sec^2, the 3 nmi IFR separation standard will provide protection against blunder accelerations of 22 ft/sec^2 and 28 ft/sec^2, respectively. Figure 3-1 shows the blunder acceleration protection for the present system. The specified level of blunder acceleration protection (safety) used in the derivation of subsystem performance requirements is 22 ft/sec^2; the return acceleration commands are assumed to be 16 ft/sec^2.

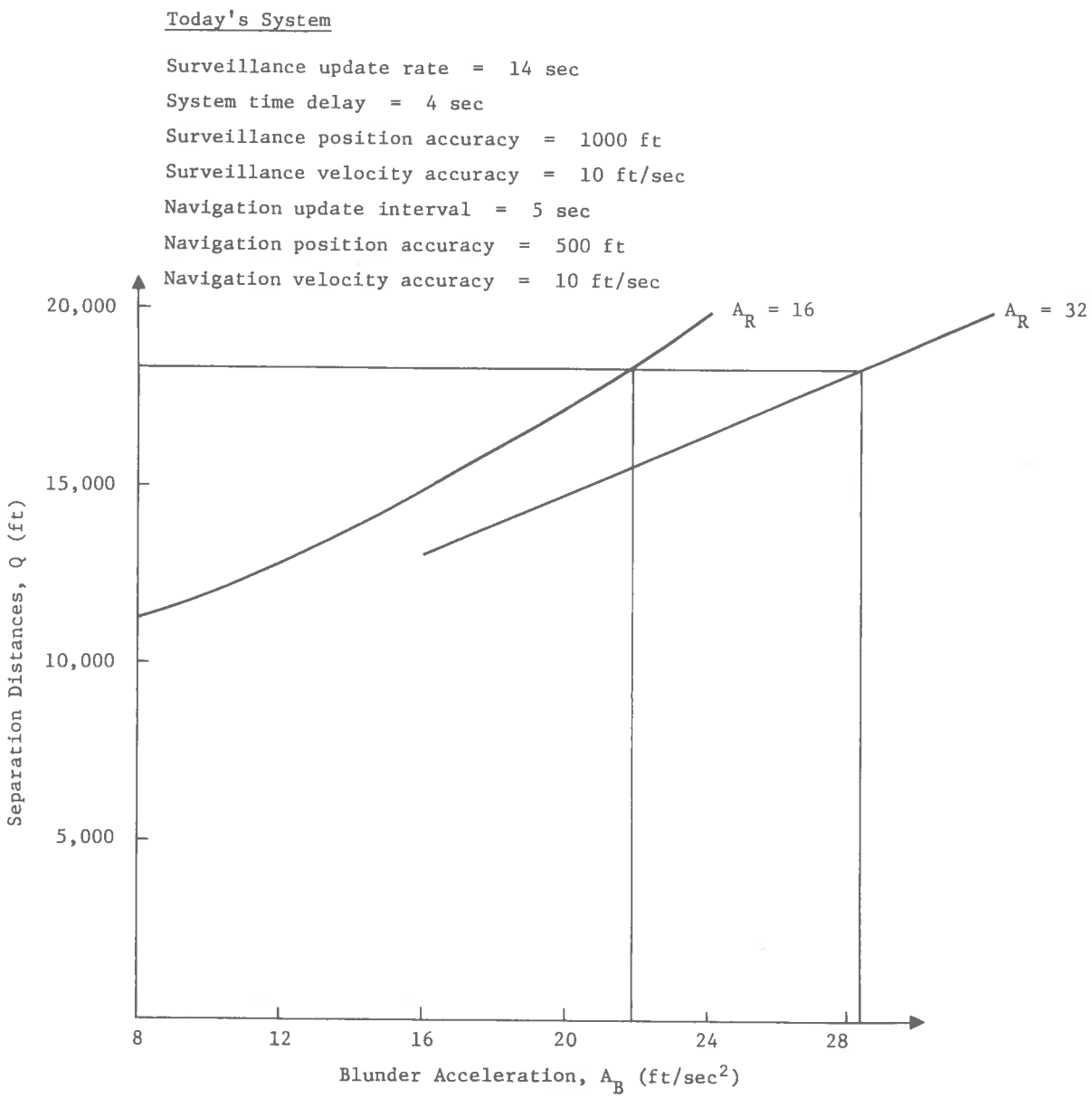

Fig. 3-1. Protected Blunder Acceleration Vs. Separation Distances for Today's System

3.1.1.2 Capacity and Delay

During the SAATMS performance evaluation, an analysis of the 1995 and post-1995 demand and capacity of the airports in the Los Angeles Basin was completed. The demand imposed upon the airports is characterized by the demand level (number of operations per hour), the mix of aircraft types comprising the demand, and the time distribution of the aircraft arrival at the airports. In all, the performance study considered 13 mixes of aircraft (see Volume V of this report) with varying proportions of three types of General Aviation (GA) aircraft and three types of aircarrier aircraft. Each of the aircraft types has different approach and landing velocities and, hence, different runway occupancy times. For any given separation standard, the capacity and delay characteristics associated with a runway will be different for different mixes. If a capacity is specified at a runway independent of the aircraft mix, it is not possible to select a separation standard which will yield a constant delay for all mixes. All three quantities, capacity, delay, and separation, cannot be specified simultaneously. Two quantities can be specified, and the third will assume some value dependent on the system and subsystem parameters.

System operation is simplified through the use of a constant separation standard rather than a different standard for each mix. The value of the common separation standard can be established by more than one method. Figure 2-9 illustrated the relationships between capacity, delay, and separation standard for a specific demand at a single runway. As depicted, if a constant delay is specified, the capacity efficiency of a runway decreases as the separation increases. If the average delay is required to be less than some maximum value, d_1, and the capacity efficiency is required be greater than some value, C_{E1}, than the intersection of those two curves defines a maximum allowable separation for that mix. If this procedure is repeated for all mixes, the minimum of all such maximum allowable separation standards could be selected as the common separation. The resulting separation requirement may be too restrictive, from both a technological and a cost standpoint. Furthermore, the designation of aircraft mixes is only representative; the actual mixes of aircraft at different times might require a smaller separation.

Another method for establishing a common separation is to simulate runway operations using a composite mix having the average composition of all mixes. This would yield a single average delay, capacity, and separation characteristic. Since different runways have different mixes, this approach would not yield a great degree of realism. The common separation standard derived in this manner might yield large average delays and small capacities for different runway mixes.

After consideration of these approaches, the values to be specified are the capacity efficiency and the separation standard; this will result in different average delays for different mixes. Four different mixes, namely M1, M8, M10, and M12, are used in the selection of the desired operating point. Table 3-1 lists these four mixes and indicates the percentage of each aircraft class in each mix.

Table 3-1. Composition of Aircraft Mixes

Mix Designation	Aircraft Class					
	A	B	C	D	E	F
	Single Engine General Aviation	Multi-Engine and Turbo-Prop General Aviation	Jet General Aviation	Ultra Short-Haul Aircraft	Lightweight Aircraft	Heavyweight Aircraft
M1	95	5	-	-	-	-
M8	35	60	5	-	-	-
M10	-	-	-	60	24	16
M12	-	15	15	10	35	25

Mix M1 consists solely of GA aircraft with the majority being the single engine class. M8 is also a GA mix; however, most of the aircraft in the mix are the higher velocity multi-engine and turbo-prop aircraft. It also contains a small percentage of GA jet aircraft. M10 is an aircarrier mix; the predominant class is the ultra short-haul jet. The remaining mixes are the lightweight jets, such as the B707 and DC8, and the heavy jets, such as the B747, DC10, and L1011. Mix M12 consists of all classes of aircraft with the exception of the single engine GA aircraft. These mixes were selected as representative for the entire ATC system, since they span the most probable runway operations.

The capacity and delay characteristics of these mixes are plotted as a function of separation in Fig. 3-2. The figure shows the relationship between capacity and separation for an average delay of 3 min. For a separation between 1 and 2 min, the capacity efficiency varies from approximately 63 operations/hour to 106 operations/hour.

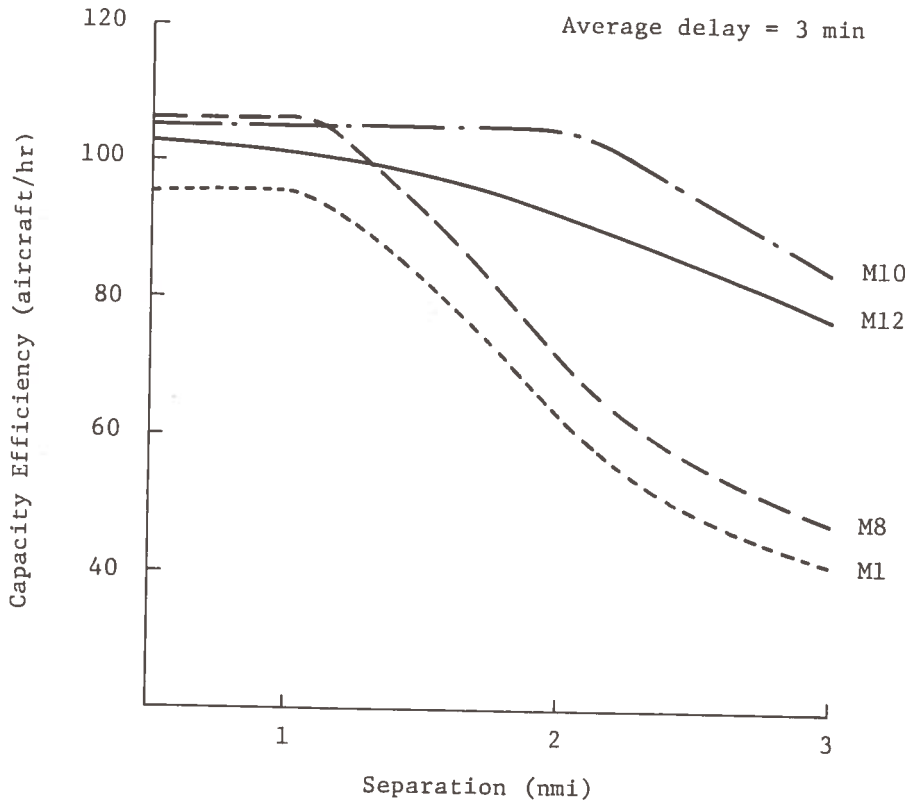

Fig. 3-2. Capacity Efficiency vs Separation Standard for Selected Mixes

From the analysis of the 1995 and post-1995 demand and capacity for SAATMS, the airports in the Los Angeles region were unable to satisfy the requirements imposed by the demand (see Volume V of this report). The major problems occurred at the feeder class airports. The overflow from the primary and secondary airports could not be accommodated by the feeder airports, considering IFR operations. By increasing the required capacity efficiency at each runway to a minimum of 100 operations/hour and by reassigning the overflow appropriately, the peak busy hour demand could be satisfied. Table 3-2 lists the capacity efficiency for the feeder airports in the Los Angeles region under the conditions of a 1.5 nmi separation and the specified delay distribution. The table shows the demand imposed on each airport and its associated capacity along with the cumulative difference for all airports. It also shows the cumulative difference assuming that the capacity is increased to a minimum of 100 operations/hour at each runway. The average delay under these conditions must increase to achieve this increased capacity and to satisfy the required demand.

Figure 3-3 shows a plot of average delay and capacity efficiency as a function of separation distance, Q, for mix M12. This type of relationship is exhibited by all mixes. For any constant average delay (e.g., 4 min) the change in capacity efficiency is large as the separation is reduced from 5 to 3 nmi and becomes much smaller as the separation is reduced further, as shown in Fig. 3-4. The most efficient separation distance in terms of runway capacity ranges from 1 to 2 nmi.

Consideration of all of these factors results in the specification of a capacity efficiency of at least 100 operations/hour during peak busy hour operations and of a separation standard of 1.5 nmi. Any smaller separation will not improve the capacity or delay characteristics for the aircarrier mixes, while any further relaxation of separation will result in large delays for the GA mixes. The average delay characteristics for each of the mixes for a 1.5 nmi separation is shown in Fig. 3-5. Under these operating conditions, the average delay for M10 would be 2.5 min and for M12 it would be 3.5 min. The GA mixes M1 and M8 would have average delays of 8 and 5 min, respectively.

Although the average delays for the GA aircraft may appear to be higher than desirable, this only represents the delays imposed during the peak busy hour. Further, in an IMC situation the GA demand will decrease and the expected delays will be reduced. During a VMC situation the actual separation could be relaxed since not all GA aircraft would fly IFR. Using these specifications on capacity and IFR separations, the system will be capable of meeting the projected demand and remain within the worst-case bound on average delay during peak busy hour operations.

Table 3-2. A Comparison of Feeder Airport Demand and Capacity

Airport	Demand (D) (operations/hr)	SAATMS Capacity Efficiency (C_E) (operations/hr)	(C_E - D)	Cumulative (C_E - D)	Required C'_E	(C'_E - D)	Cumulative (C'_E - D)
X01	129	91	-38	-38	100	-29	-29
L38	128	90	-38	-76	100	-28	-57
RIR	166	90	-76	-152	100	-66	-123
X34	101	91	-10	-162	100	-1	-124
X42	95	90	-5	-167	100	+5	-119
X17	95	90	-5	-172	100	+5	-114
X18	27	91	+64	-108	100	+73	-41
L36	168	90	-78	-186	100	-68	-109
X37	98	90	-8	-194	100	+2	-107
SBT	126	90	-36	-230	100	-26	-133
X15	61	91	+30	-200	100	+39	-94
X25	132	90	-42	-242	100	-32	-126
X31	49	91	+42	-200	100	+51	-75
X32	68	90	+22	-178	100	+32	-43
X33	49	91	+42	-136	100	+51	+8
X43	91	90	-1	-137	100	+9	+17
X44	23	91	+68	-69	100	+77	+94

*See Volume V of this report for more details concerning airport demand and delay specifications.

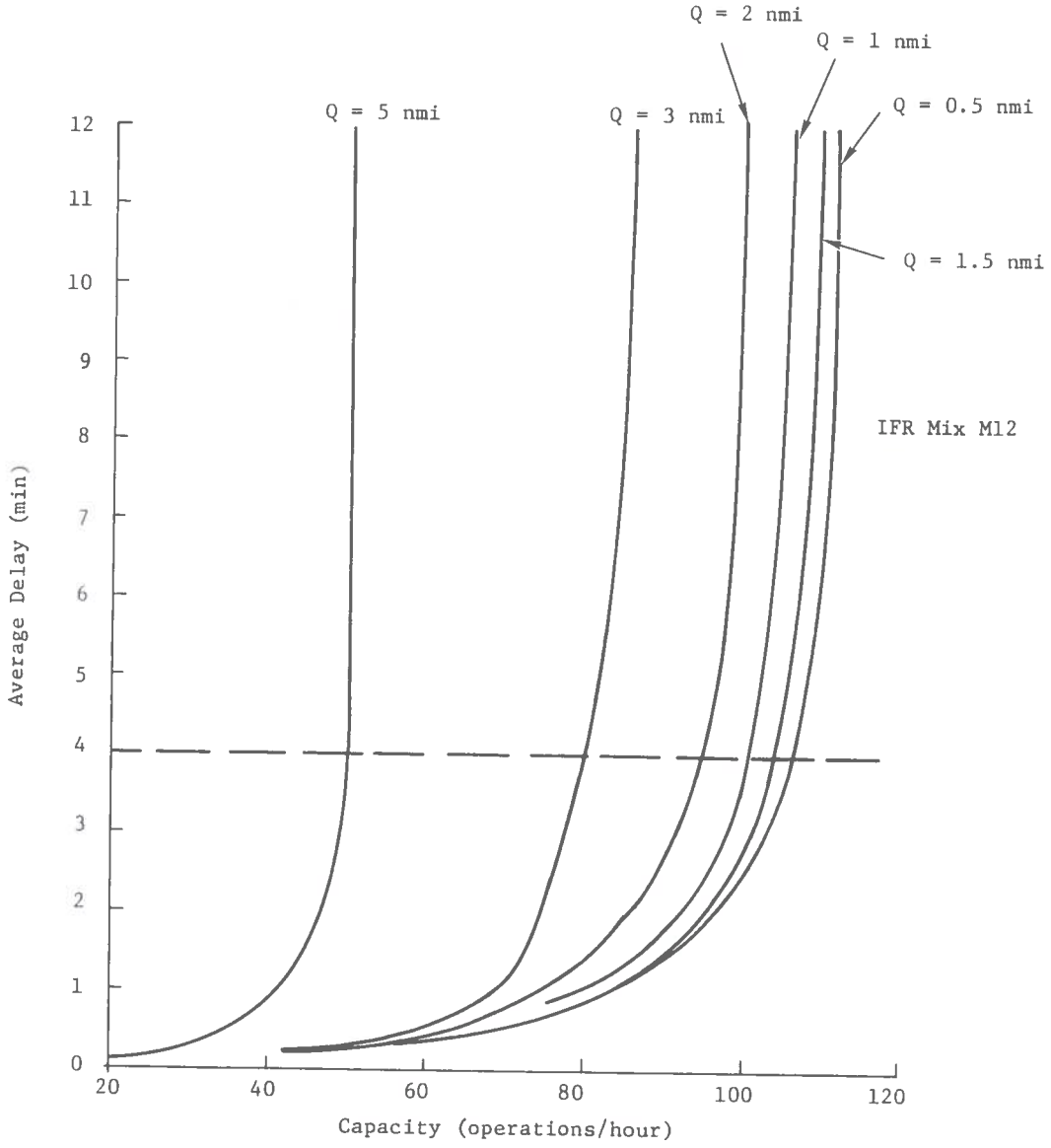

Fig. 3-3. IFR Capacity and Delay Characteristics as a Function of Separation for Mix M12

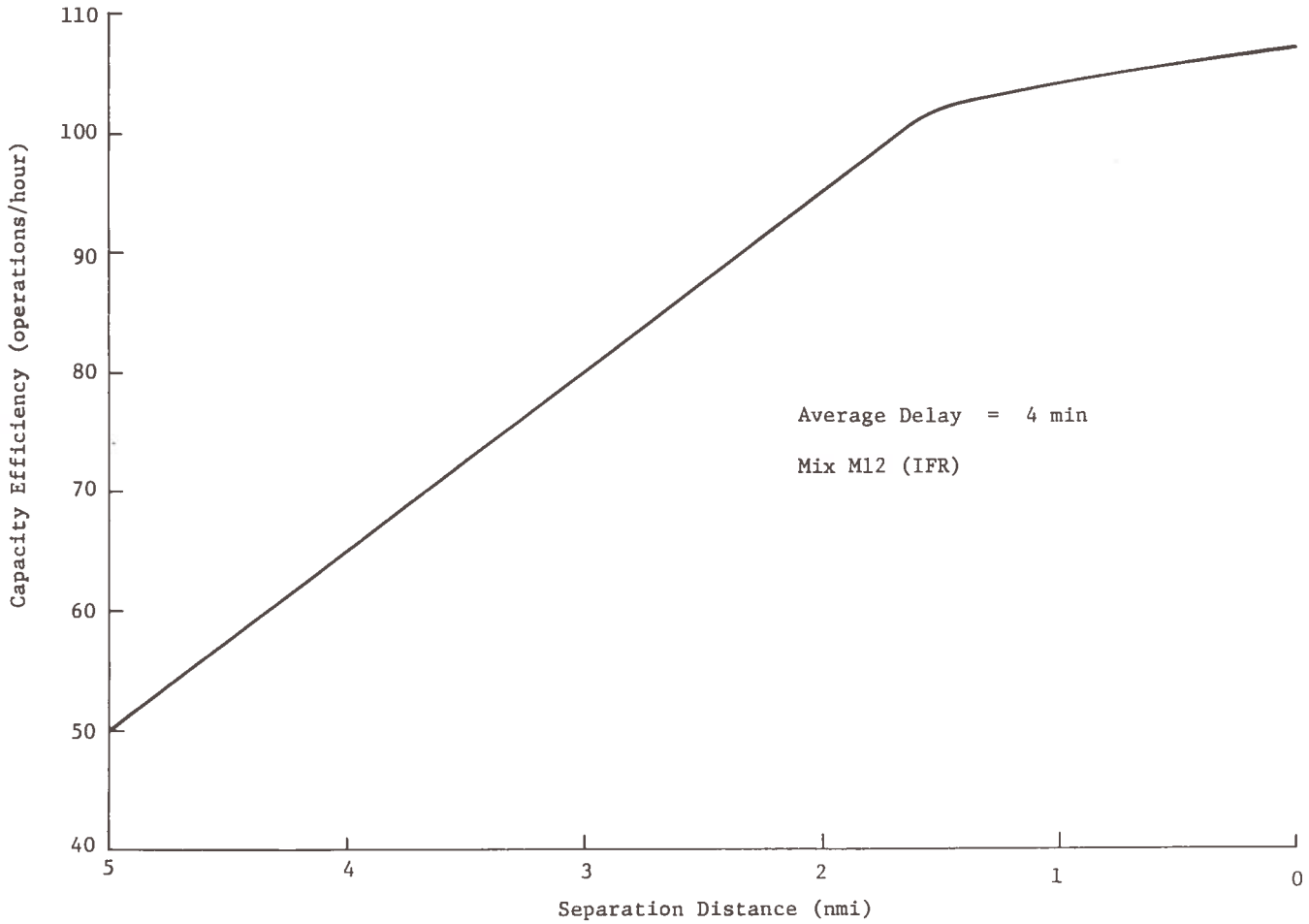

Fig. 3-4. Change in Capacity as a Function of Separation

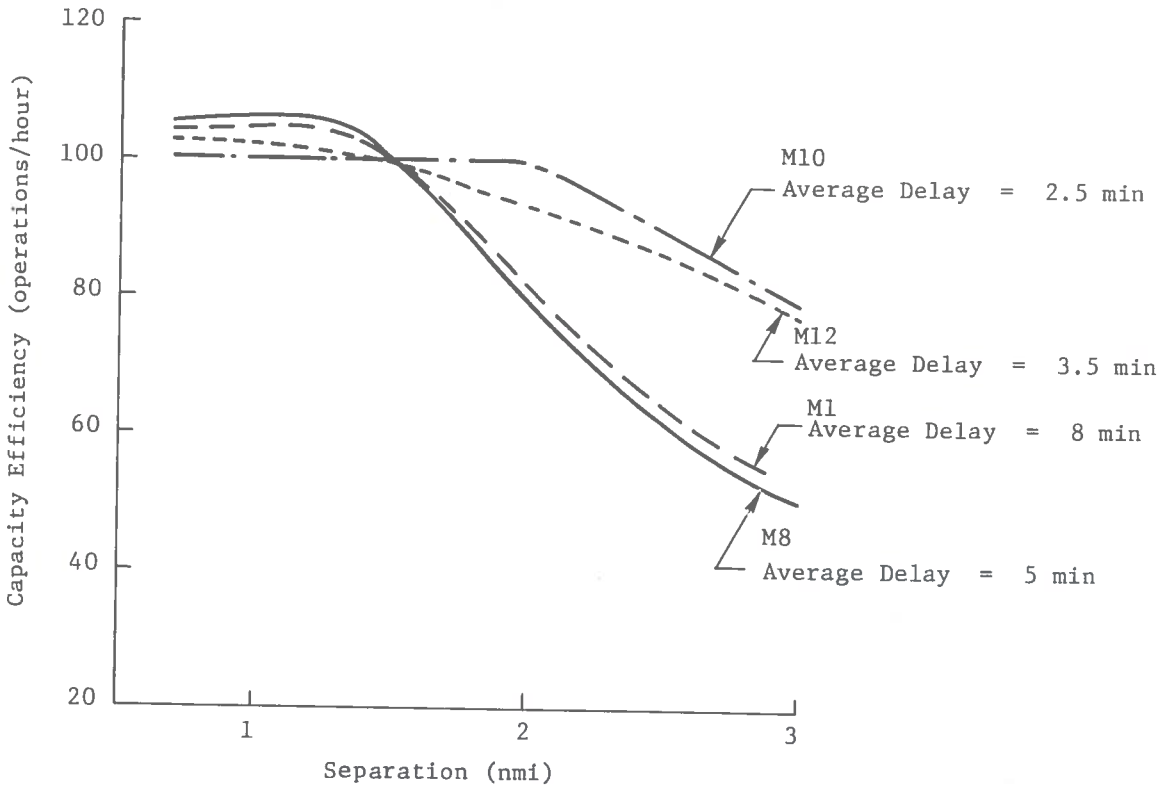

Fig. 3-5. Capacity and Delay Characteristics of All Mixes at the Selected Operating Point

The specification of separation distances of 1.5 nmi does not consider the effects of wake turbulence. The selected separation distance can only be utilized if no wake turbulence exists and if the system is aware of the wake turbulence condition. Of course, this specification is postulated for an advanced system operating in the 1995 and post-1995 time frame during busy hour operations and is not required when the demand is low. By the 1990's, it is assumed either that the wake turbulence can be dissipated by some technique or, at least, that the wake turbulence condition can be measured so that the system can institute the proper procedures for safe operation. Without the proper knowledge of turbulence conditions, separations less than 3 to 5 nmi cannot be utilized for mixes of aircraft containing large jet aircraft employing a given runway. However, all other runways can still use the specified separation, and wake turbulence problems will only affect specific localized runways or areas.

3.1.2 Subsystem Performance Requirements

To determine those subsystem parameter values which can satisfy the specified separation standard of 1.5 nmi, the functional relationships between the separation standard and the subsystem parameters must be known. The separation standard, Q_S, is a function of the width of the Normal Operating Zone, W_N, the width of the Buffer Zone, W_B, and the width of the miss distance, W_M, namely,

$$Q_S = W_N + W_B + W_M \tag{1}$$

The width of the Buffer Zone is dependent on the blunder acceleration, A_B, for which protection is assured by the system, the commanded return acceleration, A_R, the system delay time, τ_D, the surveillance update interval, τ_s, the surveillance position accuracy, σ_s, the surveillance velocity accuracy, $\sigma_s^{\bullet}$, and a number, K_s, which is related to the probability that a blunder is not recognized early enough to prevent the blundering aircraft from traveling beyond its associated blunder distance. Thus,

$$W_B = W_B\,(A_B,\ A_R,\ \tau_D,\ \tau_s,\ \sigma_s,\ \sigma_s^{\bullet},\ K_s) \tag{2}$$

The width of the Normal Operating Zone is established utilizing the Track Model. With a specified intervention rate, $\dot{N}_I$, the Normal Operating Zone is a function of the blunder acceleration, the return acceleration, the system delay time, the surveillance time delay, the surveillance position and velocity accuracies, and, in addition, the navigation update interval, τ_n, the navigation position accuracy, σ_n, and the navigation velocity accuracy, $\sigma_n^{\bullet}$. The width of NOZ can be represented as

$$W_N = W_N\,(A_B,\ A_R,\ \tau_D,\ \tau_s,\ \sigma_s,\ \sigma_s^{\bullet},\ \tau_n,\ \sigma_n,\ \sigma_n^{\bullet}) \tag{3}$$

The miss distance, W_M, has been specified as 300 ft and is unrelated to subsystem parameters. Its value was established from aircraft physical dimensions.

Using the relationships for the Buffer Zone and NOZ, the separation standard can be expressed as

$$Q_s = Q_s (A_B, A_R, \tau_D, \tau_s, \sigma_s, \sigma_s^{\bullet}, \tau_n, \sigma_n, \sigma_n^{\bullet}, K_s) \quad (4)$$

At the specified operating point, $Q_s = Q_s^*$, the separation standard can be written as

$$Q_s^* = Q_s (A_B, A_R, \tau_D, \tau_s, \sigma_s, \sigma_s^{\bullet}, \tau_n, \sigma_n, \sigma_n^{\bullet}, K_s) \quad (5)$$

Many of these variables were considered to have constant values throughout this study. The system delay time, τ_D, which includes the processing of the surveillance samples, the decision making time, the formulation of the command, the transmission and reception of the command, and the pilot and aircraft initial response to the command, is assumed to be 4 sec. This value is representative of a highly automated system and is considered suitable for a highly reliable advanced system.

The values of blunder acceleration, A_B, and K_s are established by the specification of the safety level. The blunder acceleration for which protection is afforded is 22 ft/sec^2; the value of K_s used in the study is 3.0, which yields a 99.87 percent probability of protection for aircraft experiencing the 22 ft/sec^2 blunder acceleration. The commanded return acceleration is assumed to be 16 ft/sec^2, corresponding to providing protection against a 22 ft/sec^2 blunder. The system commands a constant return acceleration since the magnitude of the aircraft's acceleration at the time it leaves its Normal Operating Zone is unknown. If the system returns the aircraft to its Normal Operating Zone with a 0.5 g (16 ft/sec^2) acceleration, the 22 ft/sec^2 blunder acceleration protection will be provided. If the blundering aircraft had less than a 22 ft/sec^2 acceleration, the return command will merely return the aircraft to its Normal Operating Zone sooner than if the aircraft had blundered with the maximum protection acceleration.

The remainder of the subsystem parameter values are established as the result of the subsystem performance requirements study.

The functional relationship to be solved, once those parameters are fixed, is

$$Q_s^* = Q_s (\tau_s, \sigma_s, \sigma_s^{\bullet}, \tau_n, \sigma_n, \sigma_n^{\bullet}) \quad (6)$$

In general, the solution is a five dimensional surface in the subsystem parameter space of six variables. When all except one of the parameters are fixed, the value of the sixth parameter can be established. The consideration of a fail-operational system has led to the assumption that the surveillance and navigation position accuracies be approximately the same; for this study, they are taken to be identical and the solution complexity is reduced. Because of this complexity and the fact that the relationship is not analytical due to the involvement of computer simulations, a graphical method of solution is used to develop the subsystem requirements.

3.1.2.1 Example of the Requirements Methodology

An example of the variation in the width of the Buffer Zone is shown in Fig. 3-6 as a function of surveillance position accuracy. The graph illustrates that the Buffer Zone width varies from approximately 3500 to 4200 ft as the surveillance position accuracy varies from 50 to 600 ft. This curve depicts the variation in W_B only for the case where the surveillance update interval (τ_S) is 4 sec and the surveillance velocity accuracy ($\sigma_S^{\bullet}$) is 30 fps. A family of curves for all τ_S and $\sigma_S^{\bullet}$ combinations is required to describe the Buffer Zone width surface. The illustration is used as an example to aid in describing the technique used to establish the subsystem requirements.

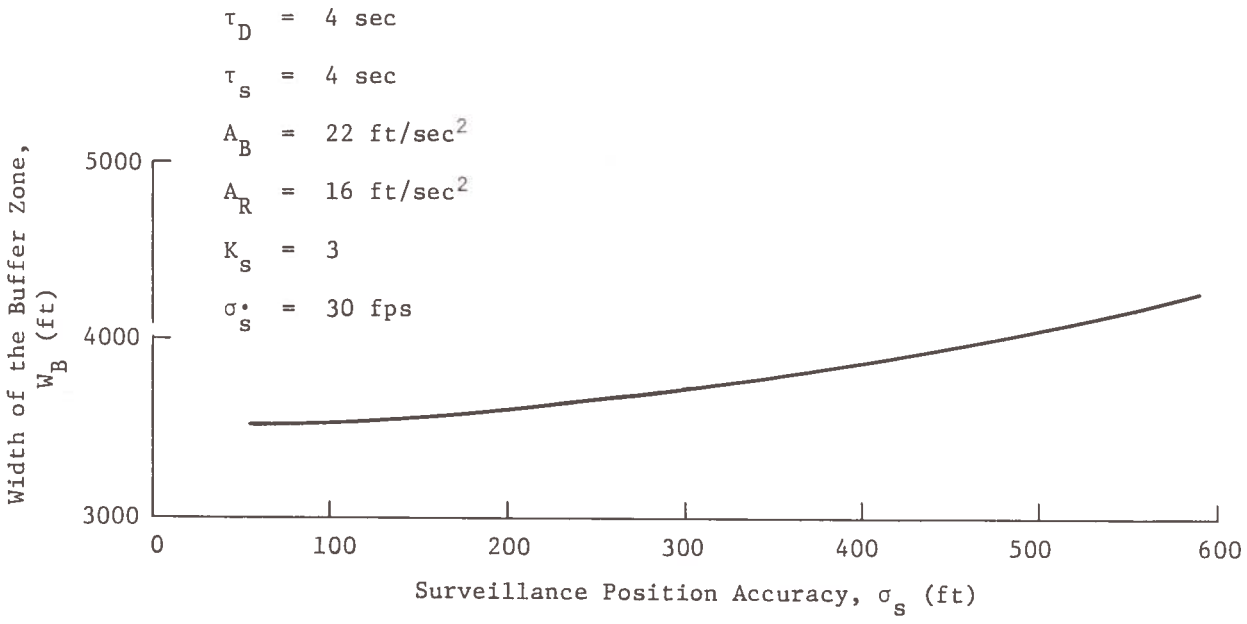

Fig. 3-6. Example Plot of the Width of Buffer Zone vs Surveillance Position Accuracy

The values of the subsystem parameters used in determining the Buffer Zone width are used directly in the Track Model simulation to establish the width of the Normal Operating Zone. The simulation also requires values for the navigation update interval, τ_n, and the navigation velocity accuracy, $\sigma_{\dot{n}}$. The Track Model is exercised iteratively to determine the value of the Normal Operating Zone width as a function of position accuracy. An example of the results is shown in Fig. 3-7 for $\sigma_{\dot{s}}$ = 10 fps and τ_n = 5 sec, assuming that the surveillance subsystem is not required to issue intervention commands at a rate greater than one intervention per aircraft per hour. The figure shows that the Normal Operating Zone varies from approximately 4000 to 6400 ft as the position accuracy varies from approximately 100 to 600 ft.

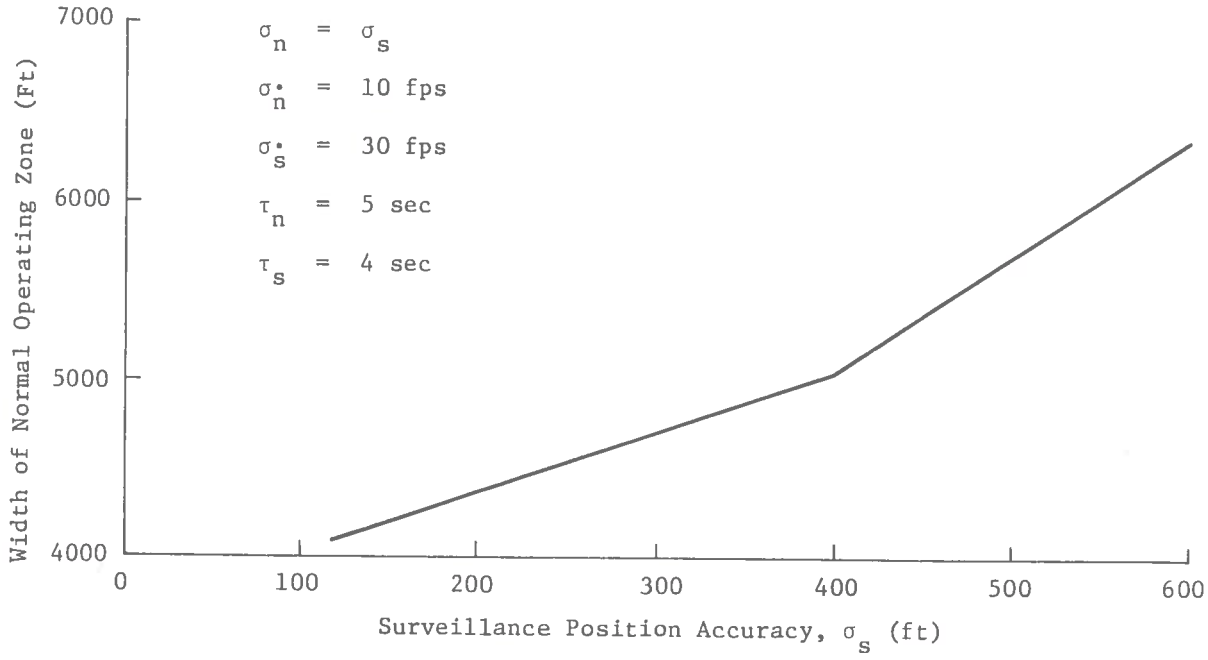

Fig. 3-7. Example Plot of the Width of the Normal Operating Zone vs Surveillance Position Accuracy

When the Buffer Zone (W_B), the Normal Operating Zone (W_N), and the miss distance of 300 ft (W_M) are summed, the separation standard, Q_s, is obtained. Figure 3-8 shows an example of the variation in separation standard as a function of position accuracy for the selected set of subsystem parameters. The graph illustrates that the separation standard ranges from about 8300 to 11,300 ft as the position accuracy is varied from 200 to 650 ft. Using the specified separation standard, $Q_s^* = 1.5$ nmi, the required position accuracy is $\sigma_s = \sigma_n = 390$ ft. The corresponding values of the Buffer Zone width of 3850 ft and the Normal Operating Zone width of 5000 ft can be obtained from Fig. 3-6 and 3-7, respectively. The sum of these two zones with the 300 ft miss distance is 9150 ft, approximately the 9120 ft (1.5 nmi) separation standard specification. This example has only considered one set of subsystem parameters; families of curves must be generated to span the ranges of all subsystem parameters to establish the subsystem requirements.

If the resulting curve of separation standard versus position accuracy lies entirely above the value of the specified separation, Q_s^*, there is no value of position accuracy which will yield the desired separation. That is, it is not possible to find a position accuracy which, together with the other subsystem parameters, can support the desired separation standard and the desired safety performance level.

An example of this is illustrated in Fig. 3-8; with the subsystem parameters listed on the graph, a separation standard of 1 nmi cannot be achieved regardless of the accuracy of the surveillance and navigation subsystems.

The procedure used to establish the subsystem requirements is essentially the same as discussed above. It has been modified in that the full range of navigation velocity accuracy $\sigma_{\dot{n}}$, and navigation update interval, τ_n, were not utilized. A preliminary analysis indicated that the separation standard is relatively insensitive to variations in those parameters. Thus, the navigation velocity accuracy ($\sigma_{\dot{n}}^*$) was taken to be 10 fps and the navigation update interval, τ_n, was fixed at 5 sec. Sensitivity data showing the effects of varying $\sigma_{\dot{n}}$ and τ_n on the separation standard are presented in the latter part of this section.

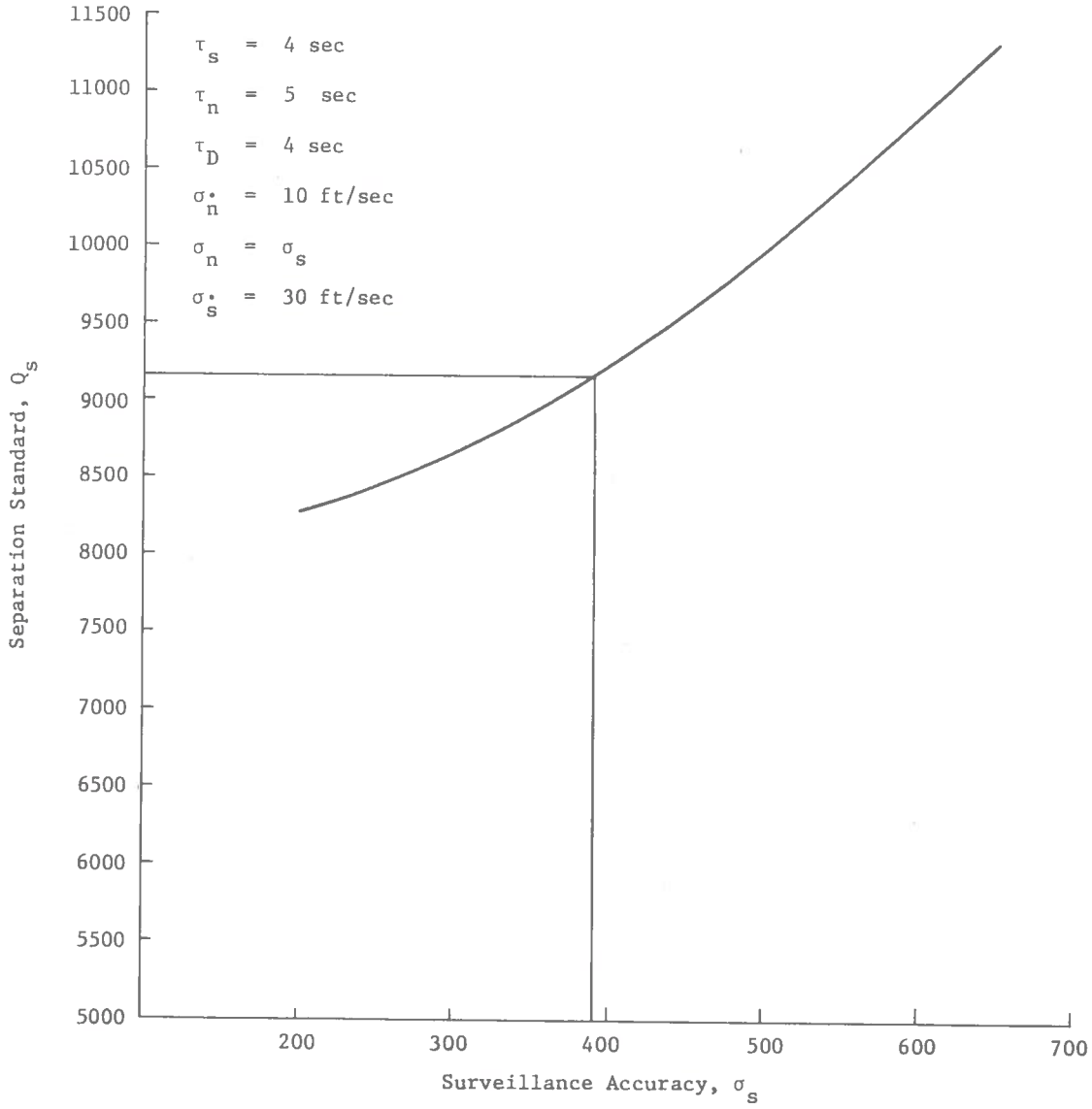

Fig. 3-8. Example of Separation Standard Vs. Surveillance Accuracy

3.1.2.2 Establishing the Terminal Area Subsystem Requirements

A family of curves has been generated to show the range of the Buffer Zone width, W_B, as a function of the surveillance position accuracy for surveillance velocity accuracy, $\sigma_{\dot{S}}$, ranging from 10 to 50 fps and for surveillance update interval, τ_S, varying from 2 to 12 sec in 2-sec increments. One such plot, for $\tau_S = 4$ sec is shown in Fig. 3-9. The same subsystem parameter values are used in the Track Model to establish the width of the Normal Operating Zone, W_N. Instead of forming a similar plot depicting W_N as a function of position accuracy, values of the separation standard (i.e., $W_N + W_B + W_M$) are plotted on the graph of W_B versus σ_S, at the intersection of the σ_S = constant and $\sigma_{\dot{S}}$ = constant. Figure 3-9 depicts the curve of $Q_S = 1.5$ nmi which defines the loci of all possible $\sigma_S, \sigma_{\dot{S}}$ combinations that yield the required separation standard for the condition that $\tau_S = 4$ sec. For each point on the iso-Q_S loci, the value of the position accuracy is determined on the abscissa, while the value of the surveillance velocity accuracy can be interpolated from the family of iso-$\sigma_{\dot{S}}$ curves. The value on the ordinate is the width of the Buffer Zone for the given conditions. The value of the Normal Operating Zone can be readily obtained by

$$W_N = 9120 - 300 - W_B \text{ (ft)} \tag{7}$$

The family of curves relating all the subsystem variables is shown in Fig. 3-10. Each curve represents the $\sigma_S, \sigma_{\dot{S}}$ combinations which support the specified separation standard of 1.5 nmi for its corresponding surveillance update interval. The values of surveillance velocity accuracy are noted along each curve. The investigation revealed that there are no combinations of $\sigma_S, \sigma_{\dot{S}}$ where $\sigma_S \geq 50$ ft and $\sigma_{\dot{S}} \geq 5$ fps (minimum values considered during this study) that can support the specified separation standard if $\tau_S \geq 12$ sec.

The curves indicate the set of subsystem parameters which satisfy the specified separation standard and illustrate the potential trade-offs among position accuracy, surveillance velocity accuracy, and surveillance update interval. Figure 3-11 has been derived from Fig. 3-10 to show the relationships between position accuracy, velocity accuracy, and update interval. The figure shows that position and velocity accuracy requirements can be relaxed if the interval between data samples is reduced. For a fixed update interval, surveillance velocity accuracy requirements are made more stringent as position accuracy requirements are relaxed. For small values of position accuracy (σ_S), the ratio of the increment in the velocity accuracy requirement to the increment in position accuracy (i.e., $|\partial\sigma_{\dot{S}}/\partial\sigma_S|$ is small. This indicates that for a fixed update interval, τ_S, a decrease in position accuracy below a given point does not permit a relaxation in other parameters requirements. From the curves of Fig. 3-11, it is evident that values of position accuracy below 200 ft, for any value of τ_S, does not relax the requirements on velocity accuracy. For larger values of σ_S, $|\partial\sigma_{\dot{S}}/\partial\sigma_S|$ increases very rapidly; at small values of $\sigma_{\dot{S}}$, the ratio $|\partial\sigma_S/\partial\sigma_{\dot{S}}|$ is very small. This illustrates that increasing velocity accuracy does not permit relaxation of position accuracy requirements. The relationship between σ_S and $\sigma_{\dot{S}}$ indicates that operation at either end of the curves is relatively inefficient. The area on the curve inside the dashed lines encloses what appears to be a reasonable combination of subsystem parameters which can support the specified separation.

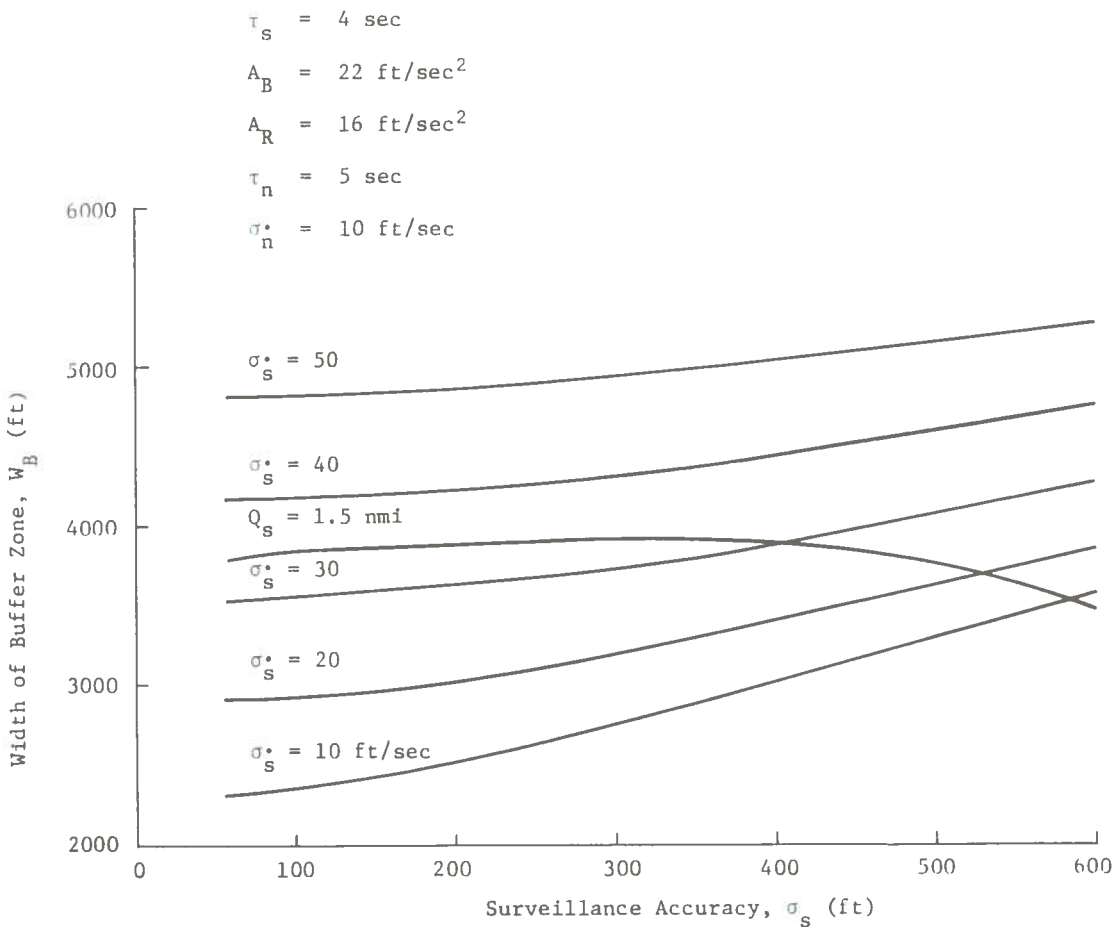

Fig. 3-9. Width of Buffer Zone Vs. Surveillance Accuracies

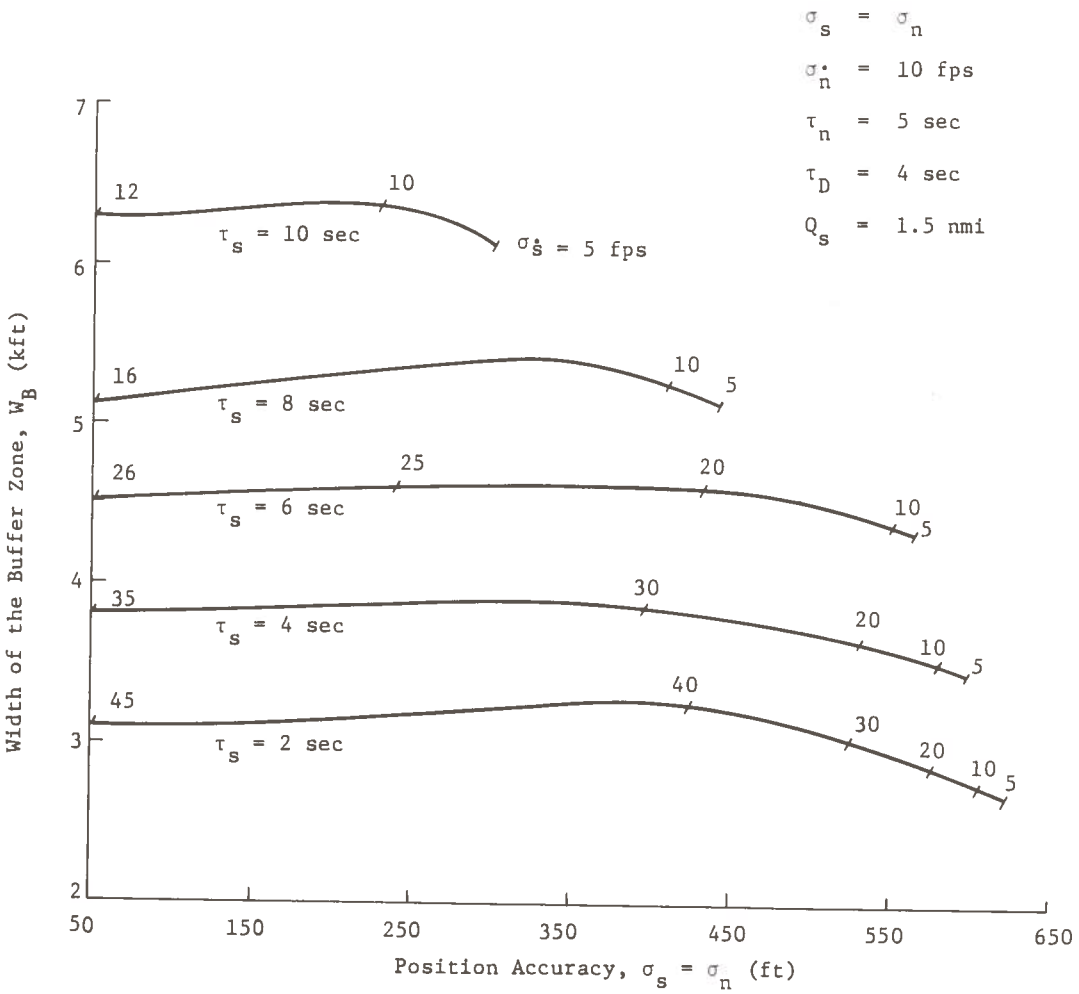

Fig. 3-10. Subsystem Performance Requirements for Terminal Area, Plot of W_B and $\dot{\sigma}_s$ vs. σ_s for Various Values of Surveillance Update Interval, τ_s

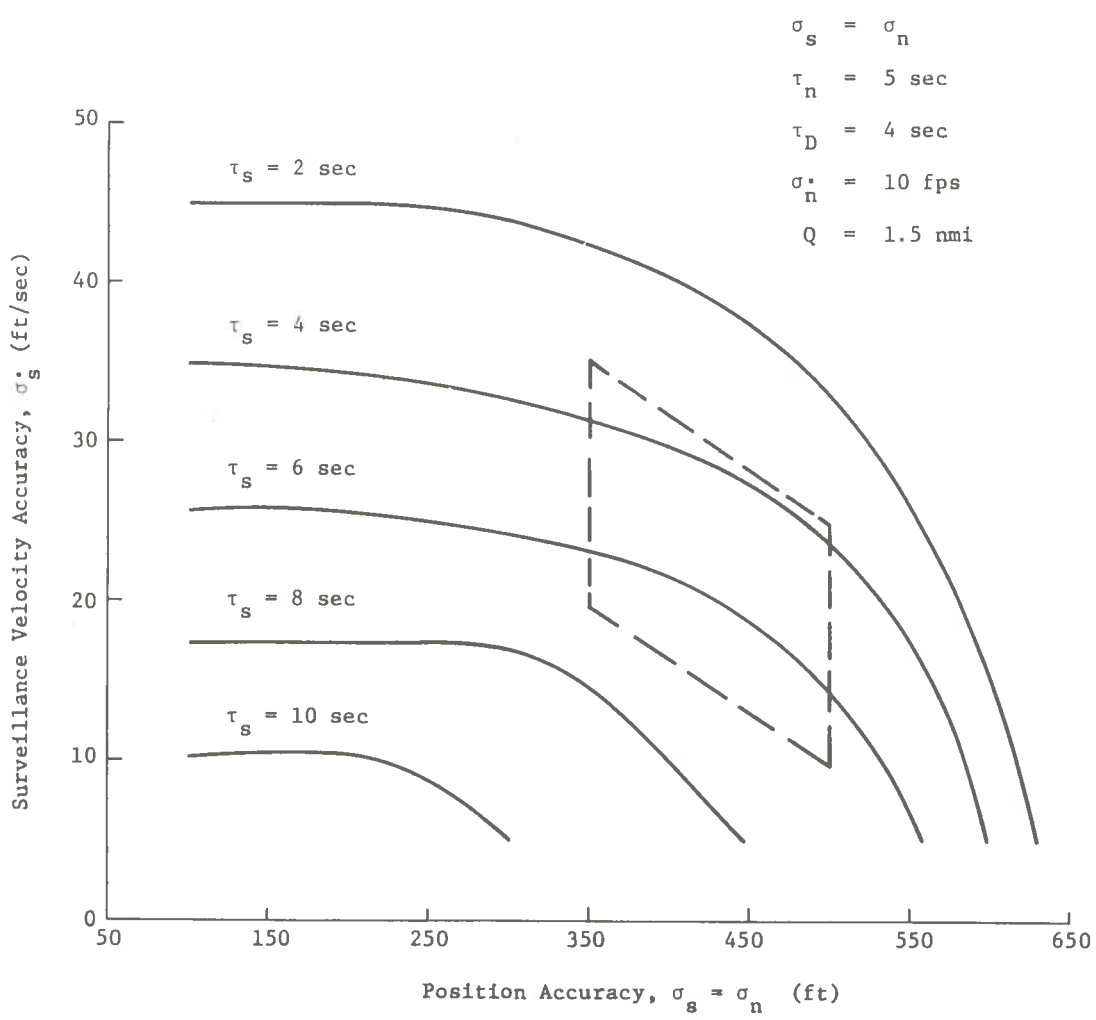

Figure 3-11. Surveillance Velocity Accuracy as a Function of Position Accuracy for Values of τ_s

A similar set of curves is shown in Fig. 3-12 to show position accuracy versus update interval for various velocity accuracies. The curves show that position accuracy must increase as update interval increases. The sensitivity of position accuracy to variations of update interval is quite high; i.e., $|\partial\sigma_s/\partial\tau_s|$ is large. For any given $\sigma_{\dot{s}}$, when τ_s is increased beyond a given point, the position accuracy must increase markedly to maintain the specified separation. For small values of τ_s and σ_s, the ratio $|\partial\sigma_s/\partial\tau_s|$ is small, indicating that decreasing the time between data samples does not permit a large relaxation of position accuracy. These relationships show that operation at either end of the curves is undesirable. The dashed area on the graph encloses what appears to be a reasonable set of subsystem parameters.

A final chart, Fig. 3-13, can be developed showing the relationship between $\sigma_{\dot{s}}$ and τ_s for constant values of position accuracy. Again, the most preferable area of operation is in the central region of the plot where variations in any parameter do not give rise to large changes in the remaining parameters.

The results of the subsystem performance requirements indicate the range of subsystem parameters which can support the specified separation standard. These ranges are depicted in Fig. 3-10. The desired subsystem parameter ranges are defined by the enclosed areas on Fig. 3-11 through 3-13. The subsystem performance requirements are as follows:

(1) Surveillance and navigation position accuracies from 350 to 525 ft

(2) Surveillance velocity accuracy from 10 to 34 ft/sec

(3) A surveillance update interval from 4 to 7 sec

These requirements are based on assumptions that the navigation velocity accuracy is 10 ft/sec and the navigation update interval is 5 sec.

The selection of the regions that established the requirements was based solely on the characteristics of the sets of subsystem parameters which can support the given separation standard. If other information such as cost were available, the subsystem requirements could be developed on the basis of a minimum cost system. Without such additional information, the lack of constraints prohibit a further refinement of subsystem performance.

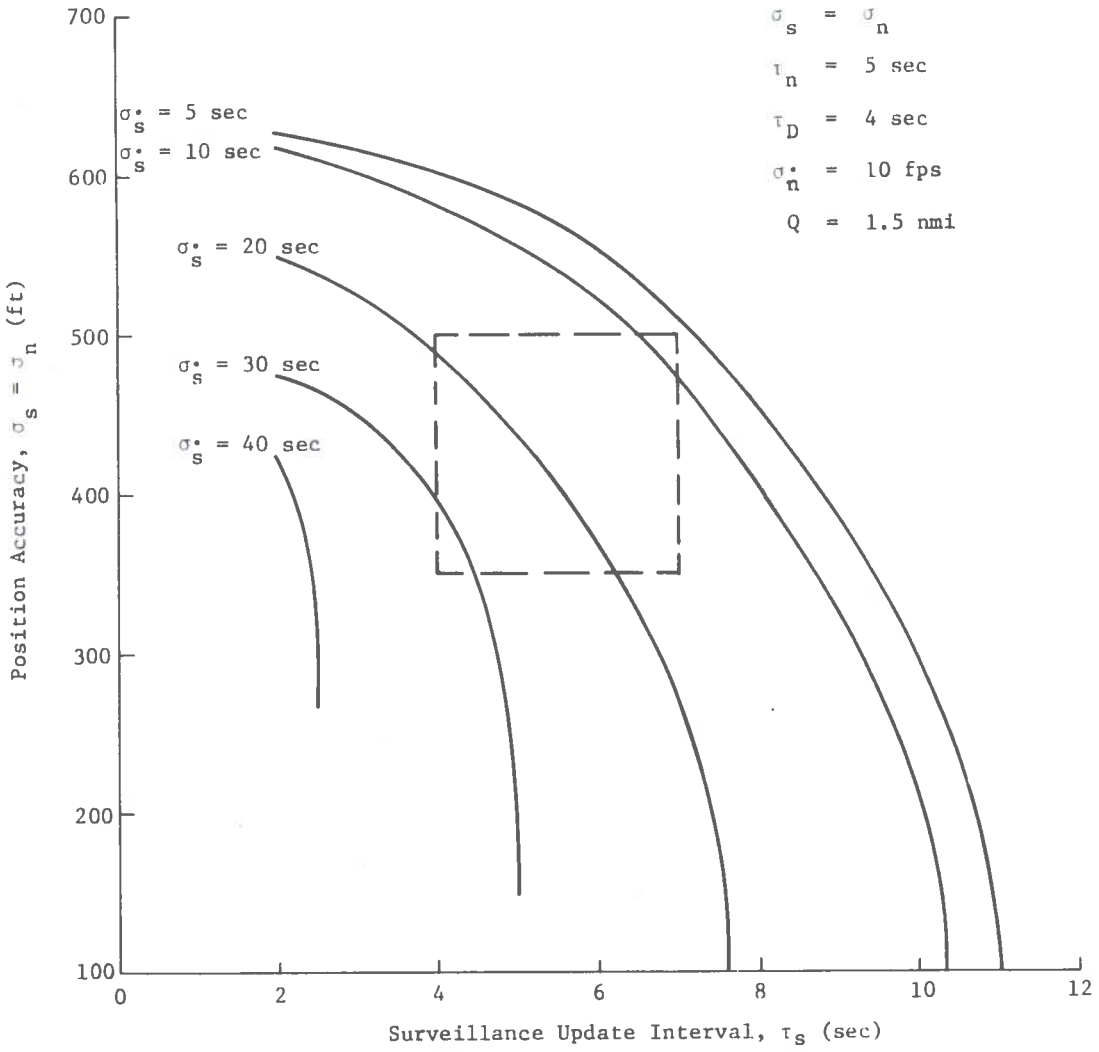

Fig. 3-12. Position Accuracy as a Function of Surveillance Update Interval for a Set of Surveillance Velocity Accuracies

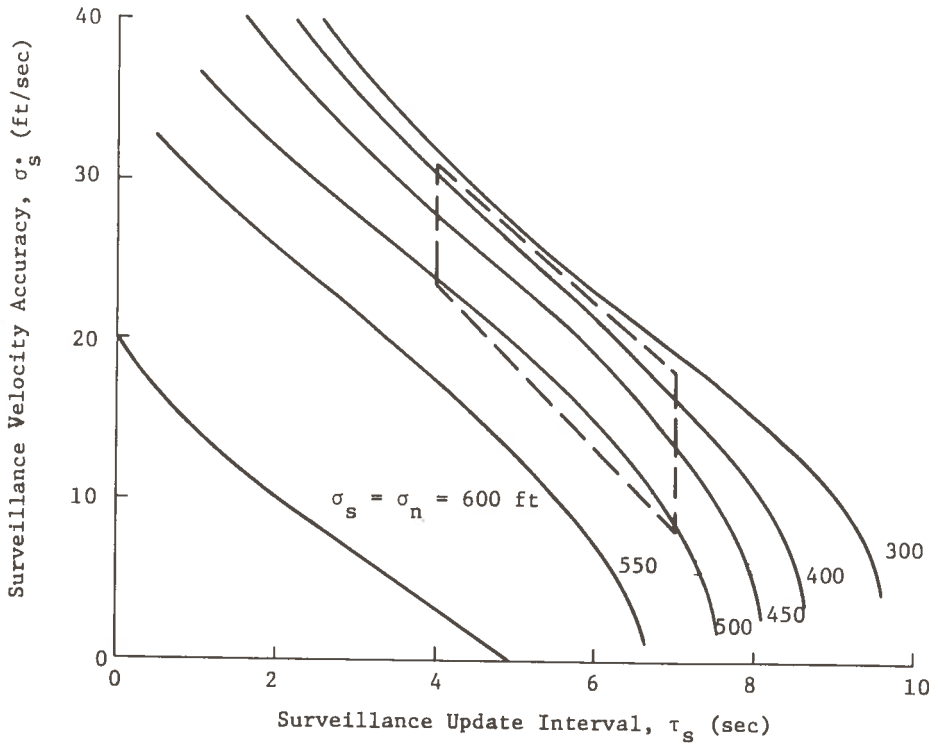

Fig. 3-13. Surveillance Velocity Accuracy Vs. Surveillance Update Interval for Various Position Accuracies

3.1.2.3 Sensitivity Data

The subsystem performance requirements were developed assuming that navigation velocity accuracy and navigation update interval were fixed. Figure 3-14 shows the relationship between surveillance velocity accuracy versus position accuracy for three values of navigation velocity accuracy. The curves illustrate that the subsystem performance requirements are not a strong function of navigation velocity accuracy in the range from 5 to 20 ft/sec. Figure 3-15 illustrates the effect of variations in navigation update interval on position and velocity accuracies. Both the velocity and position accuracies are more sensitive to variations in navigation update interval than do navigation velocity accuracy. This is especially true for small values of velocity accuracy and large values of position accuracy in the region from 5 to 10 sec. The sensitivity of the requirements to τ_n is much smaller than to surveillance update interval, τ_s. Relaxation of the navigation update interval from 5 to 10 sec would not alter the subsystem performance requirements.

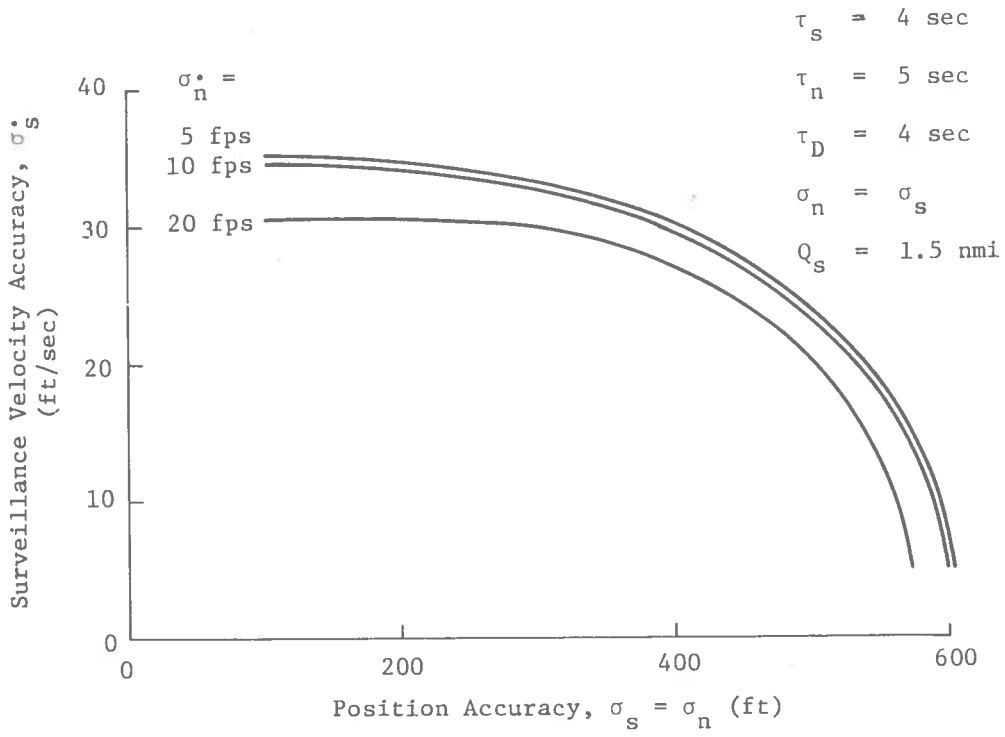

Fig. 3-14. Surveillance Velocity Accuracy vs Position Accuracy for Various $\sigma_n^\bullet$

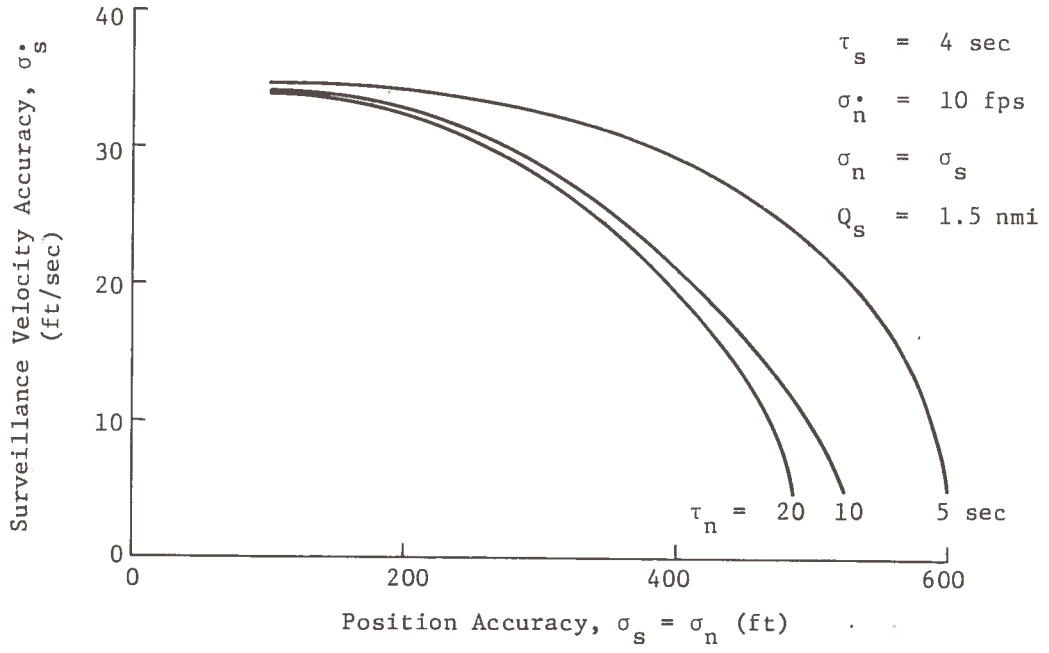

Fig. 3-15. Surveillance Velocity Accuracy as a Function of Position Accuracy for Various τ_n

The final sensitivity data concern the impact of changing the specified separation standard without altering the level of safety. Figure 3-16 illustrates the variations in position and velocity accuracies for different separation standards. The remaining subsystem parameters have been fixed with surveillance update interval τ_s = 4 sec, navigation update interval τ_n = 5 sec, navigation velocity accuracy $\sigma_n^{\bullet}$ = 10 fps, and system delay time τ_D = 4 sec. The surveillance and navigation accuracies are assumed to be identical to provide a fail-operational system.

The result of the sensitivity analysis is that the position and velocity accuracies can both be relaxed as the separation standard increases. As expected, the subsystem performance requirements are a strong function of the separation standard.

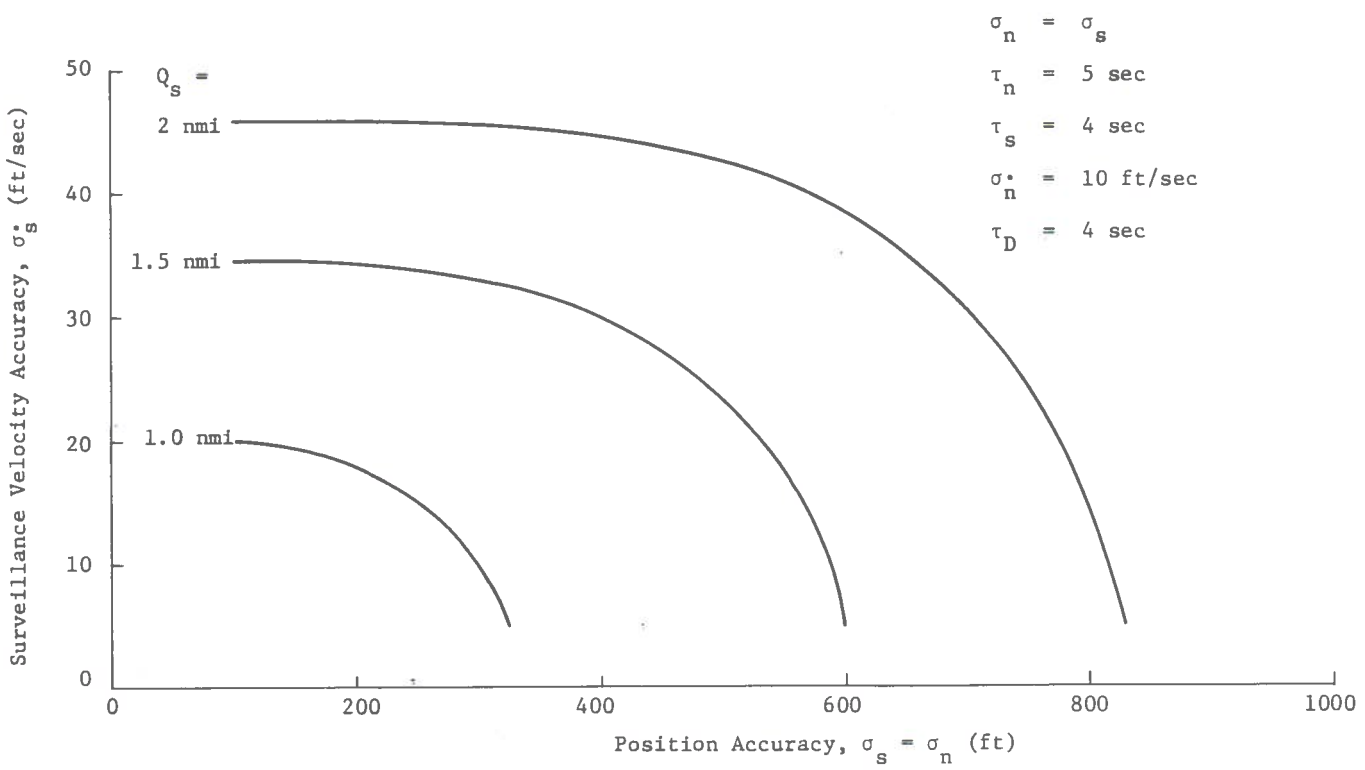

Fig. 3-16. Surveillance Velocity Accuracy as a Function of Position Accuracy for Various σ_s

3.2 Enroute Area Requirements

While the terminal areas of the airspace structure are characterized by high density air traffic, the enroute areas are, in general, sparsely populated. This is due primarily to the greater amount of available space. As a result, capacity and delay are not the primary system performance measures for enroute operations. The selection of an operating point in enroute areas cannot be based on the same constraints as in terminal areas. The primary relationship considered for enroute operations concerns aircraft separation standards and safety level. Even with the increased demand postulated for future systems, the enroute airspace will not be capacity limited. This is especially true if area navigation techniques are utilized. The separation distances used in the present system and the present safety level are assumed sufficient for future systems.

The development of enroute requirements is based on separation standards of 5, 7, and 10 nmi. The safety provided by the system is the same as that specified for terminal area operations; i.e., assuming a return acceleration of 16 ft/sec^2, aircraft will be protected against blunder accelerations up to 22 ft/sec^2.

Since the system is required to be fail-operational, the surveillance and navigation position accuracies are assumed to be the same. In the event that one subsystem fails to provide data, the data can be obtained from the other subsystem, thus maintaining the same level of performance. Since the navigation velocity errors (true airspeed) are essentially constant over a wide range of aircraft velocity, the navigation velocity accuracy is assumed to range from 10 to 50 fps, even though aircraft in the enroute areas have greater speeds than in terminal areas. The velocity errors resulting from true airspeed calculations are assumed to be at most 5 knots; the remainder of the error stems from inaccurate wind measurement data. The surveillance velocity errors are assumed to be the same as the navigation velocity errors, independent of the surveillance velocity estimation technique.

The procedures used in establishing the enroute requirements are the same as those used for the terminal area requirements. The buffer zone model was used to determine the width of the buffer zone as a function of position accuracy for various values of surveillance velocity accuracies and surveillance update rates. The Track Model is used to determine the width of the normal operating zone for the same set of subsystem parameters. The value of the miss distance is assumed to be 300 ft. The separation standard, which is the sum of the buffer zone, the normal operating zone, and the miss distance, is then plotted as a function of position accuracy.

The results of the analysis are shown in Fig. 3-17. The plot indicates the values of position accuracies required to maintain a constant level of safety for various separation standards. The curve illustrates that the requirements are independent of the velocity accuracy and the surveillance update interval. It also shows that the separation standard is essentially a linear function of position accuracy.

For surveillance update intervals from 6 to 8 sec, velocity accuracies from 10 to 50 fps, and a navigation update interval of 5 sec, the required surveillance and navigation accuracies are (1) 2200 ft (1-σ) for a separation of 5 nmi, (2) 3300 ft (1-σ) for 7 nmi separations, and (3) 4900 ft (1-σ) for a separation standard of 10 nmi.

Since many of the aircraft operating in enroute areas are either aircarriers or highly equipped general aviation aircraft, their navigation performance capabilities could be better than assumed. This study investigated the effect on surveillance position accuracy requirements when the navigation position accuracy was fixed at σ_n = 1000 ft. The results of the investigation are shown in Fig. 3-18 along with the values chosen for the other subsystem parameters. As in the previous case, where $\sigma_s = \sigma_n$, the surveillance position accuracy increases almost linearly with increasing separation standards. The 1-σ requirements on surveillance position accuracy for Q_s equal to 5, 7, and 10 nmi are 3000, 4700, and 7350 ft, respectively.

Since it is possible that the surveillance position accuracy for enroute areas will be improved in the reasonably near future, the effect on navigation position accuracy requirements of a fixed surveillance accuracy of σ_s = 1000 ft was also investigated. Figure 3-19 shows the result of the analysis. The navigation accuracy requirement is, as expected, nearly linear with separation standard. The 1-σ navigation position accuracy requirements are 3400 ft for a 5 nmi separation, 5200 ft for a 7 nmi separation, and 7900 ft for a 10 nmi separation standard.

The accuracy of the surveillance and navigation subsystems can be degraded in enroute airspace from that required for terminal operations and still maintain the required safety level. When one subsystem performance is fixed, the performance of the other subsystem can be degraded. The allowable amount of degradation is essentially the same, regardless of which subsystem is considered fixed.

A system with unequal surveillance and navigation accuracies would still be able to meet the enroute separation standards requirement under normal operating conditions, as evidenced in Figures 3-18 and 3-19. In the event that the system with the highest accuracy failed (e.g., the navigation system for Figure 3-18 or the surveillance system for Figure 3-19), the system would not be able to meet the required separation standards. If the surveillance system failed and surveillance was performed using data linked navigation information (Figure 3-19), the surveillance accuracy would be the same as the navigation accuracy (i.e., 3400 ft), assuming a 5 nmi separation standard. Under these conditions ($\sigma_s = \sigma_n$ = 3400 ft) the system could only support a 7 nmi separation standard (see Figure 3-17) at the desired level of safety. This increased enroute separation would degrade the capacity and delay performance of the system. Equal surveillance and navigation accuracies permit the system to maintain the same operational performance under failure conditions as under normal conditions, thus providing a fail-operational capability.

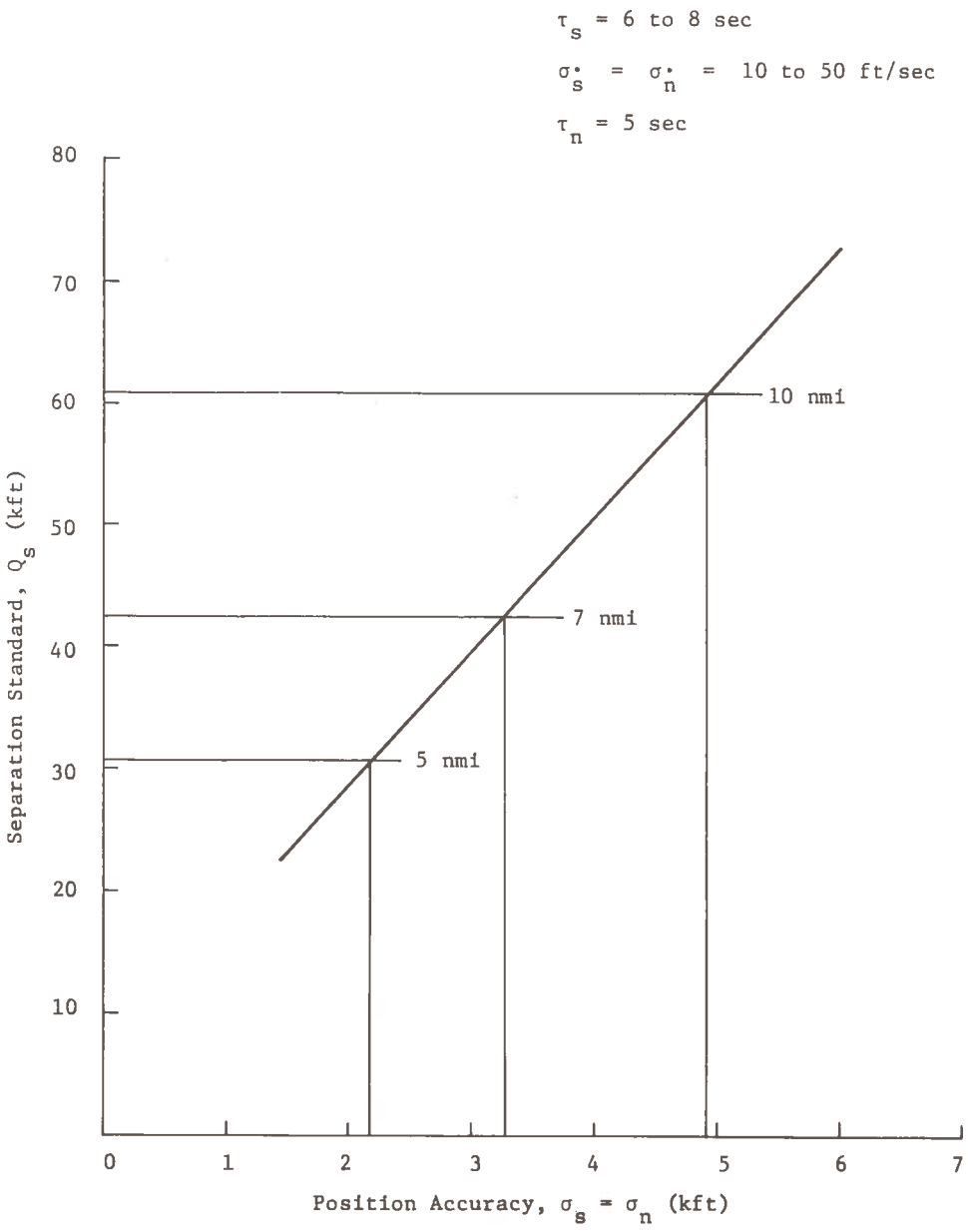

Fig. 3-17. Position Accuracy Requirements to Obtain Separation Standards for Enroute Operations

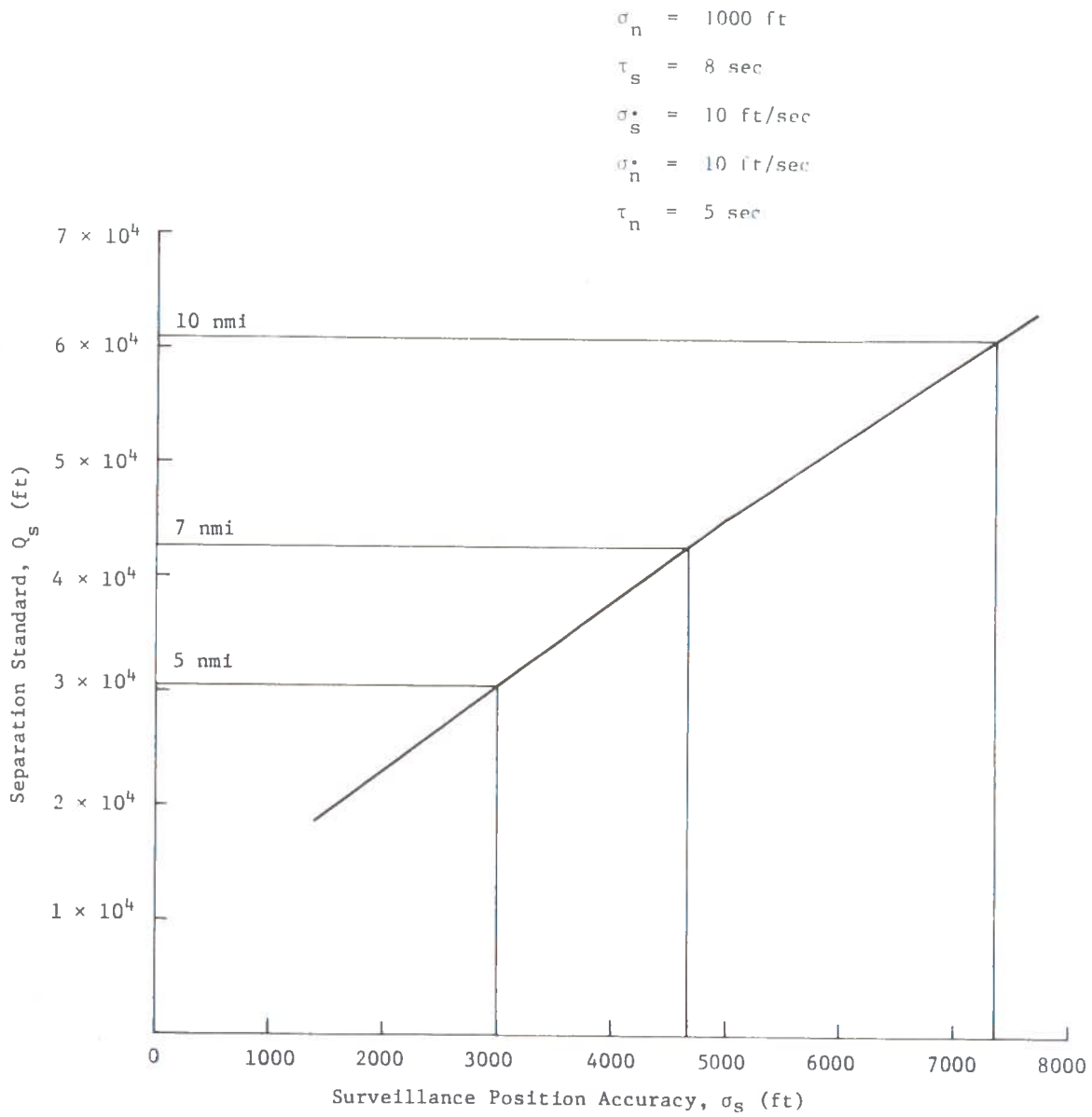

Fig. 3-18. Enroute Requirement for Fixed Navigation Accuracy

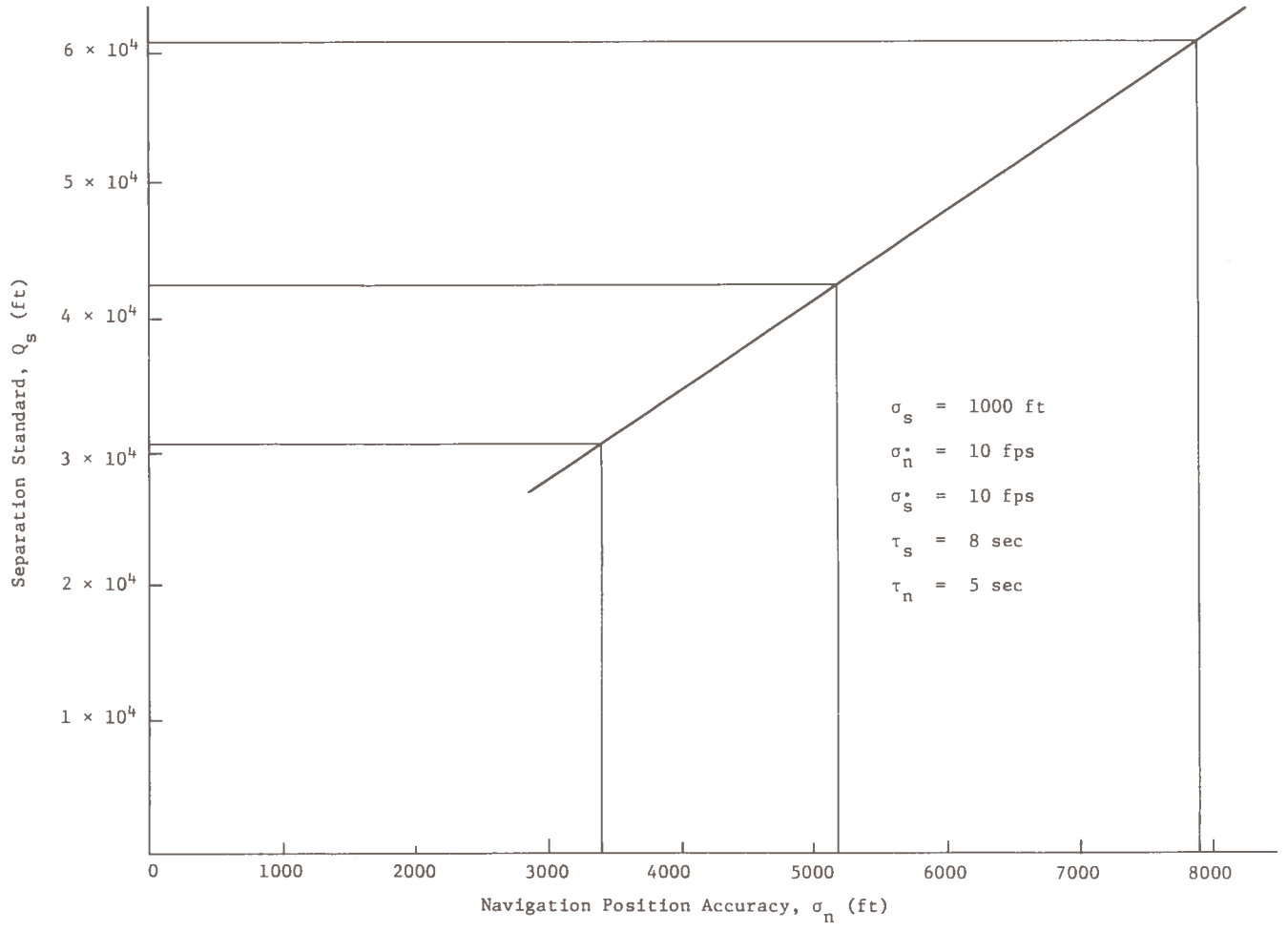

Fig. 3-19. Enroute Requirement for Fixed Surveillance Accuracy

4. SUITABILITY OF VIRTUAL VOR (VVOR) OR SATELLITE NAVIGATION FOR APPROACH GUIDANCE

This section presents a description of the Virtual VOR navigation concept. It discusses the methodology used to establish the navigation accuracy and update rate required for approach guidance. This section also presents a description of the models used in the suitability analysis. Finally, it defines the approach guidance requirements and discusses the suitability of VVOR and Satellite Navigation concepts.

4.1 Virtual VOR

Virtual VOR is a navigation scheme based on ground processing of surveillance information; it is called virtual VOR due to its operational similarity to the present VOR system from a user viewpoint. VVOR provides an area navigation (RNAV) capability, distance measuring capability (equivalent to DME), and instrument approach to airports.

The VVOR system employs a latitude/longitude grid with intersections spaced 1 $\widehat{\text{min}}$ apart. This is equivalent to covering the entire CONUS with 5,500,000 VOR sites approximately 1 nmi apart. The ground processor must obtain information from each user concerning the user's origin and distination (selected VVOR grid points). This allows the system to develop a desired course line between the origin and destination. The processor determines the aircraft position from the surveillance information and provides the user with position data and course deviation as guidance information. In an approach to an airport, the runway threshold is used as the destination VVOR ground point. The user informs the system that approach information is needed. The ground system defines a straight line on the runway heading that terminates on the runway threshold; this imaginary line is the equivalent of the ILS localizer used in the present system. The aircraft receives three-dimensional position (or derives altitude from an onboard source), range and course deviation, or steering information. Standard procedures dictate the proper aircraft altitude as a function of range. The user flies along the course line to touchdown; this process is equivalent to the present glide path procedure. The navigation information is transmitted to the user at a rate sufficient to minimize build-up of errors.

The accuracy of a VVOR system is dependent upon the specific mechanization utilized. The lower bound on the system accuracy is determined by the accuracy of the surveillance subsystem and the rate at which the user receives navigation information.

4.2 Methodology

The requirements for approach to an airport are a function of the visibility range to the threshold and the characteristics of the user aircraft. The aircraft characteristics involved in determining the window defined by the aircraft control limits include: (1) the aircraft velocity, (2) the maximum horizontal and vertical turn rates, (3) the maximum angular acceleration, and (4) the aircraft response times. The aircraft control window or the delivery window is established using a landing phase model. The delivery window routine calculates the window based on the aircraft characteristics and the distance from touchdown. A second routine in the landing phase model, the integration routine, establishes the cross-track and vertical position-keeping errors the user can be allowed to have and still intersect the delivery window with a specified probability. The revised Track Model, which simulates the navigation control system, is used to determine the position-keeping error resulting from errors in the aircraft's position and velocity information. The Track Model also determines the effect of varying the interval between navigation data samples on the position keeping errors. This approach determines the navigation accuracy and update rates required to insure (within a specified probability) that an aircraft can be inserted in the delivery window. The requirements are independent of the mechanization used to provide the navigation data. VVOR or satellite navigation can be used to provide the navigation data, as long as it meets the approach requirements.

4.3 Landing Phase Model

The landing phase of flight is primarily concerned with the task of guiding an aircraft to touchdown on the desired runway. Because runway dimensions are relatively small, high degrees of precision may be required. In some large airports, instrument landing systems are provided to meet these landing requirements. Thus, even in weather conditions which degrade visibility, the safe and expeditious handling of landing-phase demand may be accomplished. In the larger number of cases, however, auxiliary landing instrumentation is not available. The basic air traffic surveillance and/or navigation systems and range-limited visual observation by the pilot are the only sources of guidance information.

The visual ability of pilots will not in general be improved by future generation ATM systems. The various system concepts proposed, however, do predict improved accuracies in surveillance and navigation. In addition to the general improvements in capacity, delay, and safety levels, visibility-limited landing-phase operation should be enhanced. Thus, without the benefit of auxiliary landing systems, the ATM system may be capable of landing aircraft in weather conditions previously considered impossible. The requirements for approach guidance for various degraded visibility conditions are discussed in this section.

4.3.1 The Delivery Window

The basic approach used in establishing subsystem requirements for landing in limited visibility is the defining of a "delivery window." Runway-approaching aircraft which pass through this conceptual surface in space can be guided directly to the runway. Aircraft which miss the window will not be able to land safely without re-entering the traffic pattern. The basic system requirement is to minimize the number of aircraft that miss the delivery window.

The size and shape of the window are dependent upon the particular visibility condition, glide-slope angle, and nominal aircraft performance characteristics: velocity, maximum turn rate, and maximum rate-of-change turn rate. The window is at a fixed distance from the runway touchdown point, namely, the visibility range determined by weather conditions.

The problem of determining the window for any given case can be viewed as the determination of the amount of errors an aircraft can withstand in flying an along-track distance equal to the visibility range. If the time of touchdown is taken as $t = 0$ and the time scale is reversed, the window under consideration is the set of attainable points on the boundary of the cone extending from the touchdown point. In the glide-slope plane, heading angle restrictions must be met. At touchdown, it is required that the aircraft velocity be aligned with the runway, that is, its heading angle with respect to the runway axis and the associated angular rate of change, must be zero. At the point where the aircraft intersects the window, it is assumed that the heading angle is also zero. Window-to-touchdown trajectories allowed are those for which heading angle magnitude never exceeds 90 deg; the states of interest are those in which aircraft can land without circling. Except in cases of very low visibility, the width of the runway is small when compared to the width of the window. Thus, it is considered that aircraft are guided to the center of the runway; the error introduced by this assumption is very small.

In the vertical plane, it is assumed that the aircraft must stay within a correctable deviation above its nominal 3-deg glide-slope descent plane. Aircraft below the 3-deg glide-slope plane can fly level until they intersect this plane and can assume the necessary glide slope from this point of interception. A maximum instantaneous descent angle is defined, as is the rate of change of descent angle.

Simplified aircraft dynamics are assumed in deriving any particular delivery window. The velocity of the aircraft is taken to be constant through the landing phase.

Constraints concerning horizontal deviation from the desired glide-slope trajectory are considered first. It is assumed that during the interval of consideration, from window to touchdown, the aircraft never has a negative velocity component along the desired straight-in trajectory; i.e., aircraft which turn back will not be considered. The model assumes that optimal control is applied such that once visual contact of the runway has been established, the pilot will initiate position correction immediately and try to align the aircraft to the straight-in trajectory in the shortest possible time. The derivation of the window involves calculation of the minimum along-track distance the aircraft will travel in the time the correction is completed.

In the vertical direction, the turn rate and turn rate changes correspond to characteristics of the aircraft climb or dive angle. The problem is primarily concerned with aircraft having vertical deviation above the desired glide slope. This deviation may result from either altitude information inaccuracy or horizontal along-track position inaccuracy. As with the lateral case, an along-track distance corresponding to the correction of vertical deviation is calculated. This calculation again assumes optimal pilot and aircraft response. It is further assumed that the glide slope is small enough for small-angle approximations. A nominal value of 3 deg is used in the analyses. Vertical deviation is then assumed to be the same as perpendicular deviation from the glide slope. Additionally, the projection of along-track distance upon the ground plane is assumed to be equal to the along-track distance itself.

In general, an aircraft will have both lateral and vertical deviations. The resultant along-track distance required to correct both deviations is taken as the root-sum-square of the individual along-track distances required to correct the two components. The flying time is also assumed to be root-sum-square of the individual time required.

The delivery window is symmetric about the vertical plane passing through the runway center line. That is, identical approach deviations from either side yield identical requirement magnitudes. The delivery window is not symmetric about the glide-slope plane, however, primarily because an aircraft below the desired glide slope does not present a significant problem in correcting its trajectory.

4.3.1.1 Flow Diagram of Model

A general flow diagram of the window-deriving routine of the model is shown in Fig. 4-1.

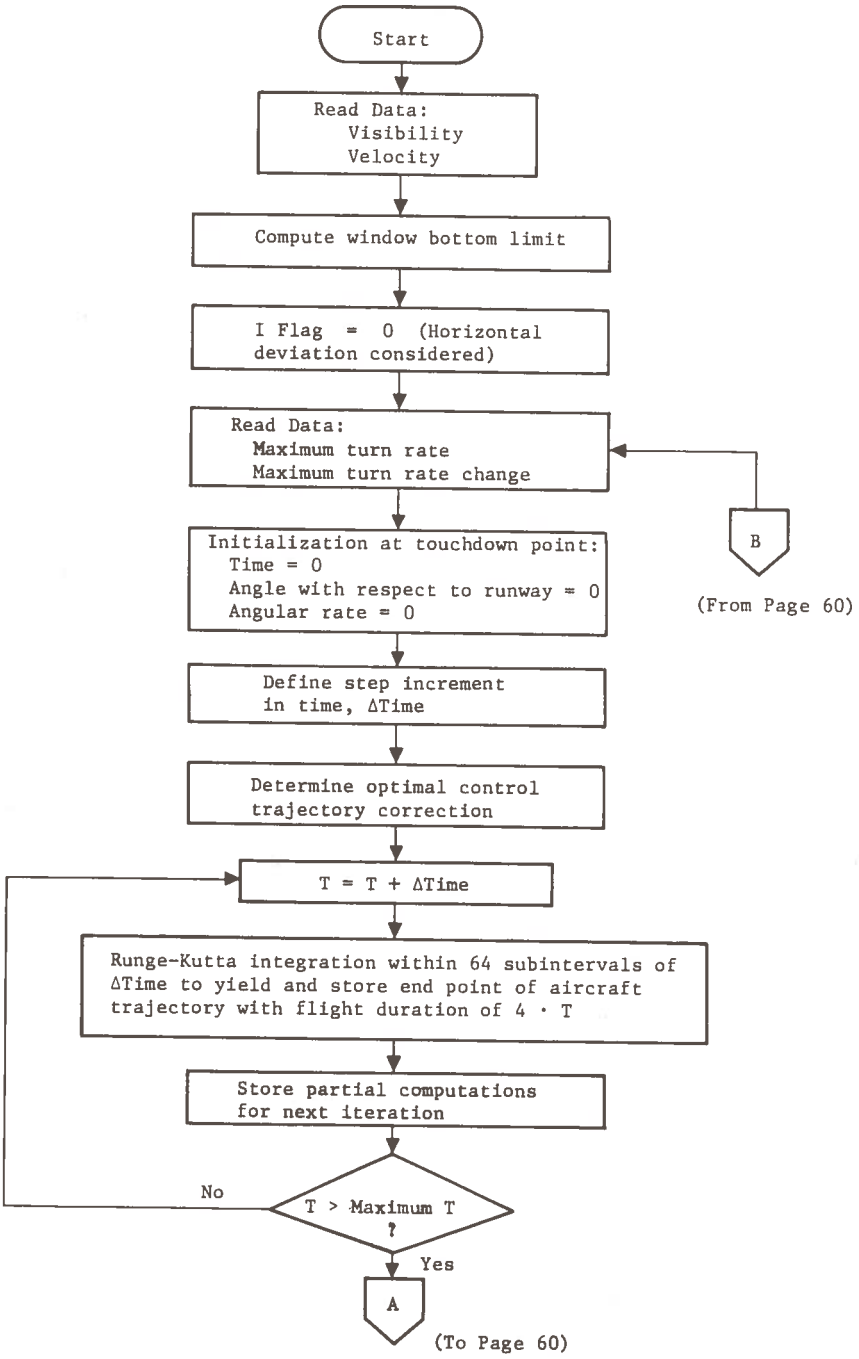

Fig. 4-1. Delivery Window Flow Diagram

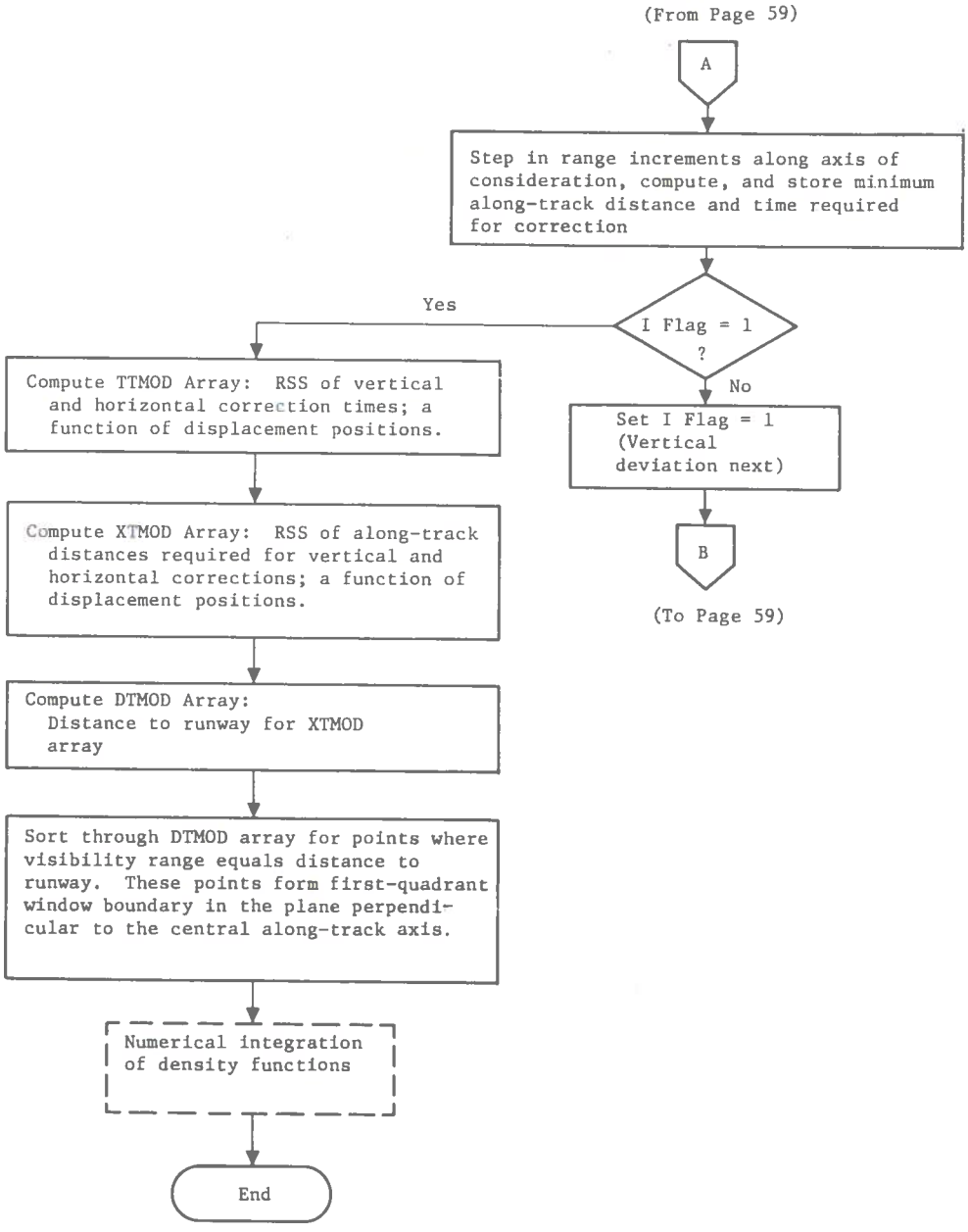

Fig. 4-1. (Continued)

It should be noticed that the bottom limit of the window is computed as one of the initial steps. Because aircraft below the glide-slope plane can easily correct by flying level or at a lesser slope until intersection with the desired glide slope, the window bottom limit is assumed to be a constant distance above the ground. For the 3-deg glide slope used in this analysis, the window bottoms are at the following altitudes:

VOR (6080 ft visibility): 50 ft

Category I (2600 ft visibility): 20 ft

Category II (1200 ft visibility): 0 ft

4.3.1.2 Landing Window Diagrams

The surface of the landing window is composed entirely of points at a distance d, the visibility range, from the landing end of the runway. Thus, it is a portion of a spherical surface with radius d. Figure 4-2 shows a sketch of a landing window with exaggerated glide-slope angle.

The general shape of the window can be represented by a two-dimensional diagram of the projection upon a plane perpendicular to the central glide slope path. This is shown in Fig. 4-3 for a visibility range of 6080 ft. The given velocity in this case is 90 knots, maximum descent angle is 5 deg, maximum horizontal and vertical turn rates are 6 and 2 deg/sec, respectively, and maximum turn rate changes are 2 and 1 deg/sec^2, respectively.

The window is symmetric about the vertical axis of the diagram. Below the glide-slope plane, it is assumed that the window projection is rectangular, since vertical deviation in this direction does not present significant limitations. The lower window boundary is assumed to be 50 ft above the ground for this 6080-ft visibility category.

The major task in deriving the window for any set of conditions is then concentrated upon that portion representing deviation above the glide-slope plane. The model computes the boundary in the upper right quadrant. Curves of this portion of the window are shown in Fig. 4-4 through 4-6.

In Fig. 4-4, window boundaries are shown for a family of different visibility ranges. For this figure, aircraft velocity is 90 knots, maximum descent angle is 5 deg, maximum turn rates are 6 deg/sec horizontal and 2 deg/sec vertical, and maximum turn rate changes are 2 deg/sec^2 horizontal and 1 deg/sec^2 vertical. It is seen from the figure that the window diminishes in size as visibility range decreases. Also shown in the figure are lines representing loci of points requiring given deviation-correction times. These lines are essentially straight and vertical. Thus, it is the horizontal or cross-track deviation which dominates in determining correction time. This, of course, is seen from the fact that much larger deviation is allowed in the horizontal direction than in the vertical.

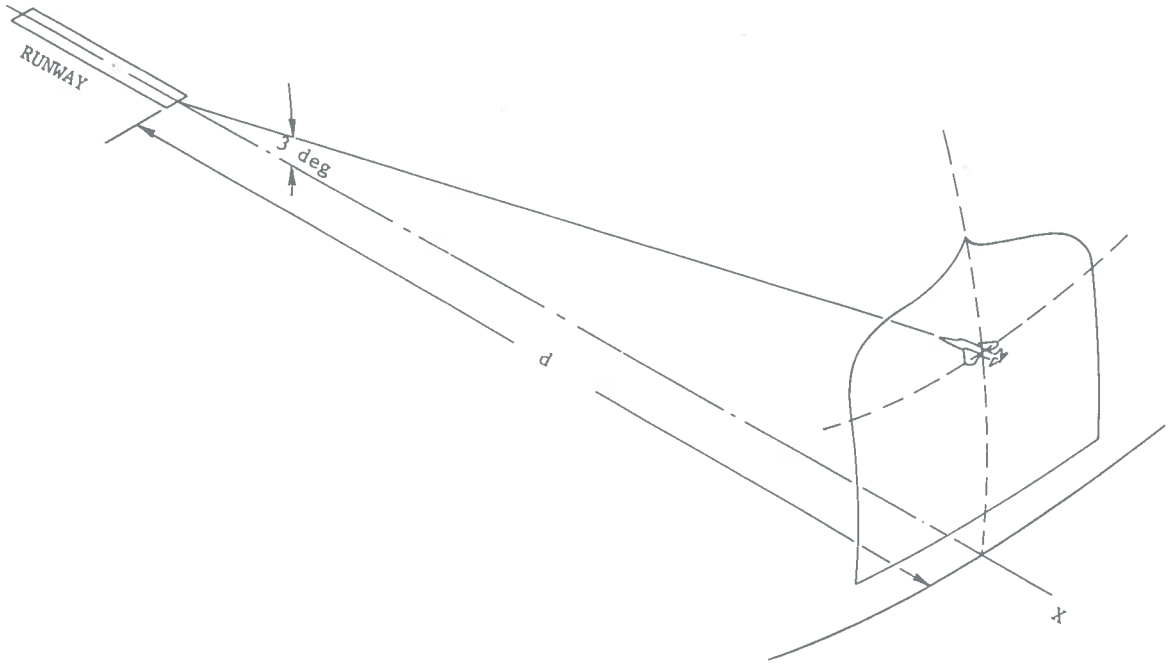

Fig. 4-2. Typical Approach Delivery Window

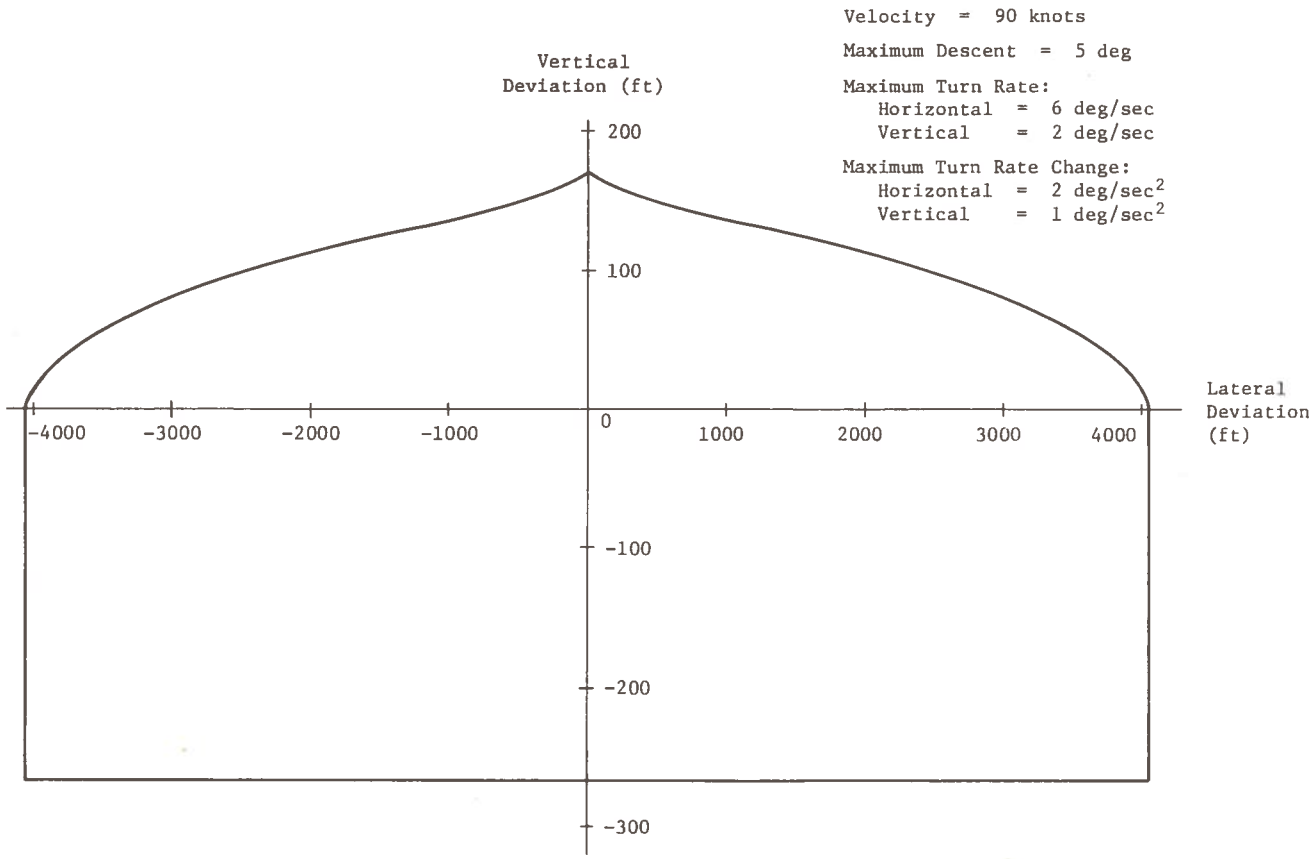

Fig. 4-3. Projection of Window Upon Plane Perpendicular to Center Path of 3-Deg Glide Slope

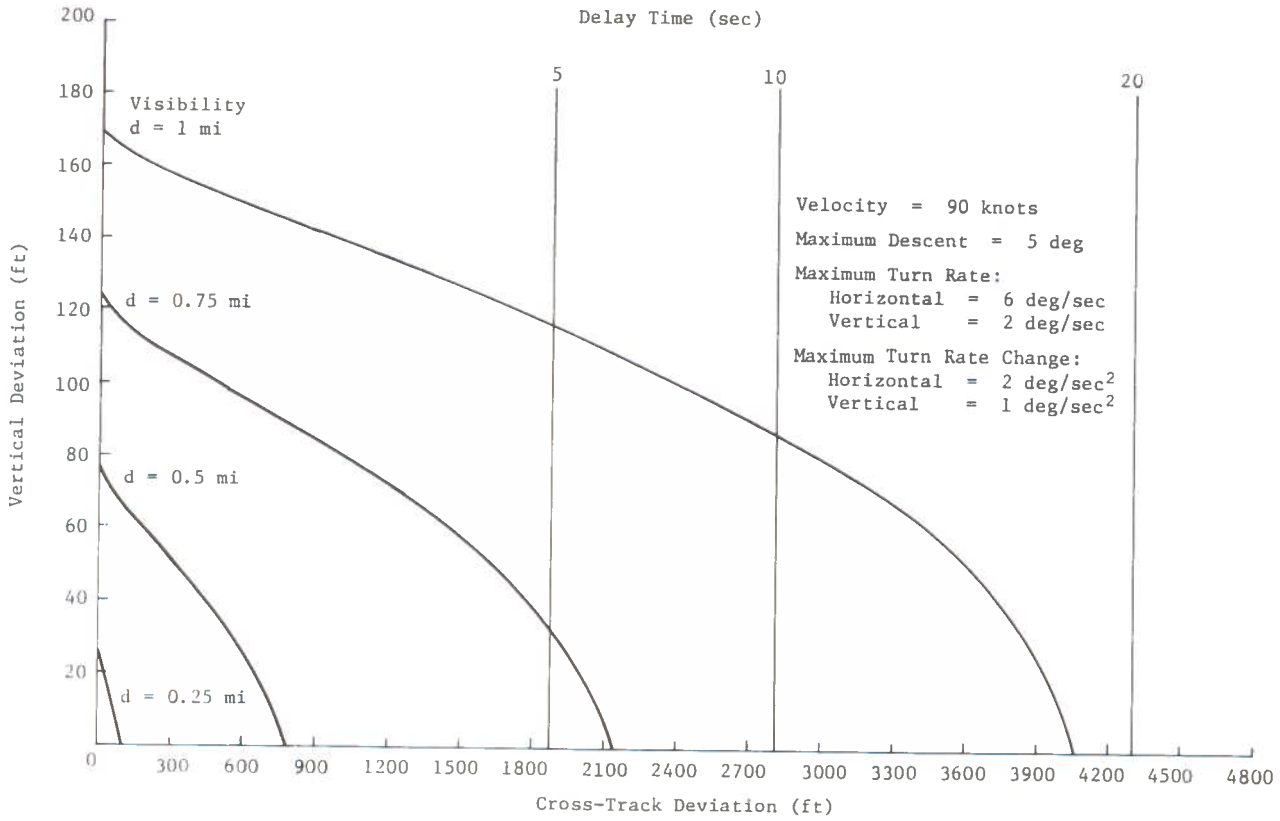

Fig. 4-4. Landing Window (Upper Right Quadrant)

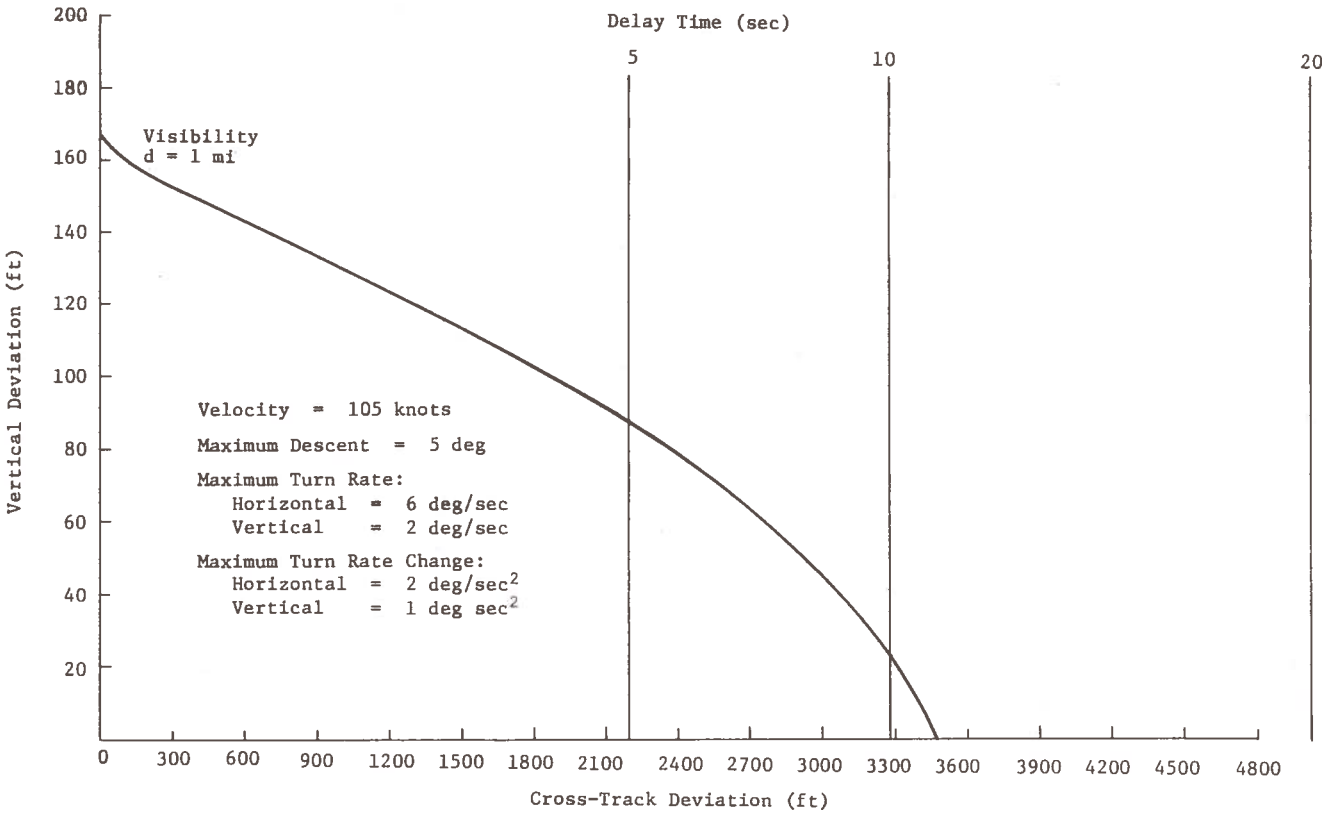

Fig. 4-5. Landing Window for Increased Velocity

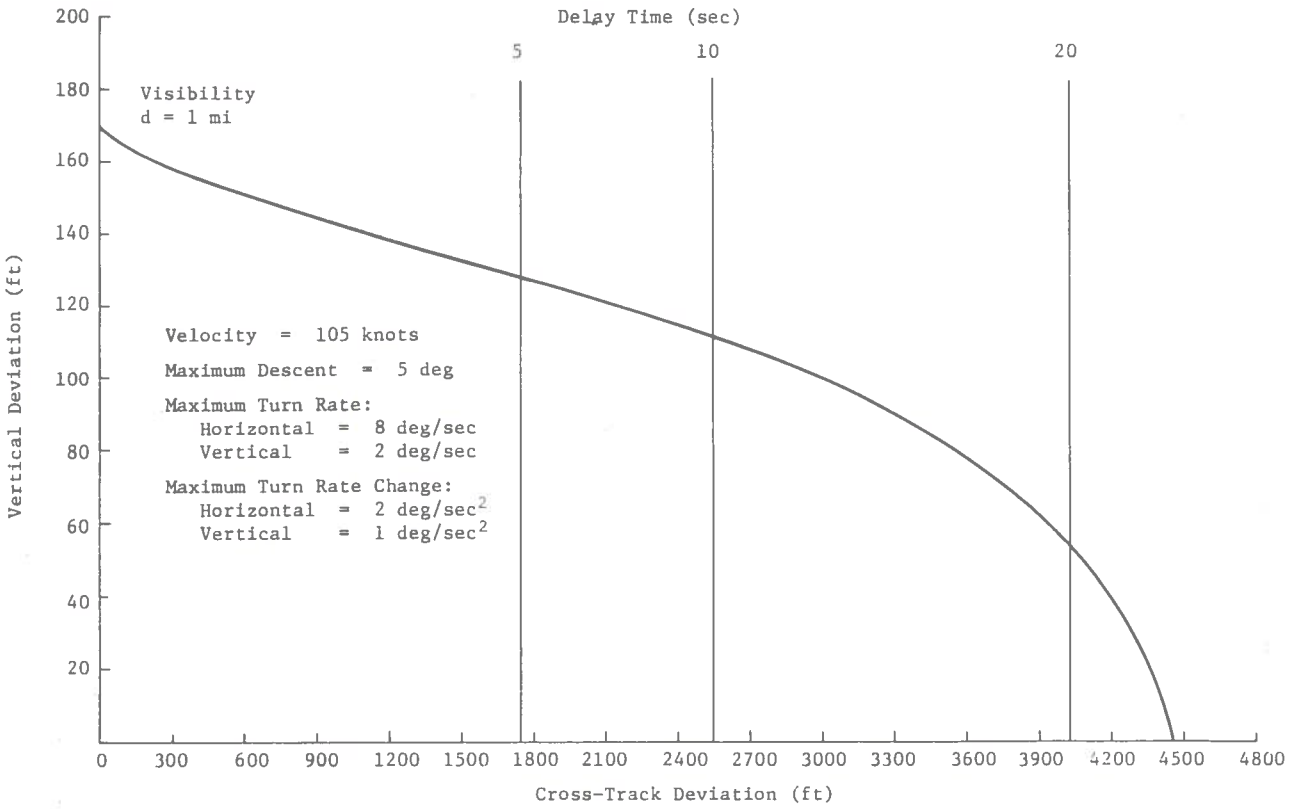

Fig. 4-6. Landing Window for Increased Turn Rate

Comparison of Fig. 4-4 and 4-5 shows that for increased aircraft velocity (105 knots in the latter figure) the window at the same 1-mile range becomes smaller. The faster aircraft has less chance to correct deviations from its desired path and must, therefore, meet stricter window requirements. Comparison of Fig. 4-4 and 4-6 shows that for an increased maximum horizontal turn rate of 8 deg/sec, the window becomes larger in the horizontal direction. The increased maximum turn rate allows for larger corrections of horizontal deviations, allowing for the less stringent window. Since the only difference in deriving the 1-mile windows of Fig. 4-4 and 4-7 is the turn rate, the window heights at zero horizontal deviation are identical.

4.3.2 Numerical Integration Routine Position-Keeping Requirements

Position-keeping errors in the cross-track direction and the altitude direction are assumed to be jointly normal and independent. The joint density function, f(y,z), can be written as

$$f(y,z) = \frac{1}{\sqrt{2\pi}\,\sigma_y} e^{-y^2/2\sigma_y^2} \cdot \frac{1}{\sqrt{2\pi}\,\sigma_z} e^{-z^2/2\sigma_z^2} \qquad (1)$$

where

y is the lateral displacement from the desired flight path

z is the vertical displacement

In the present study, the standard deviation of the altitude error, σ_z, is assumed to be some fraction of the lateral standard deviation, σ_y. Integration of the density function over a region corresponding to the delivery window yields the probability that the aircraft will arrive within the window and thus be able to successfully land on the runway. This probability is given by

$$P_{\text{A/C in window}} = \iint_{\text{window}} f(y,z)\, dy\, dz \qquad (2)$$

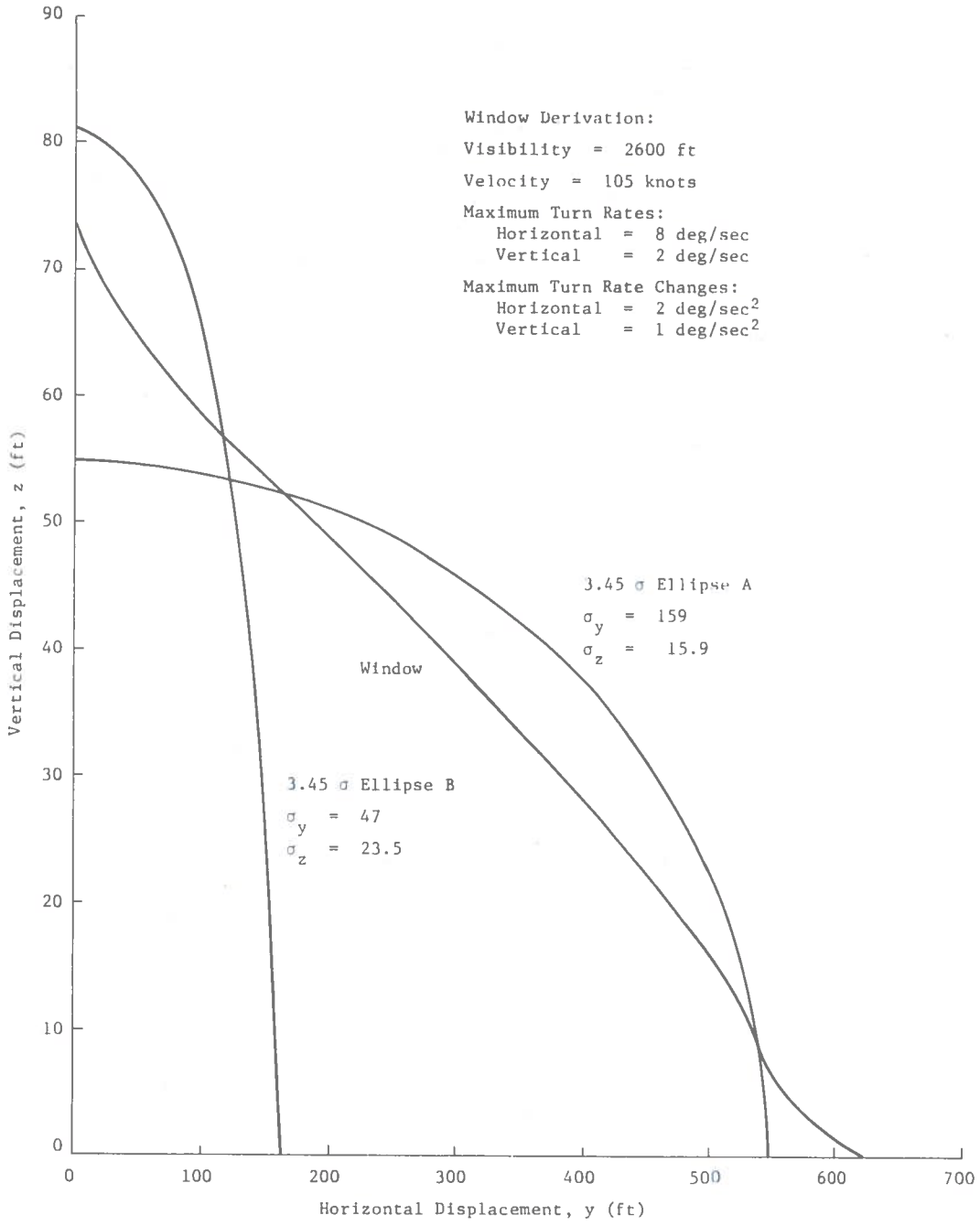

Fig. 4-7. Regions of Integration Yielding Areas of 0.9974

A probability of arriving in a window of 0.9974 is used as the criterion for determining σ_y and σ_z. This value corresponds to the integration of a single-dimensional normal density function from its negative "3-sigma" value to its positive "3-sigma" value. The joint position-keeping probability density function can be converted into a Rayleigh distribution. For such a distribution, 0.9974 corresponds to the "3.45 sigma" value. Since the delivery window is two-dimensional, the in-window probability is not a "3-sigma" criterion in the true sense. Still, the criterion does allow for a uniform condition in deriving position-keeping requirements, with a probability of successful execution equivalent to the 3-sigma level of confidence.

The integration is performed numerically, utilizing the error function, ERF(X), available in the Fortran library. This function is given by

$$\mathrm{ERF}(X) = \frac{2}{\sqrt{\pi}} \int_0^X e^{-u^2}\, du \tag{3}$$

This is the integration of the density function for a Gaussian random variable of mean zero and unity variance. Equation (1) can be substituted into Eq. (2) to yield

$$P_{\text{A/C in window}} = P = \iint_{\text{window}} \frac{1}{\sqrt{2\pi}\,\sigma_y} e^{-y^2/2\sigma_y^2} \cdot \frac{1}{\sqrt{2\pi}\,\sigma_z} e^{-z^2/2\sigma_z^2}\, dy\, dz \tag{4}$$

A numerical integration scheme is performed, summing incremental values along the y-axis. Within each y-step increment, the positive and negative vertical extents of the window are assumed to be constant. This approximation yields

$$P = \sum_{i=1}^{N} 2 \int_{y_i - a_i}^{y_i + \frac{\Delta y}{2}} \left[\int_{a_A}^{z_B} \frac{1}{\sqrt{2\pi}\,\sigma_z} e^{-z^2/2\sigma_z^2}\, dz \right] \cdot \frac{1}{\sqrt{2\pi}\,\sigma_y} e^{-y^2/2\sigma_y^2}\, dy \tag{5}$$

where

y_i = $(i-1) \cdot \Delta y$

Δy = integration step size along y-axis

z_B = allowable positive vertical deviation of window, $y = y_i$, measured from the intersection with desired glide-slope plane

z_A = allowable negative vertical deviation of window at $y = y_i$, measured as is z_B

$$a_i = \begin{cases} 0 \text{ for } i = 1 \\ \frac{\Delta y}{2} \text{ for } i > 1 \end{cases}$$

N = number of y-step intervals necessary for z_B to decrease to zero

The y-axis increment corresponding to i = 1 is only half as large as the other increments. All increments are located along the positive y-axis. Since the window is symmetric about the z-axis, the results of the integration through the positive y-axis must be doubled. This accounts for the factor of 2 in Eq. (5). It can be shown that,

$$\int_{z_A}^{z_B} \frac{1}{\sqrt{2\pi}\,\sigma_z} e^{-z^2/2\sigma_z^2}\, dz = \frac{1}{2}\,\mathrm{ERF}\,\frac{z_B}{\sqrt{2}\,\sigma_z} - \frac{1}{2}\,\mathrm{ERF}\,\frac{-z_A}{\sqrt{2}\,\sigma_z} \tag{6}$$

The vertical axis integration of Eq. (6) is constant for each horizontal increment. Thus, this term can be factored out of the horizontal integral. The remaining horizontal integral is given by

$$\int_{y_i-\frac{\Delta y}{2}}^{y_i+\frac{\Delta y}{2}} \frac{1}{\sqrt{2\pi}\,\sigma_y} e^{-y^2/2\sigma_y^2}\, dy = \frac{1}{2}\,\mathrm{ERF}\,\frac{y_i+\frac{\Delta y}{2}}{\sqrt{2}\,\sigma_y} - \frac{1}{2}\,\mathrm{ERF}\,\frac{y_i-\frac{\Delta y}{2}}{\sqrt{2}\,\sigma_y} \tag{7}$$

Equations (6) and (7) substituted into Eq. (5) yield

$$P = \frac{1}{2}\sum_{i=0}^{N}\left[\mathrm{ERF}\left(\frac{z_B}{\sqrt{2}\,\sigma_z}\right) - \mathrm{ERF}\left(\frac{-z_A}{\sqrt{2}\,\sigma_z}\right)\right]\cdot\left[\mathrm{ERF}\left(\frac{y_i + \frac{\Delta y}{2}}{\sqrt{2}\,\sigma_y}\right) - \mathrm{ERF}\left(\frac{y_i - a_i}{\sqrt{2}\,\sigma_y}\right)\right] \qquad (8)$$

This is the basic integration methodology utilized. In addition, interpolative correction is made for the general case where the positive vertical extent of the window decreases to zero at a point along the y-axis less than exactly N intervals from the origin.

An example of comparable integration regions and σ_y,σ_z combinations is shown in Fig. 4-7. The integration of the density function with σ_y = 159 and σ_z = 15.9 is equal to 0.9974 over both the region of the window and the 34.5 σ ellipse A. Likewise, the integration of the density function with σ_y = 47 and σ_z = 23.5 is equal to 0.9974 over the regions of the window and the 34.5 σ ellipse B.

The correspondence of integration values for the window and the respective ellipses may not be immediately apparent. One may question the differences in size, especially between the window and the 3.45 σ ellipse B. These differences are accounted for by the fall-off of the density function going away from the origin. The apparent unbalance of areas is attributed to the differences in total fall-off, or weighting, at different areas. The ellipses partially overlap the window in the first quadrant areas shown in the figure. Likewise, there is an identical magnitude overlap in the second quadrant, which is a mirror image of the first. In the third and fourth quadrants, however, the window is always larger than the ellipses. The first and second quadrant overlaps are weighted heavily enough to offset the relative largeness of the window in all other regions. It is pointed out, too, that integration of the density function entirely outside the 3.45 σ ellipse will yield a result of only 0.0026, while integration within the ellipse yields 0.9974.

4.4 Use of the Modified Track Model to Develop Navigation Requirements

The landing phase model, described in the previous section, determines the delivery (or control limit) window an aircraft must pass through to land safely as well as the position-keeping accuracy the aircraft must maintain so that the probability of intersecting the window is greater than the specified value of 0.9974. In the landing phase, position-keeping ability is dependent on navigation system performance, i.e., navigation accuracy and navigation data update rate. The relationship between navigation system performance and position-keeping accuracy will be discussed in this section.

A first approximation to the required navigation accuracy is to simply equate it to the established position-keeping accuracy. This may yield a more stringent requirement on navigation accuracy than may actually be necessary when small update intervals are used, since the position-keeping process filters the high frequency component of the navigation noise. Another method of deriving navigation requirements is to use computer simulations. The Track Model, described earlier in this report, has been modified to establish the relationship between navigation and position-keeping requirements. A block diagram of the modified Track Model is shown in Fig. 4-8. The parameters are defined as follows:

A_d	Disturbance acceleration
$r, \dot{r}, \ddot{r}$	Actual aircraft position, velocity, acceleration
$r_d, \dot{r}_d$	Desired aircraft position and velocity
$\Delta r_n, \Delta \dot{r}_n$	Navigation position and velocity erros
τ_n	Navigation update interval
$r_n, \dot{r}_n$	Navigation position and velocity
K_a, K_b	Aircraft response parameters
K_p, K_r	Position and velocity control loop gains
K_d	Aerodynamic drag term
A_L	Limit on commanded acceleration

The modified Track Model is simply the original Track Model with the surveillance loops deleted. Horizontal navigation errors and update rates have been observed in 20-hr simulations. For each case of navigation accuracy and update rate, the distribution of displacement from the desired path has been established. Each sample point of this distribution is taken at a navigation sample time. The instantaneous position distribution of the aircraft around its desired path is assumed to be the same as the distribution of the displacement obtained from the simulation.

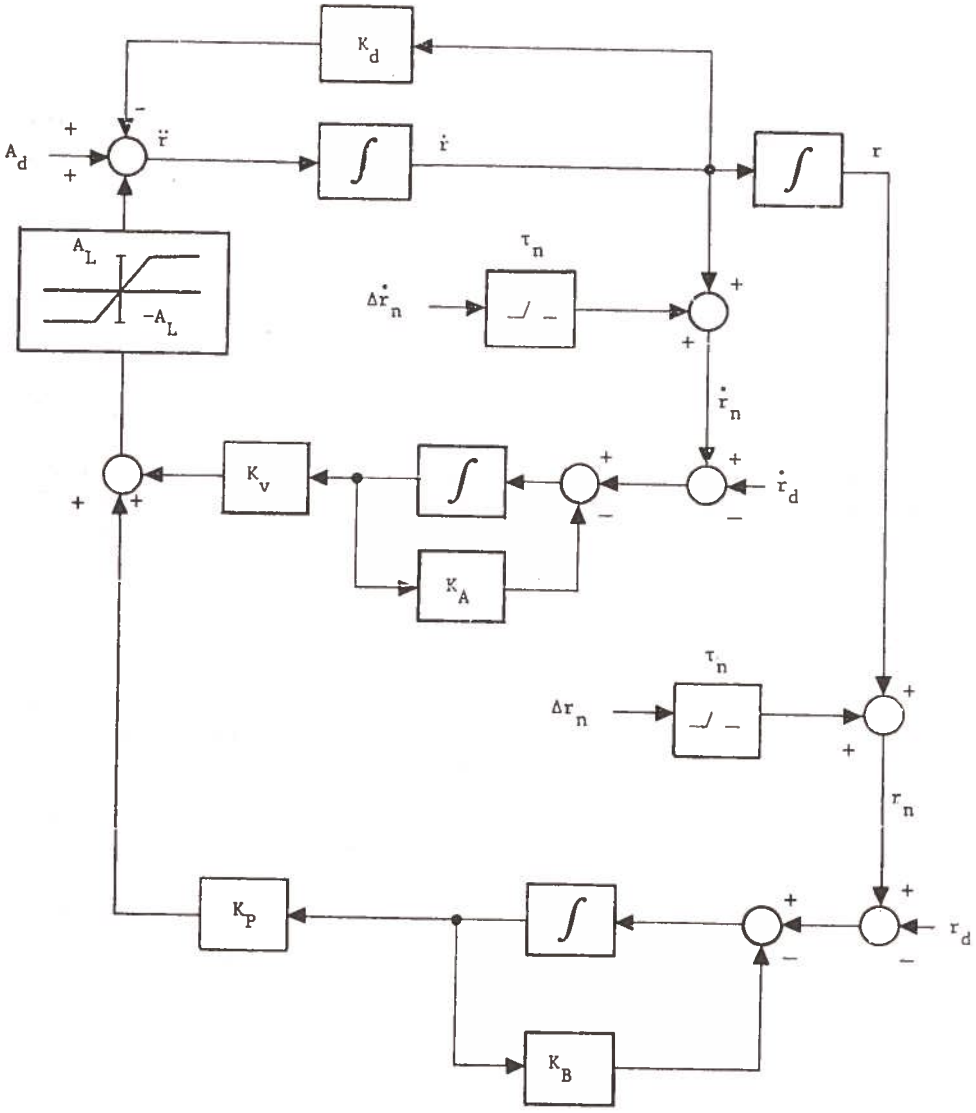

Fig. 4-8. Modified Track Model

An example of the density function of aircraft position developed over 20 simulated hours of aircraft operation is shown in Fig. 4-9. The navigation accuracy and update interval for the plot are 1000 ft and 5 sec, respectively. Superimposed on the plot of aircraft position is a Gaussian density function whose mean and standard deviation are equal to those of the simulation derived position data. Theoretically, the mean of the position deviation is zero. The non-zero mean depicted in Fig. 4-9 is attributed to the limited 20-hr simulation time.

The position-keeping requirement is a function of the visibility range (i.e., the landing conditions such as VOR, Category I, and Category II), the ratio of the vertical position-keeping accuracy to the horizontal or cross-track position-keeping accuracy, aircraft velocity, and maximum turn rates. The navigation requirements for the approach phase that must be met to provide the required position-keeping accuracies have been established using the modified Track Model. Figure 4-10 presents the results of the simulation; the relationships between navigation position and position-keeping standard deviation are shown for two values of navigation update interval, τ_n. For fixed values of navigation accuracy, the 5-sec update interval results in a smaller position-keeping accuracy than the 20-sec update interval. The closeness of the curves, however, indicates that τ_n is not a dominant factor in establishing requirements. For any given navigation position accuracy in Fig. 4-10, the resultant position-keeping accuracy increases by approximately 30 to 40 ft as τ_n is varied from 5 to 20 sec. Figure 4-11 shows a similar plot of position-keeping accuracy and navigation accuracy for uncorrelated noise samples only. The values of the position-keeping standard deviations may be slightly higher than the results shown since the non-zero mean was not considered. The values of the means are larger for the case where the noise is both correlated and uncorrelated than for the case where the noise is totally uncorrelated. In general, the position-keeping accuracies are smaller for the uncorrelated cases than for the correlated cases. However, systems with only uncorrelated noises are usually unachievable, hence, the curves of Fig. 4-11 are useful only from a theoretical standpoint.

4.5 Development of Navigation Accuracy Requirements for Approach

The navigation performance required for an airport approach has been established using the landing phase model and the modified Track Model. The first step of the procedure is to establish the size and shape of the delivery or control limit window. The required position-keeping accuracy is then determined under the assumption that aircraft deviations from a desired course can be represented by a zero mean Gaussian distribution. The final step is to establish the navigation performance requirements needed to maintain the necessary position-keeping accuracy.

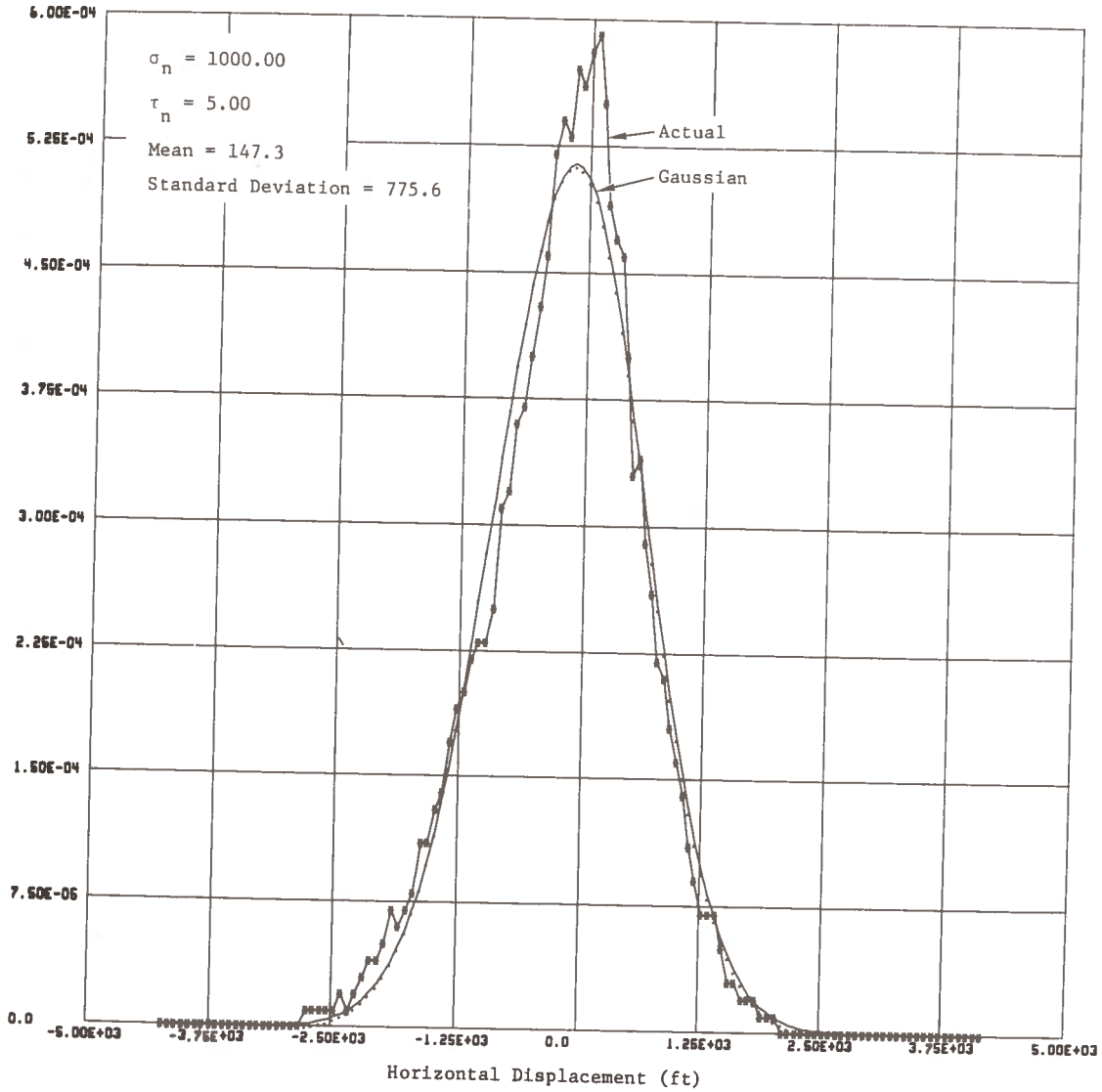

Fig. 4-9. Position-Keeping Density Functions Actual Position and Gaussian Density Functions with Identical Means and Variances

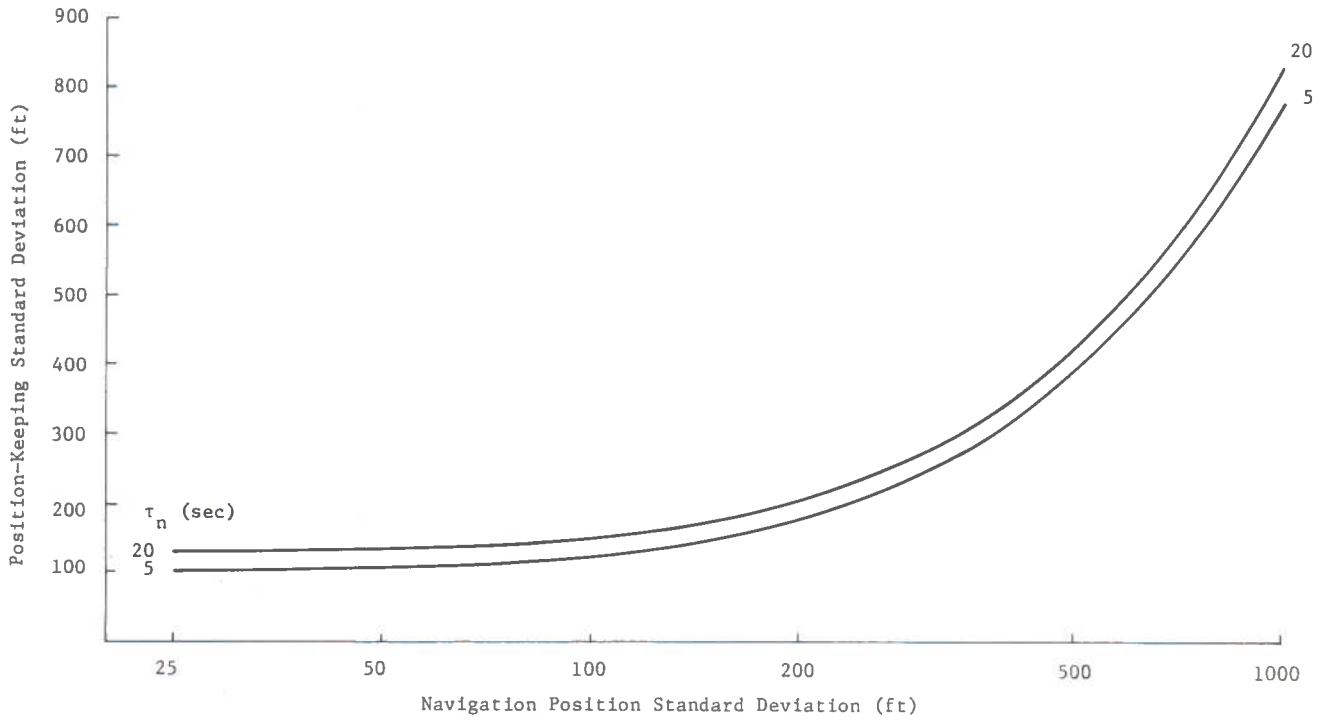

Fig. 4-10. Position-Keeping Accuracy Vs. Navigation Accuracy for Various Navigation Update Intervals, Correlated and Uncorrelated Errors

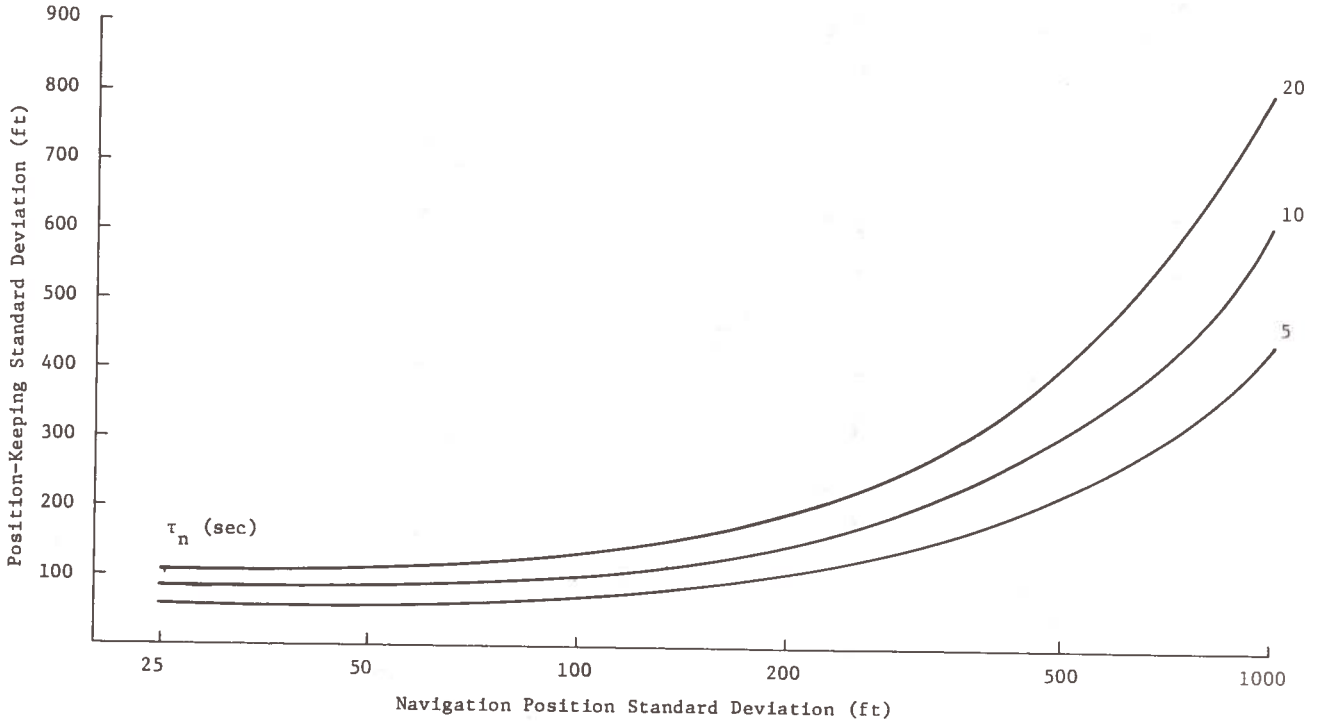

Fig. 4-11. Position-Keeping Accuracy Vs. Navigation Accuracy for Various Navigation Update Intervals, Uncorrelated Errors Only

Delivery windows were established for three landing categories (VOR, Category I, and Category II) considering aircraft with velocities of 75, 90, and 105 knots and maximum turn rates of 6 and 8 deg/sec. Other aircraft characteristics considered during the study include (1) maximum horizontal turn rate change (2 deg/sec^2), (2) maximum vertical turn rate (2 deg/sec), and (3) maximum vertical turn rate change (1 deg/sec^2). The integration routine was used to establish the vertical (σ_z) and cross-track (σ_y) position-keeping accuracies for two ratios σ_z/σ_y, namely, 0.1 and 0.5. Tables 4-1, 4-2, and 4-3 summarize the position-keeping accuracy requirements established from the landing phase model for the three landing categories.

The position-keeping accuracy becomes more stringent as velocities increase, turn rates decrease, and visibility decreases. The effect of turn rate on performance requirements is negligible. In most cases, less than 1 percent decrease in allowable error results from changing the maximum turn rate from 8 to 6 deg/sec.

The modified Track Model has been used to establish the navigation performance requirements. Whenever the position-keeping accuracy obtained from the model is smaller than the navigation position accuracy, the navigation position accuracy is used as the position-keeping accuracy in order to be conservative. Tables 4-4, 4-5, and 4-6 present the navigation requirements for VOR, Category I, and Category II landing conditions, respectively. The conditions assumed for the navigation performance requirements derivation are identical with those used for determining the position-keeping requirements. The results were obtained from Fig. 4-10 by finding the navigation position accuracy and navigation update interval which can support the position-keeping requirements delineated in Tables 4-1 through 4-3. The navigation accuracies shown in the tables were selected as the minimum of the position-keeping accuracies from Tables 4-1 through 4-3 or the navigation position accuracies from the curves of Fig. 4-10. Selection of the minimum value yields a conservative estimate of the requirements; i.e., the more stringent accuracy requirements are selected. Only one set of values is presented, since the requirements are essentially identical for maximum turn rates of 8 or 6 deg/sec.

The results of the study indicate that the navigation requirements for VOR landing conditions and a ratio $\sigma_z/\sigma_y = 0.1$ can be achieved with the same navigation performance required for terminal area operations (i.e., a separation standard of 1.5 nmi). For VOR landing conditions with $\sigma_z/\sigma_y = 0.5$ or for Category I conditions with $\sigma_z/\sigma_y = 0.1$, the navigation requirements are more stringent and may be difficult to achieve without an auxiliary landing system such as an ILS or MLS. The criterion used in this study is that 99.74 percent of all aircraft must pass through the delivery window. It is possible that a performance requirement which allows a greater percentage of the aircraft to miss the window and make additional approaches may be achievable and acceptable. These marginal cases require a more detailed analysis to establish the navigation position accuracy requirements.

Table 4-1. VOR Position-Keeping Requirements, 600-ft Visibility

Velocity (knots)	Maximum Horizontal Turn Rate (deg/sec)	Accuracy Combinations (ft)	
		Horizontal	Vertical
75	8	676	68
		140	70
90	8	656	66
		139	70
105	8	635	64
		135	68
75	6	672	67
		142	71
90	6	653	65
		138	69
105	6	628	63
		134	67

Table 4-2. Category I Position-Keeping Requirements, 2600-ft Visibility

Velocity (knots)	Maximum Horizontal Turn Rate (deg/sec)	Accuracy Combinations (ft)	
		Horizontal	Vertical
75	8	219	22
		53	26
90	8	191	19
		50	25
105	8	159	16
		47	24
75	6	218	22
		53	26
90	6	188	19
		50	25
105	6	158	16
		47	24

Table 4-3. Category II Position-Keeping Requirements, 1200-ft Visibility

Velocity (knots)	Maximum Horizontal Turn Rate (deg/sec)	Accuracy Combinations (ft)	
		Horizontal	Veritical
75	8	33	3.3
		16.5	8.3
90	8	23	2.3
		13.4	6.7
105	8	16.9	1.7
		10.2	5.1
75	6	33	3.3
		16.5	8.3
90	6	23	2.3
		12.8	6.4
105	6	16.9	1.7
		10.2	5.1

Table 4-4. VOR Landing Navigation Requirements, 6080-ft Visibility

Velocity (knots)	Position-Keeping σ_z/σ_y Ratio	Navigation Requirement Combinations		
		Update Time τ_n (sec)	Horizontal σ_{nav} (ft)	Vertical σ_{nav} (ft)
75	0.1	5	676	68
		20	676	68
	0.5	5	140	70
		20	55	70
90	0.1	5	656	66
		20	656	66
	0.5	5	139	60
		20	55	60
105	0.1	5	635	64
		20	635	64
	0.5	5	125	68
		20	50	68

Table 4-5. Category I Navigation Requirements, 2600-ft Visibility

Velocity (knots)	Position-Keeping σ_z/σ_y Ratio	Navigation Requirement Combinations		
		Update Time τ_n (sec)	Horizontal σ_{nav} (ft)	Vertical σ_{nav} (ft)
75	0.1	5	219	22
		20	219	22
	0.5	5	53	26
		20	53	26
90	0.1	5	191	19
		20	170	19
	0.5	5	50	25
		20	50	25
105	0.1	5	159	16
		20	110	16
	0.5	5	47	24
		20	47	24

Table 4-6. Category II Navigation Requirements, 1200-ft Visibility

Velocity (knots)	Position Keeping σ_z/σ_y Ratio	Navigation Requirement Combinations		
		Update Time τ_n (sec)	Horizontal σ_{nav} (ft)	Vertical σ_{nav} (ft)
75	0.1	5 to 20	33	3.3
	0.5	5 to 20	16.5	8.3
90	0.1	5 to 20	23	2.3
	0.5	5 to 20	13.4	6.7
105	0.1	5 to 20	16.9	1.7
	0.5	5 to 20	10.2	5.1

Any navigation system such as VVOR or satellite navigation which is capable of providing the navigation accuracies listed should be suitable for approach guidance. Since the SAATMS system provides surveillance accuracies approximately the same as those required for terminal area operations and thus are the same as those required for approach under VOR conditions, the VVOR concept should be suitable for approach guidance.